JIMMA UNIVERSITY

JIMMA INSTITUTE OF TECHNOLOGY

FACULTY OF ELECTRICAL AND COMPUTER ENGINEERING

MODEL AND CONTROL OF PARABOLIC TROUGH COLLECTOR FOR STEAM SUPPLY IN INDUSTRY: - CASE STUDY OF BEDELE BREWERY FACTORY

By

EPHREM ASEMAHAGN HOMA

A THESIS SUBMITTED TO THE SCHOOL OF GRADUATE STUDIES OF JIMMA UNIVERSITY IN PARTIAL FULFILLMENT OF REQUIREMENTS FOR THE DEGREE OF

MASTER OF SCIENCE

IN

CONTROL AND INSTRUMENTATION ENGINEERING

ADVISOR: DR. FITSUM BEKELE

CO-ADVISOR: MR. TESFABIRHAN SHOGA

AUGUST, 2022

JIMMA, ETHIOPIA.

JIMMA UNIVERSITY

JIMMA INSTITUTE OF TECHNOLOGY

FACULTY OF ELECTRICAL AND COMPUTER ENGINEERING

MSc THESIS

ON

MODEL AND CONTROL OF PARABOLIC TROUGH COLLECTOR FOR STEAM SUPPLY IN INDUSTRY: - CASE STUDY OF BEDELE BREWERY FACTORY

BY

EPHREM ASEMAHAGN HOMA

APPROVAL BY BOARD EXAMINERS

Dr. Fitsum Bekele		10.03.2022
Advisor	signature	Date
Mr. Tesfabirhan Shoga	----------	----------
Co-Advisor	signature	Date
Mr. Zewude Tolosa		
Internal Examiner	signature	Date
Dr. Chala Merga	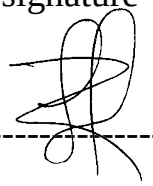	22.Aug.2022
External Examiner	signature	Date

Declaration

I declare that this thesis is my original work, here by submitted by me and has not previously been submitted for any other degree or professional qualification, all sources of material used for this thesis work have been fully acknowledged.

Ephrem Asemahagn	----------	----------
	Signature	Date

This thesis has been submitted with my approval as a university advisor.

Dr. Fitsum Bekele		10.03.2022
Advisor	Signature	Date

Mr. Tesfabirhan Shoga	----------	----------
Co-Advisor	Signature	Date

Acknowledgements

First of all, I would like to thank my God in helping me to finish my research successfully and I would like to thank Jimma Institute of Technology in giving this good chance to conduct this research.

Next, I would like to thank my advisor, Dr. Fitsum Bekele, for his knowledge and supporting me throughout my research. I appreciate his enlightening guidance and advice in helping me to complete this study. Especially his good attitude on research and his pursuit for the perfect work will help me in a long run.

I also sincerely thank my co-advisor Mr. Tesfabirhan Shoga for his kind in giving guidance on the preparation and completion of my thesis document.

Table of Contents

List of Table

List of Figure

List of Abbreviations

NDR ……..Nominal Discount Rate

CSP ……...Concentrating Solar Power

DNI……Direct Normal Irradiance

EHV ……..Existing High Voltage

CSPS …….Concentrated solar power system

LPFH ……..…low pressure feed heater

CSP ……...concentrating solar power

HCE ……..Heat Collecting Element

GSHP…….Ground Source Heat Pumps

IDR ……...Incident Direct Radiation

SEGS ……....Solar Electric Generating System

IEA ……..……International Energy Agency

NTU …….…...Number of Transfer Units

PTSC ……..Parabolic trough solar collector

PTC …….Parabolic Trough Collector

HPP ……..High pressure pasteurization

LPP ……..Low pressure pasteurization

SAM …….System Advisor Model

SCA ……..Solar Collector Assembly

CF…….Capacity Factor

DSG ……Direct Steam Generation

ST ……...Solar local time (ST)

HTF……...heat transfer fluid

FWH……Feedwater Heater

AU ……..Astronomical unit

GPM…….Gallon per minute

Re……..Reynolds number

HV…….High Pressure

FP ……..Feed Pump

LP …….....Low Pressure

NU ……..Nusselt number

Pr …….Prandtl number

CP …….…...Condenser pump

RE …….....Renewable Energies

PV ……Photovoltaic

F …….Focal Length

GHG ……..Green House Gas

ṁ(t) ……..mass flow rate

CRS ……Central Receiver Systems

CST…….Concentrating Solar Thermal

TRNSYS ……Transient system simulation program

D ……Distance between collector rows

EES ……..Engineering Equation Solver

$\dot{V}_{HTF}$ …….Volume flow rate of HTF

T_{int}……Inlet temperature

T_{steam}……Steam temperature

$q_{external}$……..External heat

N…..……Number of Days in years

L …….Length of collector

W …….Collector width

f ……friction factor

T_{amb}……Ambient temperature

q_{absorb}…….heat absorbed

T_{out}……..outlet temperature

q_{gain}…… Gain heat

$q_{internal}$……..Internal heat

List of Symbols

α ……..Surface azimuth angle

θ_z …….Zenith angle

η_{th}…….Thermal efficiency

β …….....Tilt angle

δ ……..Angle of declination

ε …….. Effectiveness

Ø …….Latitude angle

ω ……Hour angle

θ …….Angle of incidence

σ ……Stefan-Boltaman constan

ρ ……....Density

τ ……Transmittance

Abstract

Currently, most industries in Ethiopia use steam for a variety of purposes, including sanitary and pasteurization processes. This thesis shows how to use renewable energy instead of gas fuel for steam generation in a factory and how to use an advanced controller to manage the temperature level of the steam generator in a case study of the Bedele brewing factory. Currently, gas fuel is used in this factory's boiler plant, and steam temperature is controlled using a PID controller. Because gas is a non-renewable energy source with high costs and environment affect, it is preferable to replace it with a renewable energy source such as solar energy. Furthermore, in the case of solar energy systems, advanced MPC controllers are preferred over PID controllers for predict the next value.

This paper presents Model parabolic trough collector based on collected data to produce steam for pasteurization plant in Bedele brewery factory. Here, apply PTC technology using solar system. Additionally model MPC controller to supply fixed temperature of steam for pasteurization plant. Here, MPC control the temperature of steam with respect to given set point (413K). In this thesis, Analysis the performance of MPC interims of both steady state response and transient response. According to the thesis steady state error almost approximates to zero and preferable transient response result then PID controller. Therefore, MPC controller is more advisable for this temperature controlling system in this Factory.

Key words: Parabolic trough collector (PTC), Model predictive control, PID controller, Heat Transfer Fluid, Pasteurization plant and Temperature control.

CHAPTER 1
INTRODUCTION

1.1 Background of the Study

Energy is a critical component of a country's technical, industrial, social, and economic growth. Energy services are required in all civilizations to satisfy fundamental human requirements such as lighting, cooking, movement, and communication. Significant renewable energy resources exist in Ethiopia, including hydropower, wind, geothermal, biomass, and solar energy. Nonrenewable energy resources, particularly natural gas and coal, are abundant in the nation. While conventional biomass consumption now dominates the energy industry, other energy sources such as hydropower and the remainder of renewable energy resources have the potential to provide the country with significant economic growth prospects [1].

Solar energy has always been a wonderful source of energy due to its inexpensive cost of construction, operation, and the sun's unrestricted existence. Solar energy is nonpolluting, limitless, and risk-free. Additionally, it no produces hazardous emissions even when converted to power using solar or thermodynamic facilities. As a result, this renewable energy source has become increasingly important in the future of energy policy. Some advantage of solar energy are listed below [1]:

- Solar power is pollution free and causes no greenhouse gases to be emitted after installation.
- Reduced dependence on foreign oil and fossil fuels.
- Renewable clean power that is available every day of the year, even cloudy days produce some power.
- Return on investment unlike paying for utility bills.
- Greatly reduced contribution to global warming.

There are two types of solar technology used to generate electricity those are: - Photovoltaic (PV) and concentrated solar power (CSP). Solar power generation is an ancient technology. By harvesting the sun, there were several applications from domestic water heating to high heat flux weapons in history. In 1973, U.S.A began investing heavily in renewable energy sources and as a result of this act and from the concentrated solar power (CSP) point of view, the Solar Electric Generating system (SEGS) plants were built. The SEGS plants are the first large scale CSP application. Nine commercial plants were built in the Mojave Desert (average direct normal irradiance (DNI) up to 2727 kilowatt-hour per meter square in one year) in California for supplying electricity for peak demand hours to the grid. Several improvement were implemented while plants SEGS-1 to SEGS-9 were sequentially being built. After high DNI hours, the storage discharges and the hot HTF produces steam which passes through the super heater before the turbine. The aim of storage is to allow electricity generation to vary with peak demand to sell the electricity produced with the highest profit. In 1999, the storage was damaged by fire and it was not restored [3].

From other forms of renewable, Concentrating solar power are unique in that they have the option to incorporate thermal storage to store solar-generated energy for use at a later time in their design making power from concentrating solar power plants dispatch able. Thus, CSP offers firm flexible electrical production capacity to utilities and grid operators while enabling effective management of a greater share of variable energy from other renewable sources. Parabolic trough, linear Fresnel reflector, power tower and dish engine technologies fall into the Concentrating solar power category. In all of these system a working fluid is heated by the concentrated sunlight and is then used for power generation or energy storage. Some of the key advantages of concentrating solar power include the following [4]:

- It can be installed in a range of capacities to suit varying application and conditions, from tens of KW (dish systems) to multiple MWs (tower and trough systems).
- It can integrate thermal storage for peak loads as well as intermediate loads.
- It has modular and scalable components and it does not require exotic materials.

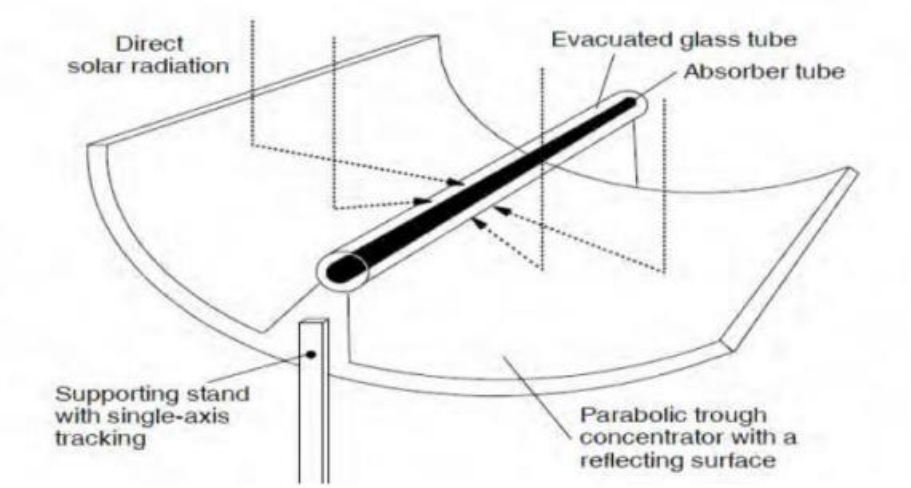

Figure 1.1: Functional principle of a parabolic trough [22]

Additionally almost all industries in our nation now utilize massive steam boiler plants that use gas fuel to create steam for various purposes such as sanitation and pasteurization of the industry's end product. Because heating systems have a high thermal inertia, maintaining excellent system managed is always a difficulty. Because this system is complicated and dynamic, precise control is difficult to achieve. The existing heating method in industry for producing steam uses non-renewable gas fuel, which is not environmentally friendly. This PID method of controlling the heating system also has its own feedback. The goal of using parabolic trough controller (PTC) technology in a solar to water source heat pump is to save money by using the energy stored in the sun or a renewable energy source. When water passes through a heat exchanger or a condenser, it gains or loses energy. However, if the water in the tank is cold, it must be heated, necessitating a good management technique to maintain the correct temperature of the water before it is poured in the tank. The solar-powered industrial process is a complicated system impacted by solar radiation uncertainty, demand temperature variations, and process time schedule unpredictability, as well as the risk of thermal stratification in the storage system when managing the heat pump, we must consider the quantity of energy consumed as well as the user's comfort. Solar thermal energy is collected using a parabolic trough, which is a kind of renewable energy. The majority of parabolic troughs are curved, with a polished metal mirror lining. The device must be portable and track the suns throughout the day and with the changing seasons in order to collect the maximum amount of energy [5].

The most essential aspect of any automation system is the design of the preferable control system. There are several sorts of controllers, including traditional and intelligent controllers. This thesis provides a technique for developing a model predictive controller (MPC) control system for steam temperature of water which supply for pasteurization. Firstly, concerned with modeling and design parabolic trough collectors (PTC) to generate steam from solar energy and design a controller to control the outlet temperature of Steam which supply to pasteurize zones. In order to design PTC first obtain the meteorology data of the Area that is solar radiation, wind speed and ambient temperature data (Bedele town). A parabolic trough technique concentrates sunlight onto an absorber tube by lining up parabolic reflectors in long rows (receiver). The heat transfer fluid is heated and circulated in the receiver, and the heat is released to produce steam. The steam is used to power a traditional steam generator, which is used to pasteurize industrial end products. To guarantee that the sun is continually focused on the receiver, the mirrors employ a single-axis Tracker, which necessitates a rather flat terrain. A parabolic trough technology uses parabolic mirrors that line up in long rows to concentrate sun light onto an absorber tube (receiver). The size of the plant and collector, as well as the temperature and pressure losses in the piping system and the unique ambient conditions all influence the design of the solar field [6].

A complete solar field contains several parallel rows of solar collectors. The distance between the collector rows is planned according to minimizing the piping costs on the one hand and having a minimal shading effect between the rows on the other. In general, the design of the solar field depends on plant and collector size, the temperature and pressure losses in the piping system and the specific ambient conditions. Parabolic trough fields can be erected in any direction, but erected in an east-west direction leads to the highest possible energy yield over the year while a north-south orientation smooth down the seasonal fluctuations. Some of the components like the metal structure, the tracking system, the controllers and other subsystems, which make up around 60 percent of the direct solar field costs, are standard components and can be ordered from several countries and in different forms. The reflectors and the absorber tube, however, are special components and have to be produced specifically for the parabolic trough solar field [8].

1.2 Solar Energy Potential

Many countries have implemented incentive programs to encourage energy generation and grid integration while minimizing environmental effect. Ethiopia has a large solar energy potential. However, only around 1 percent of the potential has been realized thus far. According to current data gathered by the energy information administration and development follow up core process, the total generated energy from solar photovoltaic over the previous 6 years has been more than 35 Megawatt hour, which is more than 6 Megawatt greater than the installed capacity. Many governments started incentive plans to promote generation and integration of energy into the grid by means that minimize the environmental impact. Ethiopia has substantial solar energy resource. Solar water heating systems with the total energy generation of 299 Megawatt hour and ten water pumps with pumping installed capacity of 10 kilo watt have been installed in different parts of the country by governmental and nongovernmental organizations [8].

Figure 1.2: Simple schematic of parabolic through technology [24]

A parabolic trough power generation uses parabolic mirrors that line up in long rows to concentrate sun light onto an absorber tube (receiver). The receiver contains a heat transfer fluid (oil) that is heated and circulated, and the heat is released to generate steam. The steam powers a conventional steam generator to produce electricity. The mirrors use a single-axis tracker to ensure that the sun

Is continuously focused on the receiver requiring a fairly flat land. Solar collector is a mechanical device which captures the radiant solar energy for use as a Source of energy for the heating of water for the production of electricity as well as for different industrial application. There are 4 main categories of Solar Collectors [12]:

- **Low temperature unglazed collectors:** consists of black color matting or tubes made from rubber or plastic based materials. If it is not insulated it can't efficiently operate in cooler conditions or when hot water (showering Temperature) is required. They are often referred to as "unglazed" as they don't have a glass Cover like flat plate or evacuated tube collectors.
- **Flat plate collectors:** the design is very simply an insulated box with an absorber sheet welded to copper pipe through which the heat transfer liquid circulates through. No insulation above the absorber is an inherent disadvantage of the design and leads to high heat loss. This heat loss means flat plates are unable to deliver hot efficiently at higher temperatures (greater than 70℃), and performance is greatly reduced in cold weather.
- **Evacuated tube collectors:** comprised of an array of single or twin wall glass tubes with a vacuum that provides excellent insulation against heat loss. The design is very similar to a glass hot water flask used to keep hot water. Single wall evacuated tubes normally have a fin that has the absorber coating, similar to that used in the flat plate collector. Twin wall evacuated tubes have absorber coating on the inner tube and the space between the two tubes is evacuated to form the vacuum.
- **Concentrating collectors:** a concentrating collector uses mirrors to concentrate the sunlight onto an absorber tube or Panel, allowing much higher temperatures to be reached. Such collectors normally require 1 Or 2 axes tracking to follow the sun and ensure optimal reflection angle. Due to the size and Complexity of these systems they are primarily used for large scale projects. Therefore use this type of solar collector for this application.

Parabolic trough collectors consists of a linear parabolic reflector that concentrates light onto a receiver positioned along the reflector's focal line. The receiver is a tube positioned directly above the middle of the parabolic mirror and filled with a working fluid. The reflector follows the sun during the daylight hours by tracking along a single axis. Parabolic trough collectors (PTCs)

represent a proven source of thermal energy for industrial process heat and power generation; unfortunately it is still not highly implemented due to technical and economic barriers. In recent years, environmental issues have focused attention on green energy resources, improving the chance for PTCs to be commercially competitive in the market. The Middle East region is considered an interesting area for implementing solar energy projects since the sun is shining most of the year with high direct irradiance values [12].

1.3 Statement of the Problem

Bedele brewery factory is one of well-known industry in Ethiopia. In this factory using steam supply for different purpose such as sanitary and pasteurization process. Therefore steam production and control this steam temperature level are most well-known activity in this industrial processes. Current steam production techniques are using massive steam boiler plants that use gas fuel (non-renewable source) and steam temperature controlling system was PID controlling system(non-adaptive and non-robust system). Generally, this sort of system has the following three effects on the factory. Firstly, its expense since use non-renewable energy such as gas fuel. Secondly, the waste products of this gas fuel from the boiler plant has a direct affect environmental. Thirdly, PID control has high percentage of overshoot, long settling time and not fast response time. Additionally, to deal with multiple and simultaneous disturbances, it would be necessary to design advanced control strategies such as model predictive control (MPC).Therefore this thesis deal to overcome above listed problem.

1.4 Objectives

1.4.1 General Objective

The main objective of this thesis to model and design MPC controller to control steam temperature of parabolic trough collector (PTC) to supply for pasteurization plant in Industry.

1.4.2 Specific Objective

This research aims to achieve the following objectives at completion:

- To modeling parabolic trough collector (PTC) and pasteurization plant.
- To design MPC controller to control steam temperature of the system.
- To analyses the result using Matlab simulation system.
- To evaluate the performance of MPC control result compare to PID controller result.

1.5 Scope of the study

The scope of this research is to model parabolic trough collectors (PTC) to produce steam based on environmental data (solar radiation and ambient temperature) of Industry location. Secondly, Modeling and developing a model predictive controller (MPC) for regulating the collector's output temperature steam to supply for pasteurization systems in industry using MATLAB/Simulink software.

1.6 Limitation of the study

There are certain limitations that have been faced in this thesis. The first limitation was that it was impossible to obtain exact solar radiation data per some minute variation since the data record averagely per day. The second limitation was because of the budget allowed by Jimma University is not enough for this thesis works.

1.7 Significance of the Study

The significance of these study content two ideas. The firstly, replace gas fuel to renewable energy solar energy for the purpose of steam generation in Bedele brewery factory. For this process design parabolic trough collectors (PTC) based on solar intensity of the factory location and steam temperature level needed for pasteurization plant. Secondly, model adaptive MPC controller to control this steam temperature level and predict the next values in the system.

The advantage of this research is to reduce the fuel cost, protect environment pollution and to replace advance controlling system in the factory as well as initiate future researcher to develop this type of controller in this factory.

1.8 Thesis Organization

This thesis is organized into seven chapters.

- In chapter one include introductions, the problems Observed Industry specifically in pasteurization plant, objective of the thesis and scope of the thesis are stated clearly.
- In chapter two different types of literatures related with this thesis are reviewed and summarized.
- In chapter three gives a short definitions, types, component and principle of operations of parabolic through collector. Also describes about the derivation of nonlinear

equations of the parabolic trough collector (PTC) and calculate the solar radiation which reach the earth discuss in detail.

- In chapter four gives definitions, block diagram and model of Pasteurization plant described briefly. Additionally, the combination Model of PTC and Pasteurization plant described.
- In chapter five, mathematical model of nonlinear system of combination plant designed, model of linearization and discrete the linearize system are explain in detail.
- In chapter six discus result and discussion of the final matlab Simulink model described briefly. Additionally, compare final MPC control result with respect to PID controller and analysis the performance of controller. Finally, chapter seven conclusion and recommendation as well as future work are presented.

CHAPTER 2

LITERATURE REVIEW

There are a number of researches and articles which address the parabolic trough collector (PTC) and Model predictive control (MPC) controlling system of steam supply in industry. There are several efforts spent on simulation of performance models, benchmarking these simulations with several PTC plants and optimization of different parameters and locations.

Xiaolei Li and Ershu Xu (2018) [12] has discussed on the title of modeling and dynamic simulation of a steam generation system for a parabolic trough solar power plant. In a parabolic trough solar power plant, the steam generation system is the junction of the heat transfer fluid circuit and the steam circuit. Due to the discontinuous nature of solar radiation, the dynamic characteristics of working fluid physical parameters, such as mass flow rate, temperature, and pressure, are more evident in the steam generation system in this kind of plant, increasing the complexity of system operation. Here, based on the developed model, four typical single-parameter disturbance processes were simulated, and then the control strategy was obtained. System-level simulations on different days (clear and cloudy) and in different seasons (spring, summer, autumn, and winter). The simulation results show that PI control can be used to adjust the water level and water temperature, that system operation on cloudy days should be avoided, and that the system can continue to generate steam after the sun sets. The simulation results can provide a useful reference for plant operators. According to this paper use proportional Integral (PI) controller to control the outlet temperature of the HTF. But this type of controller is not adaptive and not robust type of controller. Additionally, in this paper Control strategy can only deal with the single disturbance scenarios. To deal with multiple, simultaneous disturbances, it would be necessary to design advanced control strategies such as model predictive control.

Bosong Lin, Theodore Wiesner (2018) [11] here, an open source model for parabolic trough solar field. According to this paper presents an open-source model of a parabolic trough collector solar field the intention is to provide a foundational tool for the solar energy research community purpose.

The volume flow rate of the heat transfer fluid (HTF) and the angle of incidence are the manipulated variables of the model. The size of the solar field may be altered. According to this paper use proportional Integral (PI) controller to control the outlet temperature of the HTF. But this type of controller is not adaptive and not robust type of controller. Additionally, in this paper Control strategy can only deal with the single disturbance scenarios. To deal with multiple, simultaneous disturbances, it would be necessary to design advanced control strategies such as model predictive control (MPC).

Paul Verrax (2018) [2] model predictive control applied to ground source heat pumps. In this thesis Ground Source Heat Pumps (GSHP) are efficient heating systems, particularly popular in the Nordic countries. However, the GSHPs available for the consumer market today typically only utilize basic control schemes that are relatively inflexible. More advanced strategies such as model predictive control (MPC) appear as a promising approach to improve comfort while reducing consumption. The present this thesis considers a typical user case of a single family house heated by a ground source heat pump willing to reduce its environmental impact. Here, design a MPC controller to be used on top of the existing heat pump system and with almost no additional hardware needed. Specific attention is dedicated to the systems efficiency in order to reflect the real working performances of a ground source heat pump. The controller is evaluated in simulation on different scenarios using an identified model of a single family house. The results show the MPC strategy becomes most beneficial when including time varying prices or reduced comfort during certain hours of the day. According to this paper, it focus on ground source heat pumping system. Here, MPC control the level of heat pump from ground. But, its drawback is it does not consider the disturbance parameter in this plant. According to my thesis consider two types of disturbance those are solar radiation and ambient temperature.

Sanan T.mohammad and Hussain H.AL-kayiem (2018) [5] have done a paper in the title of an integrated program of a stand-alone parabolic trough solar thermal power plant. In this paper Solar thermal systems produce steam after being energized by solar parabolic trough concentrators, are incorporated with a steam turbine-generator assembly to produce electricity. This study presents a code for prediction of performance, while under-taking preliminary plant-sizing for a variety of parabolic trough solar fields operating under nominal conditions.

The thermal efficiency of stand-alone parabolic trough solar thermal power plant in commerce. The conceptual design of the standalone parabolic trough solar involves: selection and sizing of system components, power generation cycles, working fluid types, and power block sizing. In addition, this code is able to provide a flexibility in terms of temperature, heat transfer, and pressure range. This is to reproduce real working conditions and obtain actual electricity production under effective solar radiation data. But, in this paper discuss only to produce electricity using parabolic trough collector and not explain way of controlling the steam which supply to turbine for production of electricity.

Eduardo F.Camacho (2017) [34] model predictive control in solar trough plant. In this thesis the main goal of a control system for a parabolic trough field is to maintain the outlet temperature of the field close to desired a set point since the primary energy source solar energy cannot be manipulated the oil flow q is used as a control signal. The set point may change substantially throughout the daily operation due to changes in the production requirement solar radiation condition, solar hour. According to this paper control the outlet temperature using angle of incidence. Adjust the angle of incidence and control level of temperature which collects to system. But, in this paper discuss only angle of incidence is manipulated variable for the system to adjust output temperature of system and not include volume flow rate of heat transfer fluid. In my thesis using volume flow rate of heat transfer fluid as manipulated variable of the system to adjust outlet temperature.

Sigh.r;Eerapetritou M (2017) [11] modelling, transient simulations and parametric studies of parabolic trough collectors with thermal energy storage. In this thesis, a mathematical model of a parabolic trough collector field with a two tank molten salt thermal energy storage is developed. The model is built in TRNSYS and by using Mat Lab, novel valve and thermal energy storage control algorithms are implemented. The model is sensitive to transient states inside the components and variations in weather and demand. Optimum parabolic trough collector length is determined for different insolation values to show the relation between direct normal insolation and collector string length. The mathematical model is used in an economic model, which contains initial investment costs of the parabolic trough collector field and thermal energy storage costs only Depending on the economic model, different sizes of plants are created at fixed initial

Investment costs by changing collector field area and storage size in the mathematical model. A parametric study is done by using economic model data and by simulating the mathematical model at various initial investment costs, two different locations in Turkey, and four different load profiles. As result of the parametric study, maximum solar fraction cases are selected and a generalized trend is observed. Effect of thermal energy storage on solar fraction is discussed and the change in thermal energy storage with optimum plant size is investigated. After an optimum investment, linear increment behavior of solar fraction is disappears and increases asymptotically by increasing the plant and storage size. But it's not deals about type of controller which control the thermal energy produce using this PTC model.

Alexander Arnitz (2017)[13] has done a research on Model based predictive control of a heat pump system, this thesis presents and investigates a model based predictive control (MPC) approach to control the heating of a thermal storage with a heat pump. Aside from achieving the required temperatures in the storage the heat pump ought to maximize the utilization of electricity produced from an on-site photovoltaic (PV) installation. Predictions for the PV output and the electricity price are combined with characteristic diagrams of the heat pump and a model of the thermal storage to determine an optimum heat pump operation. The optimum is found through solving a convex optimization problem. Different hydraulic circuits for the connection of the heat pump to the thermal storage are investigated. The nonlinear charging process of the thermal storage required an iterative MPC routine. The simulation results for the various hydraulic circuits are analyzed for a defined set of parameters. But, in this thesis discus direct the heat store by photovoltaic (PV). Here, MPC controller control the direction of photovoltaic to maximize the storage of heat. But, According to my thesis using parabolic trough collector (PTC) to generate steam and MPC controller control the temperature of steam using volume flow rate of heat transfer fluid (HTF) as manipulated variable (MV) of the system.

Zhenun Maaand,(2017)[8] has discussed on the title of Simulation of Parabolic Trough Concentrating Solar Power Generation System, In this work, theoretical performance of concentrated solar power system (CSPS) using parabolic trough collectors (PTC) is investigated.

More express about parameter consider in PTC design as well as solar radiation collect. The TRNSYS software and the Solar Thermal Electric Components (STEC) library are used to model the power system design and simulations. Input data and results of the simulation of the already existing SEGS VI plant were used for validating the current model. Therefore this paper focus on how to generate 30MW power using PTC technology. Here, the combination plant include PTC plant and turbine. In this thesis, its drawback is it does not include the controlling system of the steam temperature produce by parabolic trough collector to supply fixed steam temperature for given turbine.

Md Adulselam (2016) [9] has discussed on the title of automatic control of the 30 MWe SEGS parabolic trough plant. For the 30 MWe SEGS PTC plant, maintain a specified set point of the collector outlet temperature is the main task by adjusting the volume flow rate of the heat transfer fluid circulating through the collectors. The PTC outlet temperature is mainly affected by changes in the sun intensity, by the collector inlet temperature and the volume flow rate of the heat transfer fluid. For development of next generation SEGS plants and to obtain a control algorithm that approximates an operator's behavior, a linear model predictive controller is developed for use in a plant mode. In this thesis focus only on volume flow rate of the system to control the collector outlet temperature, not include mass flow rate of the system.

CHAPTER 3

MODEL OF PARABOLIC TROUGH COLLECTORS

3.1 Introduction

Among utility-scale solar thermal plants, parabolic trough technology is the most common. This method concentrates sunlight onto an absorber tube by lining up parabolic reflectors in long rows (receiver). This sort of concentrating collector has a lot of potential and can deliver output fluid temperatures of up to 550 ℃ (823K). To ensure that the sun is continuously focused on the receiver, the mirrors use a single-axis Tracker, which necessitates a rather flat land. Figure 3.1 illustrates a simple schematic. The solar field in this technology is made up of parabolic-shaped glass mirrors that reflect direct normal radiation. The entire structure is made of lightweight metal and is usually equipped with a single axis tracking system. As a result, PTC is a solar energy conversion technique that is utilized to generate heat. Solar energy strikes the reflector and is reflected back to the receiver, which contains a fluid that can be used for a variety of purposes. PTC is employed in a thermal and power generation application in an industrial setting. It includes a primary component, the reflector, which has a significant impact on PTC performance. The heat transfer fluid is convered in glas (HTF) through the absorber pipe, which is covered in glass (HTF). The pumped heat transfer fluid (HTF) collects solar energy and raises its temperature before returning to the hot side header pipes. The parabolic heat collecting element (HEC) is made up of the following components:

- Glass envelope.
- Absorber.
- Heat transfer fluid (HTF)
- Partial vacuum between envelope and absorber.

Long (10-100meter) parabolic cross section mirrors focus light to a glass encased vacuum absorber tube situated at the focal point of the parabola in parabolic trough collectors (PTC). A selective absorbent coating on the absorber tube maximizes solar energy absorption (high absorbance for short wavelengths) while minimizing near-infrared losses (low emittance for near infrared region).

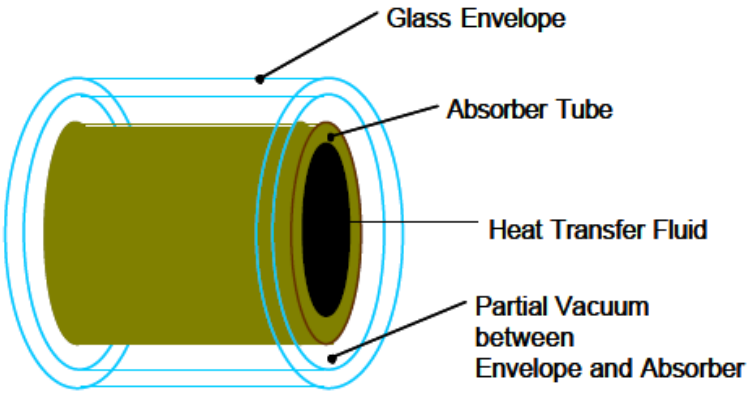

Figure 3.1: Heat collection element [32]

The glass envelope creates a vacuum between the absorber tube and the glass tube, reducing convective and conductive losses from the absorber tube to the air. Furthermore, the outer glass tube transmits solar light but is opaque to the near-infrared radiation emitted primarily by the absorber tube, which aids in keeping heat in the glass annulus. Due to the difficulties in maintaining the vacuum over long periods of time, an evacuated glass envelop may not be a cost-effective solution for low temperature systems (below 25℃). The HTF that passes through the absorber tube is heated by concentrated solar energy and piped to a heat exchanger, where it can be transported to a power block for electricity generation or stored for later use. While most commercial PTCs use thermal oil as the HTF and use a heat exchanger to connect to the load, direct steam generation (DSG) systems are being developed in which water is used as the HTF in the PTC and this water is sent directly to the load in the form of steam, eliminating the need for the heat exchanger. The parabolic collector is a closed box made up of the following components. There are flexible metallic hoses, between the solar collector area (SCA) themselves and between the collector loops and the headers. The heat transfer between the different parts of the HCE is shown in figure 3 .1.

- The suns energy, reflected by the mirrors, falls on the absorber after passing through the glass envelope.
- This absorbed solar energy is not fully transmitted to the HTF.
- There are heat losses from the absorber to the glass envelope.
- The glass envelope in turn is losing heat to the environment.

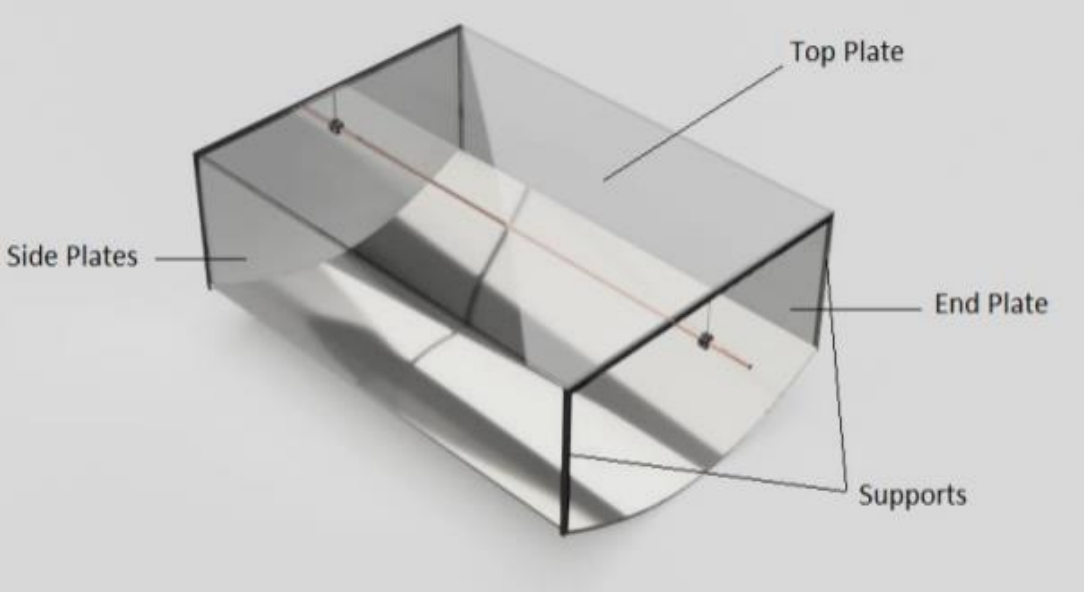

Figure 3.2: Parts of parabolic collector [21]

These energy considerations lead to the development of the collector model. Differential equations for the temperatures of the HCE, the absorber and the glass envelope are established. The differential equations are coupled through relations for the heat transfer between the different parts of the HCE.

- Heat transfer between the absorber and the HTF.
- Between the absorber and the envelope, and
- Between the envelope and the environment is considered.

Finally, the estimation of the absorbed solar energy from the direct normal solar radiation after optical losses is discussed.

3.2 General description of selected site for PTC

There are several locations in Ethiopia that have a lot of solar potential. One of these areas is the Oromia region. Those who live in this region are split into zones. Buno Bedele is one of them; it is made up of a variety of land topologies, the most of which are flat. In this thesis Bedele city has been chosen from this list of zones. The Bedele beer factory is located in this area, and several factors were considered while choosing this location.

- **Land:** assessment must be considered when determining the best location for collector solar power (CSP) installation. Some of the criteria that will be applied are optional. Flat lands is selective for CSP plant locations.
- **Geomorphologic features:** for CSP project flat land is requirement. The feature of the land of Bedele is flat and suitable for CSP installation considering plan surface of this area.
- **Technical potential:** a site is considered to have a technical potential for a CSP plant when the yearly average direct irradiation is 1750kWh/m2/year and above. Taking into consideration economic factors, CSP starts to become feasible with a higher irradiation and the selected site yearly average direct irradiation qualifies a suitable value for operating a CSP plant.
- Data for specific location of the research is Bedele, Ethiopia. Elevation 2007m, latitude 8.456 degree, longitude 36.355 degree.

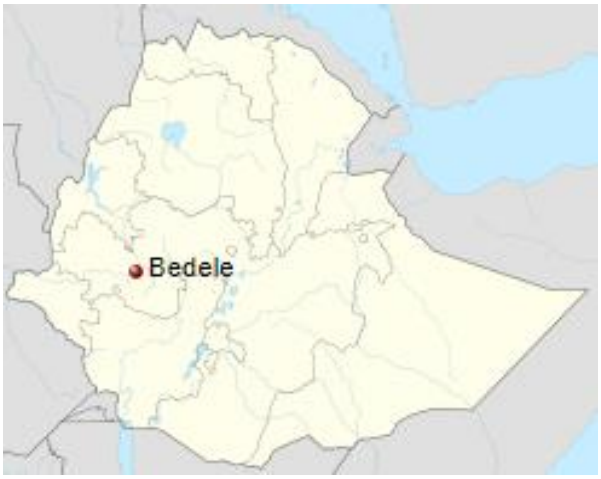

Figure 3.3: Location of Bedele from Ethiopia map [37]

3.3 Parameter consider to design the PTC

To model of parabolic trough collector consider the following three points:

- Estimating the solar radiation that reaches the collector.
- The Optical analysis used to determine the optical efficiency of the PTC which is the ratio of the amount of energy arriving to the absorber tube to the reflector.

- The thermal analysis used to predict thermal efficiency of PTC which the ratio of energy absorbed by the heat transfer fluid (HTF) to the reflector.

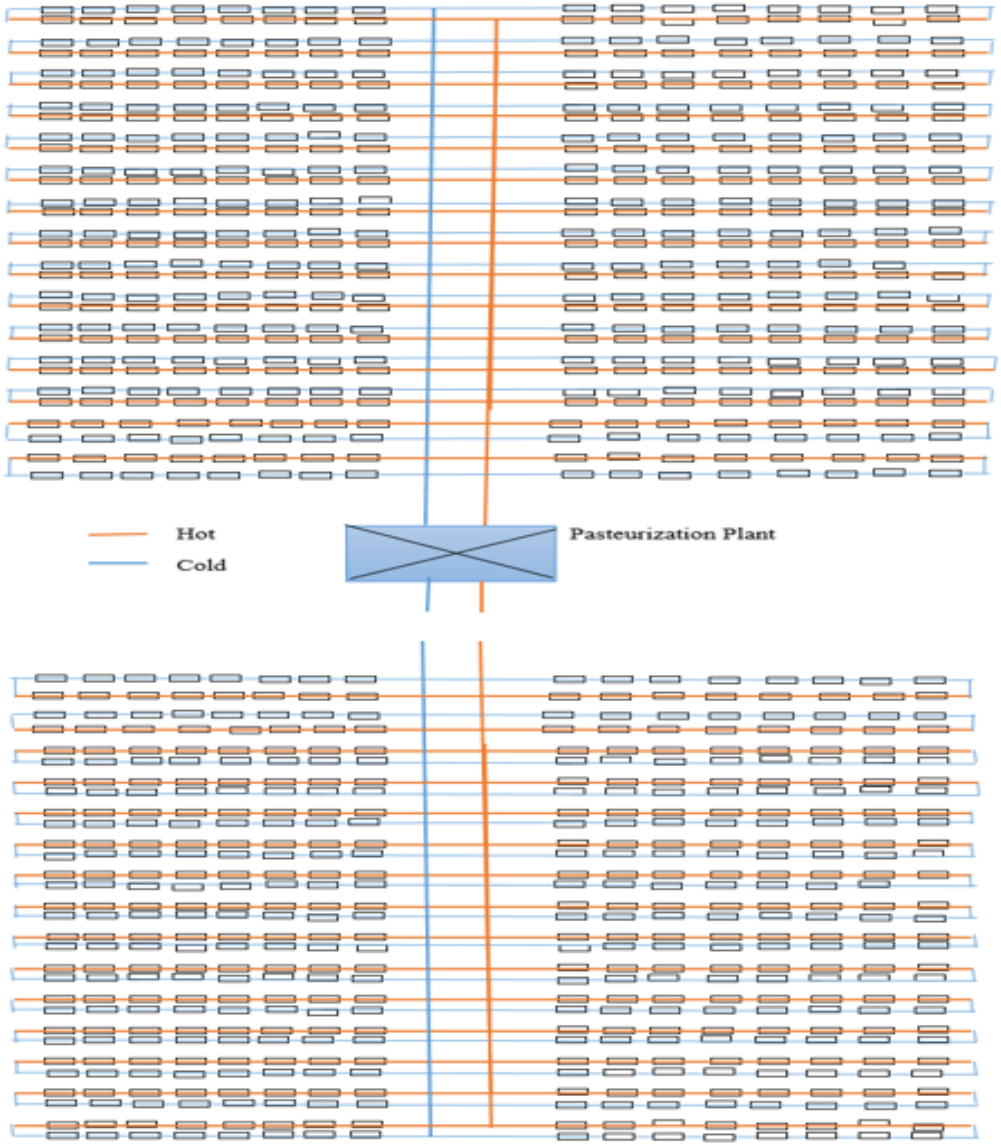

Figure 3.4: Layout of PTC Plant Model

The solar trough collector field can be divided into four quadrants. Each quadrants with 15 solar trough collectors each and for a total of 60 solar trough collectors. One of these 60 collectors is formed by a loop of 16 solar collector assemblies (SCA).

The overall efficiency of a parabolic trough collector is a function of both the fraction of direct normal radiation absorbed by the receiver (the optical efficiency) and the heat lost to the environment when the receiver is at operating temperature. The outputs of solar collector merge in central header, which connected to the pasteurization plant. Here, in pasteurization plant insert hot heat transfer fluid is used to heat working fluid that is steam. After transferring heat energy to given pasteurization plant then cold heat transfer fluid leaves this pasteurization plant and feeds the parabolic trough collectors (PTC) field through condenser. A loop of 16 solar collector assemblies (SCA) forms one of the 60 solar collectors. Cold heat transfer fluid flows through this collector on one side and is heated by absorbed solar energy before leaving the collectors on the other side. The solar collector's outputs are combined in a central header, which is connected to the power plant. In this case, a hot heat transfer fluid is used to heat a working fluid, which is steam, in a power plant. After transmitting heat energy to a given power plant, cold heat transfer fluid exits the power plant and feeds the field collectors.

The design layout of the parabolic trough collectors (PTC) is shown in figure 3.4. General speaking, consider different parameter to design parabolic trough collector (PTC) such as collector mirror width, envelope heat capacity, absorber heat capacity, density of envelope, density of absorber, energy absorber, Cross sectional area of glass of envelope and Energy absorb by heat transfer (HTF). There are two sorts of inputs used to construct the suggested model in MATLAB software: input parameters and input variables. The input parameters are inputs that do not change over time and have constant values.

Input parameters: are inputs that do not change over time and have constant values. Here, different input parameters are considered such as geometrical properties input, optical properties input and geographical coordinates input are exist.

- Inner and outer diameter of the absorber and the glass envelope.
- Aperture area of the PTSC.
- Longitude and latitude of the system location.

- All the optical specifications that do not depend on the temperature. Such as absorptivity, transmissivity and emissivity of the glass envelope and absorptivity, emissivity of the absorber.

Input variables: are input which vary with time, and these variables must be fed into the code in order to complete the simulation:

- Date and time.
- Inlet temperature and ambient temperature.
- Thermal properties of the working fluid.

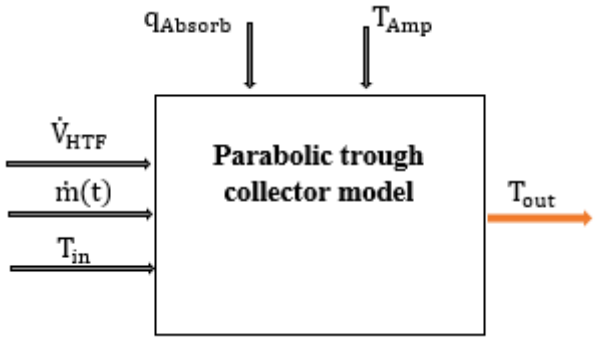

Figure 3.5: a solar field model as block with inputs and output

Additionally, Hydraulics Pipes connect all of the troughs, as well as pressure and temperature gauges, make up this hydraulic system. Stainless steel piping was chosen for this purpose. When working fluids run through it, the type of piping material utilized must not cause chemical reactions. The lowest temperature evaluated for solar collector applications is 390 kelvin. As a result, the piping material must be able to withstand temperatures more than 390 kelvin without failing. Because parabolic trough collectors are permanently located outside and exposed to the ambient temperature this piping material must resist corrosion induced by the elements. In other case, a thermocouple is an electrical device used for measuring temperatures. It consists of two dissimilar conductors. Once the junction is heated or cooled by attaching it to the place where the temperature needs to be measured, a voltage is created which will be transformed to a temperature using a thermocouple reader. A pump is required to circulate heat transfer fluid (HTF) from the storage to the system in order to conduct tests.

3.4 Mathematical model of PTC

3.4.1 Partial differential equations for temperature

To model solar collector first start from concept of energy balance for heat transfer fluid that leads to partial differential equation for the HTF temperature. Let the distance along the collector is indicated by k. The equation for the heat transfer fluid heat change over time t on an element of length k at position k is [9]:

$$\frac{\partial(\Delta\, Q_{HTF}(k,t))}{\partial t} == Q_{HTF}(k, t) - Q_{HTF}(k+ \Delta k, t) + q_{gained}(k, t)\, \Delta k \qquad (3.1)$$

From thermodynamics, it follows that [9]:

$$\Delta\, Q_{HTF}(k, t) = \rho_{HTF} c_{HTF}\, A_{ABS\,i}\ \Delta k T_{HTF}\,(k, t) \qquad (3.2)$$

With ρ_{HTF} is density of HTF, c_{HTF} is specific heat of HTF and T_{HTF} is temperature of HTF, where the first two depend on the latter. The cross-sectional area of the inside tube of the absorber is $A_{ABS\,i}$:

$$\dot{Q}_{HTF}(k, t) = \rho_{HTF} c_{HTF} \frac{V_{HTF}(t)}{n_{collectors}} T_{HTF}(k, t) \qquad (3.3)$$

Notice the overall HTF volume flow rate (V_{HTF}), is depends only on the time t since the fluid is considered to be incompressible. $n_{collectors}$, is number of collector. From Appendix 1 it is known that $n_{collectors}$= 60. After inserting equation (3.2) and (3.3) into equation (3.1), it follows that:

$$\rho_{HTF} c_{HTF}\, A_{ABS\,i}\, \Delta k \frac{\partial T_{HTF}(k,t)}{\partial t} = \rho_{HTF}\, c_{HTF} \frac{V_{HTF\,(t)}}{n_{Collectors}} T_{HTF}(k, t) - \rho_{HTF}\, c_{HTF} \frac{V_{HTF\,(t)}}{n_{Collectors}} T_{HTF}(k + \Delta k, t) + q_{gained}(k, t)\, \Delta k. \qquad (3.4)$$

From the definition of the derivative it follows:

$$\frac{\partial T_{HTF}(k,t)}{\partial t} = \lim_{\Delta k \to 0} \frac{T_{HTF}(k,t) - T_{HTF}(k+\Delta k,t)}{\Delta k} \qquad (3.5)$$

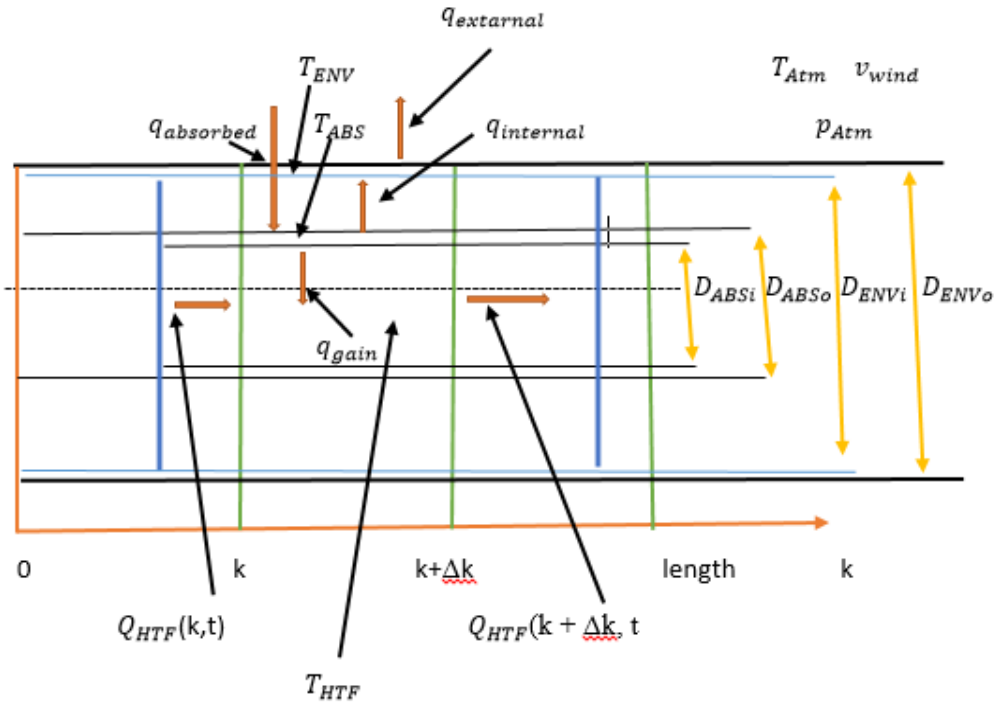

Figure 3.6: Schemata of heat collector element (HCE)

Dividing equation (3.4) by Δk, letting Δk →0 and considering equation (3.5), yields the following partial differential equation for the HTF temperature:

$$\rho_{HTF} c_{HTF} A_{ABS\,i} \frac{\partial T_{HTF}(k,t)}{\partial t} = - \rho_{HTF}\, c_{HTF} \frac{V_{HTF\,(t)}}{n_{Collectors}} \frac{\partial T_{HTF}(k,t)}{\partial t} + q_{gained}(k, t) \quad (3.6)$$

Where, $T_{HTF}(0, t) = T_{HTF,inlet}(t)$ is boundary condition and $T_{HTF}(k, 0) = T_{HTF,init}(k)$ is initial condition for equation (3.6). $T_{HTFinlet}$ = HTF collector field inlet temperature. In analogy to equation (3.1), the differential equation for the absorber temperature, T_{ABS} , is obtained:

$$\frac{\partial(\Delta Q_{HTF}(k,t))}{\partial t} = (q_{absorbed}(t) - q_{internal}(k, t) - q_{gained}(k, t))\, \Delta k \quad (3.7)$$

Here, $q_{internal}$ is the heat transfer per length between the absorber and the glass envelope. The absorbed solar energy is $q_{internal}$. From thermodynamics it is known that

$$\Delta Q_{HTF}(k, t) = \rho_{ABS} c_{ABS} A_{ABS}\, \Delta k\, T_{ABS}(k, t) \quad (3.8)$$

With ρ_{ABS}= absorber density, c_{ABS}, is Absorber specific heat, A_{ABS} is Cross sectional area of the absorber and T_{ABS} is Absorber temperature. Then substituting equation (3.8) into equation (3.7) yields after a division by Δk:

$$\rho_{ABS} c_{ABS} A_{ABS} \frac{\partial T_{ABS}(k,t)}{\partial t} = q_{absorbed}(t) - q_{internal}(k, t) - q_{gained}(k, t) \quad (3.9)$$

Where, $T_{ABS}(k, 0) = T_{ABS,init}(k)$ is initial condition for equation for (3.9).

The glass envelope is assumed to have no radial temperature gradient. The differential equation for the envelope temperature is gained through considerations similar to those used to obtain the absorber temperature (3.9).

$$\rho_{ENV}\ c_{ENV}\ A_{ENV}\ \frac{\partial T_{Env}(k,t)}{\partial t} = q_{internal}\ (k, t) - q_{external}\ (k, t) \quad (3.10)$$

Where, T_{ENV} (k,0) = $T_{ENVinit}$ (k) is the initial condition for equation (3.10). Here, ρ_{ENV} is Envelope density, C_{ENV} is Envelope specific heat and T_{ENV} is Envelope temperature. The heat transfer per length between the envelope and the enviroment is $q_{external}$.

3.4.2 Heat transfer between the Absorber and the HTF

In Internal flow, the heat transfer (q_{gained}) is calculated through the dittus-boelter equation for fully developed turbulent flow in smooth circular tube [28]. Here, the local Nusseit number ($NU_{D_{ABS\,i}}$) is given by:

$$NU_{D_{ABS\,i}} = 0.023 Re^{4/5}_{D_{ABS\,i}} Pr^{n}_{HTF} \quad (3.11)$$

Where n=0.4 for heating ($T_{ABS} > T_{HTF}$) and 0.3 for cooling ($T_{ABS} < T_{HTF}$).

With $Re_{D_{ABS,i}}$ is Reynolds number for flow in circular tube, is given by:

$$Re_{D_{ABS,\ i}} = \frac{4\rho_{HTF} V_{HTF}}{\pi D_{ABS,i}\ \mu_{HTF}\ n_{Collectors}} \quad (3.12)$$

Where, Pr_{HTF} (Prandtl number) = V_{HTF}/α_{HTF}, V_{HTF} (kinematic viscosity of the HTF) = μ_{HTF}/ρ_{HTF}, α_{HTF} (Thermal diffusivity of the HTF) = $K_{HTF}/\rho_{HTF}C_{HTF}$ and μ_{HTF} is Viscosity of the HTF. Calculated heat transfer Coefficient ($h_{ABS,HTF}$) by using the local Nusselt number ($Nu_{D_{ABS,i}}$) and thermal conductivity of the HTF (K_{HTF}) as follow equation (3.13).

$$h_{ABS,HTF} = \frac{Nu_{D_{ABSi}} K_{HTF}}{D_{ABS,i}} \quad (3.13)$$

Where $D_{ABS,i}$=0.058m (Inside diameter of the absorber tube) and the HTF properties:C_{HFT}, K_{HFT}, μ_{HFT} and ρ_{HFT} are functions of the HTF temperature (T_{HFT}).

Generally, calculate, q_{gained} (heat transfer between the absorber and the HTF) is:-

$$q_{gained} = h_{ABS,HTF} A_{ABS\ surf,i} (T_{ABS} - T_{HTF}) \quad (3.14)$$

With the inner surface area per length of the absorber ($A_{ABS,surf,i}$):

$$A_{ABS,surf,i} = \pi D_{ABS,i} \quad (3.15)$$

3.4.3 Heat transfer between the Absorber and the Glass Envelope

Consider both conventional and radiation calculate heat transfer between absorber and glass envelope ($q_{internal}$) is [9]:

$$q_{internal} = q_{internalconvection} + q_{internalradiation} \quad (3.16)$$

Since the absorber is usually hooter than the glass envelope ($T_{ABS} > T_{ENV}$), the air ascends along the absorber and descends along the glass envelope. The convection heat transfer ($q_{internalconvection}$) may be expressed as:

$$q_{internalconvection} = \frac{2\pi K_{eff,Air}}{\ln(\frac{D_{ENV,i}}{D_{ABS,o}})} (T_{ABS} - T_{ENV}) \quad (3.17)$$

Where $D_{ENV,i} = 0.112m$ (Inside diameter of the glass envelope) and $D_{ABS,o}$ =0.07m (outside diameter of the absorber). The effective thermal conductivity ($K_{eff,Air}$) is the thermal conductivity that the stationary air should have to transfer the same amount of heat as moving air. A suggested correlation for $K_{eff,Air}$ is:

$$\frac{K_{eff,Air,}}{K_{Air,}} = 0.386(\frac{Pr_{Air}}{0.861+Pr_{Air}})^{1/4}(Ra_c)^{1/4} \quad (3.18)$$

Where

$$Ra_c = \frac{[\ln(D_{ENV,i}/D_{ABS,o})]^4}{L^3(D_{ABS,o}^{-3/5}+D_{ENV,i}^{-3/5})^5} Ra_L \quad (3.19)$$

In equation (3.18), Pr_{Air} is the prandtl number of air in the annulus. The thermal conductivity of air is k_{Air}. From equation (3.19), L= the effective length and is given for the annulus through:

$$L= 0.5(D_{ENv,i} - D_{ABS,o}) \quad (3.20)$$

Where Ra_L = Rayleigh number of air, and defined as

$$Ra_L = \frac{g ß_{Air}(T_{ABS}-T_{ENV})L^3}{\alpha_{Air} V_{Air}} \quad (3.21)$$

Where, g =9.81ms^{-2} (gravitational acceleration), $ß_{Air}$ (volumetric thermal expansion coefficient of air), α_{Air} (thermal diffusivity of air) =K_{Air}/ ($\rho_{Air} C_{p,Air}$) , ρ_{Air} (density of air in the annulus), $C_{p,Air}$ (specific heat of air), μ_{Air} (viscosity of air) and V_{Air} (kinematic viscosity) =μ_{Air}/ρ_{Air}.

The properties of air in the Annulus: α_{Air},$ß_{Air}$,$C_{p,Air}$, K_{Air},μ_{Air},V_{Air}, Pr_{Air} and ρ_{Air} are dependent on the mean temperature in the annulus ($T_{Annulus}$).

$$T_{Annulus} = 0.5(T_{ABS} + T_{ENV}) \quad (3.22)$$

In addition,the density ρ_{Air} depends on the evacuation pressure in the annulus, $P_{evac.}$ A value of $P_{evac.}$ =7kPa is used in the model. This value was chosen such that the calculated collector outlet temperature fits the measured collector outlet temperature best.

The heat transfer through radiation between long, concentric cylinders, $q_{internalradiation,}$ may be expressed as [9]:-

$$q_{internalradiation} = \frac{\sigma A_{ABS\ surf,o}(T_{ABS}^4 - T_{ENV}^4)}{\frac{1}{\varepsilon_{ABS}} + \frac{1-\varepsilon_{ENV}}{\varepsilon_{ENV}}\left(\frac{D_{ABS,o}}{D_{ENV,i}}\right)} \quad (3.23)$$

In equation (3.23), σ (Stefan-Boltzmann constant) = 5.670* 10^{-8} W/m^2. K^4

The outer surface area per length of the absorber,$A_{ABS,surf,o}$, is given by:-

$$A_{ABS,surf,o} = \pi D_{ABS,o} \quad (3.24)$$

Where, ε_{ABS} (emissivity of the absorber) and ε_{ENV}= 0.9 (emissivity of the glass envelope) as measured by SANDIA. The emissivity of the absorber (ε_{ABS}) increases with the absorber temperature (T_{ABS}). SANDIA provides a linear function for ε_{ABS} from their measurement:

$$\varepsilon_{ABS} = 0.000327[\ T_{ABS} - 0.065971] \quad (3.25)$$

If $\varepsilon_{ABS} < 0.05$ then the value is set to $\varepsilon_{ABS} = 0.05$.

3.4.4 Heat Transfer between Glass Envelope and Environment

The heat transfer between the envelope and the environment is assumed to be due to convection and radiation:

$$q_{external} = q_{externalconvection} + q_{externalradiation} \quad (3.26)$$

The heat transfer due to convection ($q_{externalconvection}$) is estimated through a correlation suggested for a circular cylinder in cross flow [28].

Considering overall average conditions, the calculation starts by using following correlation for the Nusselt number ($\overline{NU}_{D_{ENV,o}}$):

$$\overline{NU}_{D_{ENV,o}} = 0.3 + \frac{0.62 Re_{D_{ENV,o}}^{1/2} pr_{Air,amb}^{1/3}}{[1+(0.4/pr_{air,amb})^{\frac{2}{3}}]^{1/4}} \left[1 + \left(\frac{Re_{D_{ENV,o}}}{285000}\right)^{5/8}\right]^{4/5} \quad (3.27)$$

For the circular glass envelope cylinder, the Reynolds number ($Re_{D_{ENV,o}}$) is defined as:

$$Re_{D_{ENV,o}} = \frac{\rho_{Air,amb} V_{wind} D_{ENV,o}}{\mu_{Air,amb}} \quad (3.28)$$

Were $\rho_{Air,amb}$ is the density of the ambient air, $D_{ENV,o}$ is the outside diameter of the glass envelope ($D_{ENV,o}$ = 0.094m), $\mu_{Air,amb}$ is the viscosity of the ambient air and the prandtl number of the ambient air ($pr_{Air,amb}$). Then calculate heat transfer coefficient ($\bar{h}_{ENV,Enviroment,}$) as follow:

$$\bar{h}_{ENV,Enviroment,} = \frac{\overline{NU}_{D_{ENV,o}} K_{Air,amb}}{D_{ENV,o}} \quad (3.29)$$

The thermal conductivity of the ambient air, $K_{Air,amb}$ and the other properties of the air,$\mu_{Air,amb}$, $Pr_{Air,amb}$ and $\rho_{Air,amb}$ are dependent on the mean ambient temperature:

$$\overline{T}_{amb} = 0.5\ (T_{ENV} + T_{amb}) \quad (3.30)$$

Where, T_{amb} is the ambient temperature of the environment. In addition, $\rho_{Air,amb}$ depends on the atmospheric pressure (p_{atm}). Finally, the heat transfer to the environment due to convection is:-

$$q_{externalconvection} = \bar{h}_{ENV,Enviroment} A_{ENV\ surf,o}\ (T_{ENV} - T_{amb}) \quad (3.31)$$

With the outer surface area per length of the glass envelope ($A_{ENV\ surf,o}$) calculated through

$$A_{ENV\ surf,o} = \pi D_{ENV,o} \quad (3.32)$$

The heat transfer to the enviroment due to radiation, $q_{externalradiation}$ may be expressed as [9].

$$q_{externalradiation} = \varepsilon_{ENV} \sigma A_{ENV\ surf,o} (T_{ENV}^4 - T_{amb}^4) \quad (3.33)$$

With ε_{ENV} as the emissivity of the glass envelope. This relationship describes the radiation of a small convex object, the glass envelope, in a large cavity, the environment. The suns energy is the energy source that acts on the absorber and induces the heat transfer discussed above. It governs the amount of energy finally transferred to the HTF and thus to the pasteurization plant for pastures end product. Thus, it is necessary to estimate the amount of absorbed solar energy ($q_{absorbed}$).

3.4.5. Solar Radiation

The sun is a fully gaseous entity with a complicated physical structure. When solar radiation enters the earths atmosphere, a part of the incident energy is removed by scattering in the atmosphere due to interaction of the radiation with air molecules. Water (vapor) and dust. Another part of the incident energy is removed in the earths atmosphere by absorption of radiation in the solar energy spectrum due to ozone in the ultraviolet and to water vapor and carbon dioxide in bands in the infrared. The scattered radiation is called diffuse radiation. A portion of this diffuse radiation goesback to space and a portion reaches the ground.

The remaining part of the solar radiation that enters the earths atmosphere, the radiation arriving on the ground directly in line from the solar disk without having been scattered by the atmosphere or having been absorbed is called beam radiation. Beam radition incident on a plane normal to the radiation is called the direct normal radiation.The total solar radiation or global radiation, that is

the sum of the diffuse and beam solar radiation on a surface is important for the design of flat plate collectors or for the calculations of heating and cooling loads in architecture. For concentrating systems like the solar trough collector field only the beam radiation or direct normal radiation is used [28].

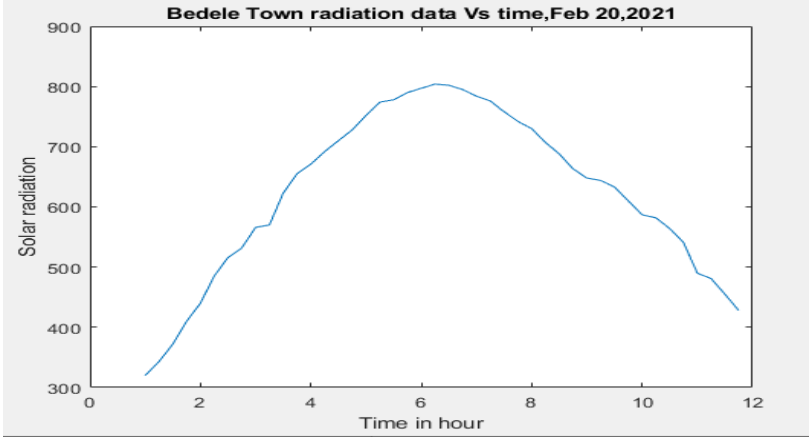

(a)

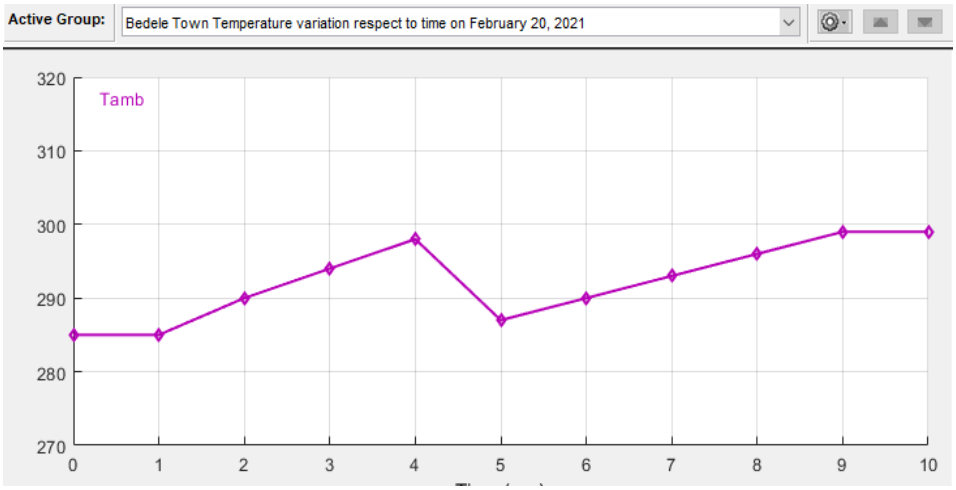

(b)

Figure 3.7: (a) Variation of module solar radiation, (b) Variation of ambient temperature for Bedele town on February 20, 2021.

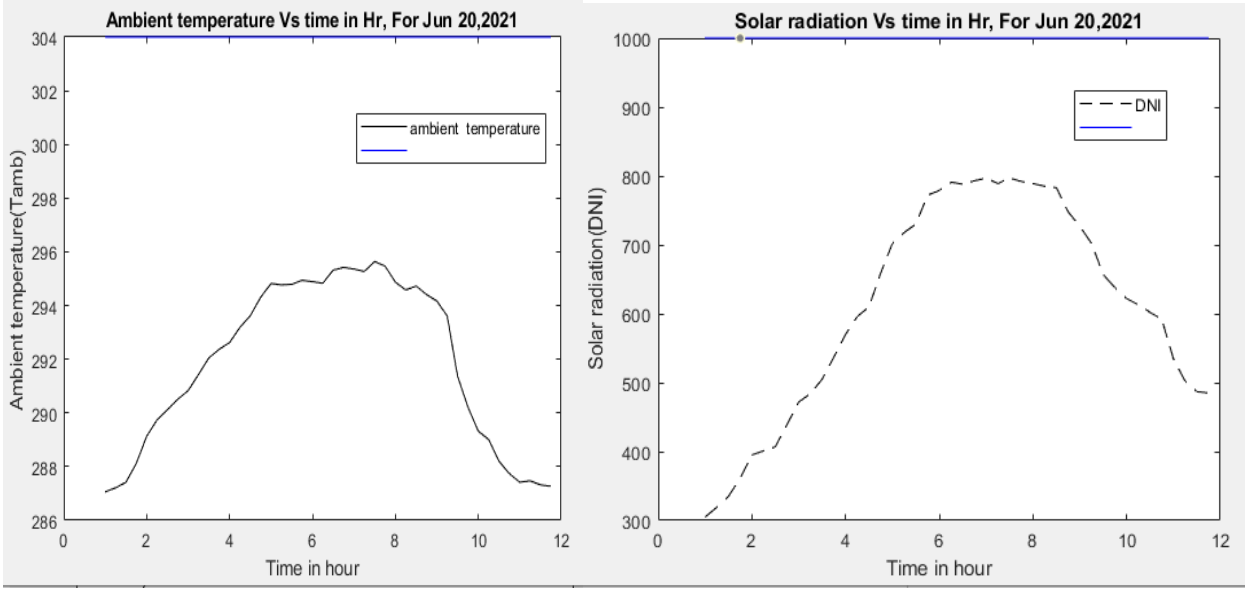

(a) (b)

Figure 3.8: (a) variation of module solar radiation, (b) variation of ambient temperature for Bedele town on June 20, 2021.

The direct normal radiation (DNI) can be measured by using a normal incidence pyrhelionmeter (NIP). The NIP is an instrument for measuring solar radiation from the sun and from a small portion of the sky around the sun at normal incidence. Notice the direct normal radiation is not constant between sunrise and sunset because the effects of the atmosphere in scattering and absorbing radiation are variable with time as atmospheric conditions and air mass change. In order to maximize the energy from the solar beam radiation through the concentrating trough collectors, the surface normal of a collector has to be collinear to the vector of the incoming solar beam radiation. The angle of incidence, is the angle between the beam radiation on a surface and the normal to that surface. Consequently, during a day the vector of the incoming solar beam radiation changes its direction as well. To minimize the angle of incidence, the solar collerctors must track the sun by moving in prescribed ways. The best way to track the sun is by rotating the collectors surface about two axis. The solar collector troughs for this case are tracking the sun by rotating around a single axis, which is the horizontal north-south axis. Due to this costraint movability, only the component of the solar beam radiation vector, which is collinear to the normal of the single axis tracking collector surface, remains to heat the absorber.

This component of the solar beam radiation vector may be found by multiplying the amount of solar beam radiation with the cosine of the angle of incidence. Therefore a relationship for the angle of incidence is needed [28].

3.4.6 Earth-Sun geometric relationship

The annual amount of solar radiation received by the earth varies due to the changeable distance between the earth and the sun as shown in figure 3.9. The earth-sun distance has a minimum values of 1.47 (10^{11}) m which is called, perihelion, on December 21 and a maximum value of 1.512 *10^{11} m which is called, aphelion, on june21. The average distance between the earth and the sun that is called astronomical unit (AU) is 1.419 (10^{11}) m. The earth revolves around itself within an axis that has tilted angle of 23.45^{o} with respect to its orbital plane axis. This angle is the cause of the changeable solar radiation throughout the year [31].

To calculate the solar radiation first understand varies earth to sun angles, those are:

- Hour angle (**ω**) and Latitude angle (ϕ)
- Solar declination (δ) and Zenith angle (θ_z)
- Solar altitude (α) and Solar azimuth angle (γ_{sun})
- Angle of incidence (Θ)

Let express those angle detail:

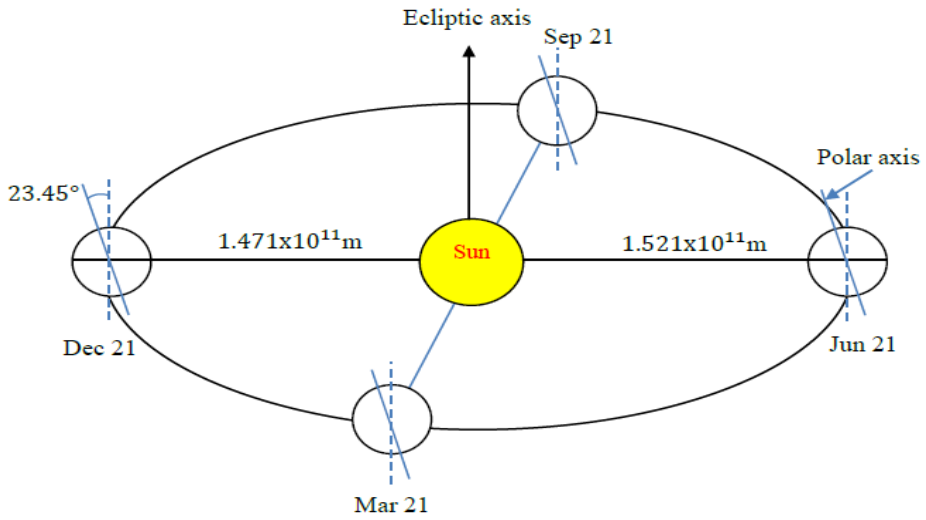

Figure 3.9: Motion of the earth around the sun [31]

- **Hour angle (ω)**: is the hour angle can be known as the angle through which the earth has to resolve to get the meridian of any point straight under the sun [32]. Hour angle varies throughout the day as shown in figure 3.10 for any place, at sunrise the hour angle has maximum negative values of -180^o, then it slowly increase 15^oper hour, while the sun is rising until it reaches zero at noon. For the period from afternoon to sunset, hour angle increases from zero to the maximum positive value which is $+180^o$[33]. The hour angle (ω) can be calculated using the following equation [32]. Solar local time (ST) is not the same as the standard time. Therefore, it is important to convert the local clock time to solar time. For this thesis plant located at Bedele town at local longitude (L_{loc}) of 36.1^o E. local clock time is measured with respect to the standard longitude (L_{st}) of 36.84^o E for the standard time. The conversion depends on the longitude, local standard meridian and day of the year. Sun takes 4 minute to transverse 1^o of longitude. It given using the following equation. [28].

$$\omega = 15(ST - 12) \quad (3.34)$$

$$\text{Solar time} = \text{Standard time} + 4(L_{st} - L_{loc}) + E \quad (3.35)$$

Where L_{st} = Stands for the standard meridian of local zone time (36.84^o E)

L_{loc} = Represent longitude of the location (36.2^o E)

The term E called the equation of the time (in minutes) and it can be determined applying the following equation [28].

$$E= 229.2(0.000075 +0.001868\cos B – 0.032077 \sin B - 0.014615\cos 2B - 0.04089\sin 2B) \quad (3.36)$$

Where B measured in degrees can be calculated using the next equation [28].

$$B= (n- 1)\frac{360}{365} \quad (3.37)$$

Where n represents the day of the year ($1 \leq n \leq 365$).

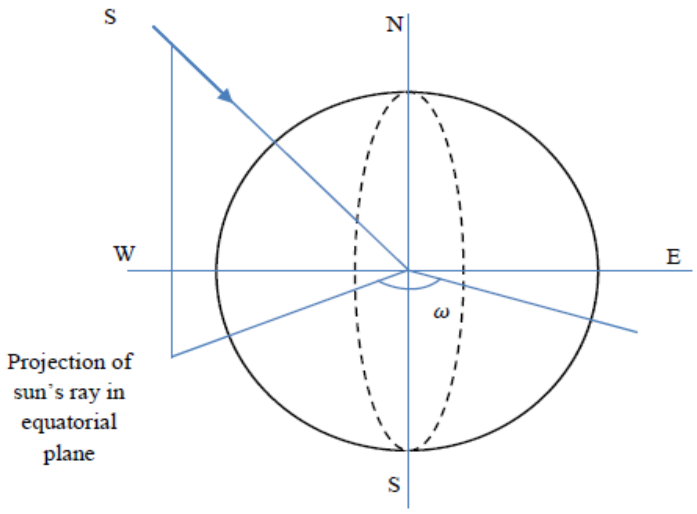

Figure 3.10: Hour angle (ω) [34]

- **Latitude angle (ϕ):** is assume that there is a point P at a location on the earth by drawing a radial line connecting the earth center with the projection of this radial line on the equatorial plane, an angle is derived, and it is known as the latitude angle (ϕ) [33] as shown in figure 3.11. It varies between +90 and -90 (18^o for this thesis selected area, Bedele).

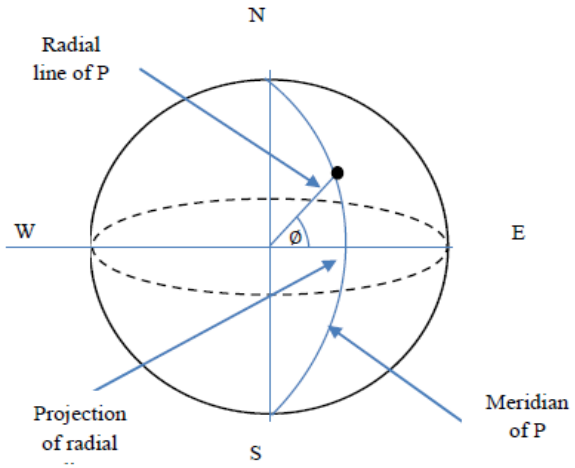

Figure 3.11: Latitude angle (ϕ) [34]

- **Solar declination (δ):** is an angle between a line connecting the earth's and the sun's centers and the projection of the line upon the equatorial plane of the earth [33]. The solar declination varies throughout the year because of the earth's revolving around its axis. It varies between values of $+23.45^o$ on June 21 and a value of -23.45^o on December 21[31].

Solar declination angle can be determine below equation [33].

$$\delta = 23.45\sin\left[\frac{360}{365}(284 + n)\right] \quad (3.38)$$

Where n = the day of the year ($1 \leq n \leq 360$).

- **Zenith angle (Θ_z):** let consider a point P on a surface of the earth, the direction PN is called zenith direction and the direction SP is known as sun's beam direction. The angle between the zenith direction (PN) and the ray of the sun direction (SP) is called as the zenith angle (Θ_z) at sunrise or sunset the zenith angle(Θ_z) is about 90^o however, at noon, the zenith angle become very close to 0^o [34].
- **Solar altitude (α):** is the angle between the horizontal direction S′P and the sun beam direction (SP). The summation of zenith angle and solar altitude is equal to 90^o[32].

$$\Theta_z + \alpha = 90^o \quad (3.39)$$

The solar altitude angle changes with the sun movement. At sunrise or sunset, the solar altitude angle is near to zero while at noon, it becomes near to90^o. Solar altitude angle can be determined using the following expression [32].

$$\text{Sin}(\alpha) = \sin(\phi)\sin(\delta) + \cos(\phi)\cos(\delta)\cos(\omega) \quad (3.40)$$

Solar altitude angle can be determined using the following expression [32].

- **Solar azimuth angle (γ_{sun}):** is the angle measured between the south direction and the sun ray as shown in figure 3.12. The expression used to estimate the solar azimuth angle is given by [32].

$$\text{Sin}(\gamma_{sun}) = \frac{\cos(\delta)\sin(\omega)}{\cos(\alpha)} \quad (3.41)$$

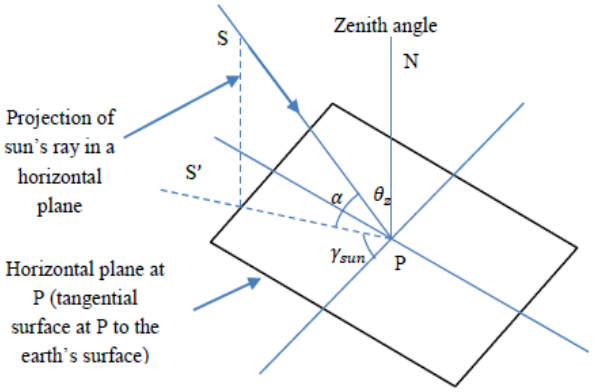

Figure 3.12: Zenith, solar altitude, and solar azimuth angles [34]

- **Angle of incidence (Ɵ):** according to duffie [28], the angle of incidence is defined as the angle between the sun rays hitting a surface and the normal to theat surface. The angle of incident varies throughout the day and the year and it greatly affects the solar energy gained by the receiver. In other words, the solar radiation is reduced by increase the cosine of this angle. For a plane tilted with an angle of β as shown in figure 3.13, the angle of incidence correlation is given by [28].

$$\cos\Theta = \sin\delta \sin\emptyset \cos ß - \sin\delta \cos\emptyset \sin ß \cos\gamma + \cos\delta \cos\emptyset \cos ß \cos\omega + \cos\delta \sin\emptyset \sin ß \cos\gamma \cos\omega + \cos\delta \sin ß \sin\gamma \sin\omega \quad (3.42)$$

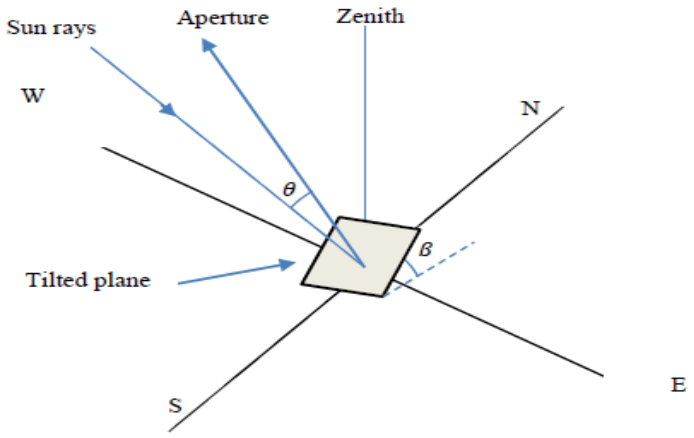

Figure 3.13: Angle of incidence (θ) [33]

In order to minimize the angle of incidence and then maximize the solar radiation, the solar collectors must move in prescribed ways to track the sun. There are two tracking systems for the collectors. First the collectors rotate about two axes which is considered the best way. The second system is that the collectors rotate about single axis, horizontal north-south and horizontal east-west, vertical or parallel to the earth axis.

3.5 Tracking and controlling

Parabolic troughs consist of a trough collector, reflectors, heat collection receivers and a drive or tracking system. There have been various tracking systems used around the world to extract energy from the sun, among this double and single axis solar tracking are well known. More of the time parabolic trough uses a single axis solar tracking.

For this thesis select single axis solar tracking. Like its name suggest, this type of tracking relies solely on one axis which means it has one degree of freedom only. Single axis tracking can be basically realized using a stepper motor and light dependent resistor (LDR) sensors. Their job is simple making sure that sun ray's make a right angle with the panels at all times. This simple tracking can increase energy production by up to 50 Percent [1]. Single axis solar tracking can classified as north-south and east- west tracking. It was shown that the east west placed solar tracker is more efficient than the north-south placement. Therefore for this thesis use east west single axis solar tracking as shown below figure 3.14.

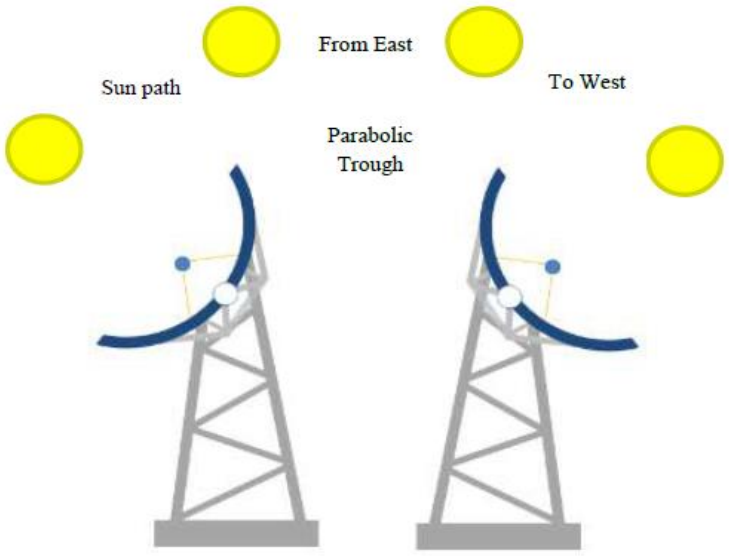

Figure 3.14: Horizontal east-west tracking system [9]

The tracker is navigated through a small motor/actuator related to the lengthy crucial power arm which rotates east to west. The tracking is according to the position of the sun and the requirement of the power block. Therefore a solar sensor is used to evaluate the sun position. Sensors consisting of a convex lens focus the sun light to a small photovoltaic cell, reaching a resolution of around 0.05 Percent. These kinds of sensors are used in the SEGS plants, where they prove most effective. The tracking system must have sufficient torque to operate the collectors even at higher wind speeds. In existing plants, the controlling of the field takes place in two separate stages. The overall control is located in the central control room and the second stage is placed on each collector unit. The local units take care of the incoming irradiation, wind speed and mass flow of heat transport medium.

CHAPTER 4
PASTREURIZATION PLANT MODEL

4.1 Introduction

Pasteurization is the process of heating product to a specific temperature for a predefined length of time. The purpose of this process is to kill bacteria by heating. After produce steam from parabolic trough collector move to designed pasteurization plant. In this chapter model the pasteurization plant as the following figure 4.1.

In this pasteurization plant steam use as working fluid. It consist feed water heating, superheating and reheating, then the working fluid leaves the condenser as a condensate and is pressurized by the condensate pump to a pressure sufficient to pass through the low-pressure feed water heaters. The water is heated up in the low-pressure feed water heaters (LPFH) through hot steam extractions withdrawn from the low-pressure pasteurization (LPP1). The water then enters the dearator where it is mixed with hot steam from the first extraction of the low-pressure pasteurization (LPP1). Through the mixing with steam, the efficient removal of non-condensable as well as the heating of the water occurs. Feed water pump after the dearator pumps the water to a higher pressure to allow the working fluid to pass through the following high-pressure feed water heaters and enter the heat exchanger trains. The water is further warmed up in the high-pressure feed water heater through steam extractions from the high-pressure pasteurization before entering the heat exchanger. Heat exchanger consist of a preheater (economizer), a boiler (steam generator) and a super heater. The water that was warmed up through feed water heating enters now the preheater, which is a counter flow heat exchanger, and is heated by heat exchange with the hot HTF. The working fluid that leaves the preheater enters the steam generator (boiler) and is essentially in the saturated liquid state. In the steam generator (boiler), the working fluid changes its state from liquid to vapor through the heat energy transmitted by the hot HTF. Leaving the steam generator, the saturated steam flows into the superheated. The superheated is also a counter flow heat exchanger and the steam is superheated through heat exchange with the hot HTF that is directly coming from the collector field. The steam generated from heat exchanger is expanded in a high pressure section of the pasteurization, after which it is entering the re heaters.

Here, the incoming steam is reheated to a temperature near that of the superheated steam before the expansion. The reheated steam now expands in the low-pressure section of the pasteurization to the condenser pressure. While the steam is expanding in the pasteurization, the end product of the factory pasteurize. Then completely expanded fluid is cooled down to saturated water by heat rejection to a cooling water in the condenser. The below plant model is pure solar mode means that nothing other than solar energy is used to heat the pasteurization plant working fluid.

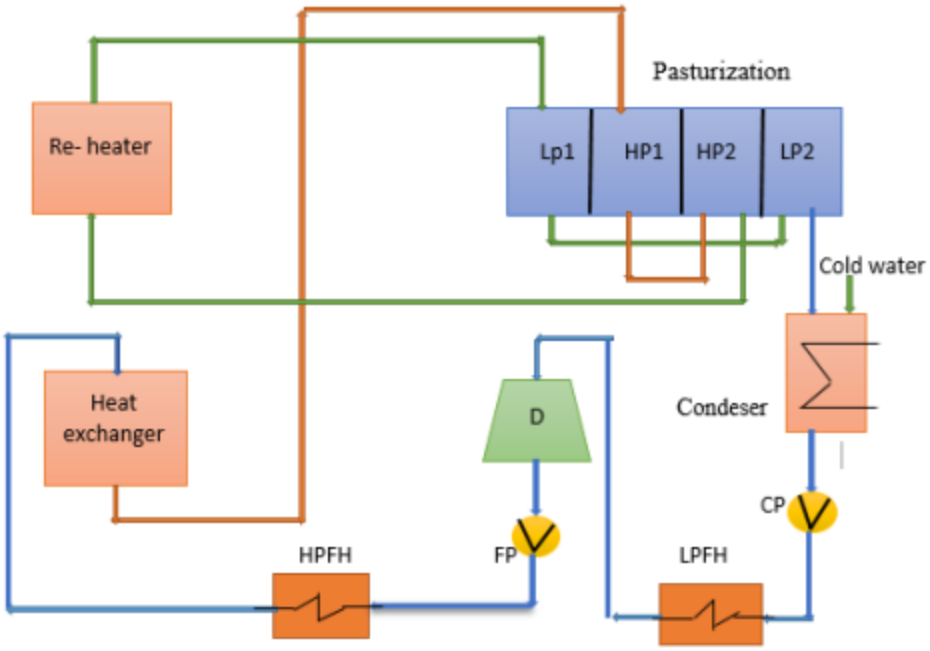

Figure 4.1: Pasteurization plant model

4.2 Model of pasteurization plant

Let explain the below block diagram of pasteurization plant with working principles:

I. **Condensate pump (CP):** for the case of condensate pump (CP), internal irreversibility is primarily the result of fluid friction occur. Engineering equation solver (EES) is a commercial software package used for solution of systems of simultaneous non-linear equations. Here, calculate the enthalpy and temperature at specific pressure according to Engineering Equation solver (EES).

The enthalpy,$h_{2,rev}$ gained, is calculated from fluid property functions as the enthalpy of water.

$$h_{2,rev} = f_h(\text{Water}, S = s_1, P = p_2) \quad (4.1)$$

Where, entropy s_1 is calculate using $s_1 = f_s$ (steam, H $= h_1$, P $= p_1$) and the pressure p_2 is calculated through equation (4.31). The EES inbuilt fluid property functions (Klein, 2001) are used for the calculation of $h_{2,rev}$ the enthalpy h_1 is known from equation (4.46). Then to calculate h_2 use isentropic efficiency of CP ($\eta_{is,CP}$) which shown below equation (4.2). Assume $\eta_{is,CP}$ (isentropic efficiency for CP) = 0.7125.

$$\eta_{is,CP} = \frac{h_{2,rev} - h_1}{h_2 - h_1} \quad (4.2)$$

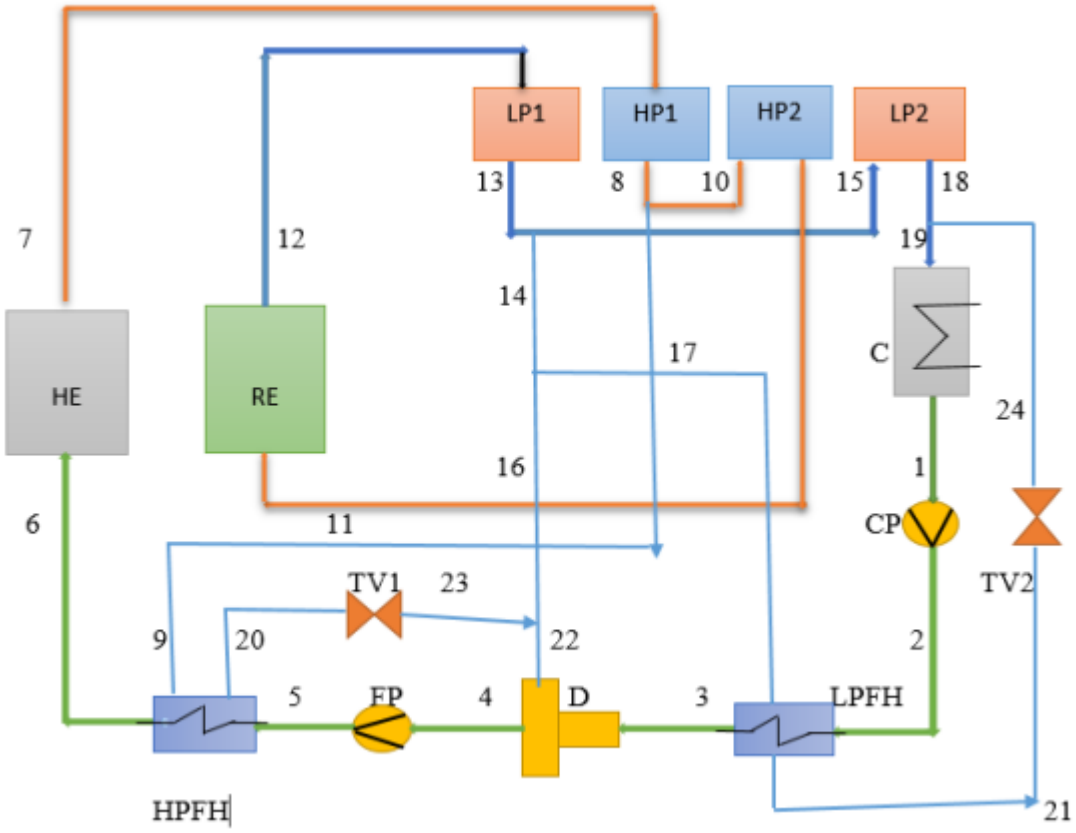

Figure 4.2: Internal diagram of pasteurization plant

Then the temperature T_2 and entropy s_2 are also calculated from EES fluid property functions with the enthalpy h_2 at the pressure p_2 using T_2 = f_T (water, H =h_2, P =p_2) and s_2= f_s (water, H =h_2, P =p_2).

II. **Feed water pump (FP):** feed water pump (FP), have the same calculations with condensate pump. Where the enthalpy h_4 is known from equation (4.34). Calculate $h_{5,rev}$ from fluid property functions as follow equation.

$$h_{5,rev} = f_T(\text{Water, S} = s_4, \text{P} = p_5) \quad (4.3)$$

With the entropy *S*4, using S_4 = f_S (steam, H = h4, P =p_4) and the pressure p_5, from equation (4.41). Then to calculate h_5 use isentropic efficiency of FP ($\eta_{is,FP}$) which shown below equation (4.4). Assume $\eta_{is,FP}$ (isentropic efficiency for FP) = 0.7125.

$$\eta_{is,FP} = \frac{h_{5,rev} - h_4}{h_5 - h_4} \quad (4.4)$$

Then the temperature T_5 and entropy S_5 are also calculated from EES fluid property functions with the enthalpy h_5 at the pressure P_5 using T_5 =f_T (water, H =h_5, P =P_5) and S_5 = f_s (water, H = h_5, P = P_5). A mass balance completes the model equations for FP is:

$$\dot{m}_4 - \dot{m}_5 = 0 \quad (4.5)$$

From above equation (4.5) calculate mass flow rate 4($\dot{m}_4$), since mass flow rate 5 ($\dot{m}_5$) is calculate from concept of ($\dot{m}_4 - \dot{m}_5 = 0$).

Measurements of the mass flow rates available in the heat exchanger in order to use these measured flow rates as possible inputs to the pasteurization plant model, the mass flow rates in all the different elements of the plant are calculated from $\dot{m}_6$ through mass balances for the devices following or preceding the heat exchanger. Thus $\dot{m}_2$ is determined from $\dot{m}_3$ through a mass balance for the low-pressure feed water heater (LPFH), equation (4.29), and $\dot{m}_1$ is calculated from $\dot{m}_{19}$ through the condenser model, using ($\dot{m}_{19} - \dot{m}_1 = 0$).

III. **High pressure pasteurization (HPP1 and HPP2):** in pasteurization consider the internal irreversibility.

For both, the high-pressure and low-pressure section of the pasteurization plant, exhaust is to the two-phase region. Hence the entropy increase in the pasteurization does not result in a temperature increase but in an increase in enthalpy. Taking the high-pressure section of the pasteurization, HTP 1, as an example, the ideal work through expansion, if the pasteurization section were adiabatic reversible, is *h*7 - $h_{8,rev}$ but the actual work is *h*7 - *h*8. The irreversible losses in the pasteurization are represented by an isentropic efficiency, i.e. for the high pressure section, $\eta is;HP\ T\ 1$*:* The enthalpy $h_{8,rev}$ is calculated from EES fluid property functions as the enthalpy of steam with the entropy *S*7 and the pressure *P*8.

$$h_{8,rev} = f_h\ (steam, S = s_7, P = P_8) \qquad (4.6)$$

Where the entropy S_7 is calculated from $S_7 = f_s$ (*steam; H* =h_7, *P* =P_7) and the pressure P_8 is determined from P_7 and a constant pressure ratio for HPP 1 ($R_{p,HPP1}$)

$$P_8 = P_7\ R_{p,HPP1} \qquad (4.7)$$

The pressure *P*7 in turn is known from equation (4.61). The enthalpy *h*7 is calculated using, *h*7 = *hsteam:HE*. Then to calculate *h*8 use isentropic efficiency of HPP1 ($\eta_{is,HPP1}$) which shown below equation 4.8. Assume $\eta_{is,HPP1}$ (isentropic efficiency for HPP1) = 0.84 and $R_{p,HPP1}$ (constant pressure ratio for HPP1) =0.45.

$$\eta_{is,HPP1} = \frac{h_7 - h_8}{h_7 - h_{8,rev}} \qquad (4.8)$$

Then the temperature T_8 and entropy S_8 are also calculated from EES fluid property functions with the enthalpy h8 at the pressure p8 using $T_8 = f_T$ (water, H =h_8, P =p_8) and $S_8 = f_s$ (water, H =h_8, P =P_8) equation. In order to calculate the mass flow rate $\dot{m}_8$, a mass balance has to be considered.

$$\dot{m}_7 - \dot{m}_8 = 0 \qquad (4.9)$$

Calculate mass flow rate exhoust from heat exchanger ($\dot{m}_7$) from equation (4.60).Then calculate $\dot{m}_8$ from equation (4.9). To calculate mass flow rate between HPP1 and HPP2:

$$\dot{m}_8 - \dot{m}_9 - \dot{m}_{10} = 0 \qquad (4.10)$$

$$\frac{\dot{m}_9}{\dot{m}_{10}} = R_{m,HPP1} \quad (4.11)$$

$R_{m,HPP1}$ Is constant mass flow rate for HPP1, this value changes for different days, let take for February 20, 2021 $R_{m,HPP1}$= 0.1463. The split streams are assumed to be in the mechanical and thermodynamic equilibrium. Therefore fulfil the following values. (*T*8 = *T*9 = *T*10)*;* (*P*8 = *P*9 = *P*10)*;* (*h*8 = *h*9 = *h*10) *and* (*S*8 = *S*9 = *S*10). Calculate overall pressure drop of high pressure as well as low pressure from a mass flow rate as follow from [9].

$$\Delta P_{HP}=0.197 + 0.087\ \dot{m}_7 - 0.021\ \dot{m}_7^2 \quad (4.12)$$

$$\Delta P_{LP} =0.096 – 0.0387\dot{m}_{12} + 0.0567\ \dot{m}_{12}^2 \quad (4.13)$$

These polynomials are found from measurement of the turbine outlet pressures at different days. The mass flow rate $\dot{m}_{12}$ is known from equation (4.63). The same to HPP1, calculate the temperature, pressure and enthalpy in HPP2 using, $T_{11} = f_T$ (steam, $H=h_{11}$, $P=p_{11}$) and $S_{11} = f_s$ (steam, $H=h_{11}$, $P=p_{11}$).

$$h_{11,rev} = f\ (\text{steam}, S=s_{10}, P=p_{11}) \quad (4.14)$$

$$P_{11} = \frac{P_{10} * \Delta P_{HP}}{R_{p,HPP1}} \quad (4.15)$$

$$\dot{m}_{10} - \dot{m}_{11} = 0 \quad (4.16)$$

Assume $R_{p,HPP1}$=0.45. since calculate $\dot{m}_{10}$ from equation 4.10, its possible to calculate $\dot{m}_{11}$ for equation 4.16.

IV. Low-pressure pasteurization (LPP1 and LPP2): Where the enthalpy h_{12} is known that h_{12} =$h_{steam,RH}$. Then calculate $h_{13,rev}$ from fluid property equation.

$$h_{13,rev} = f_h\ (\text{steam}, S =s_{12}, P =P_{13}) \quad (4.17)$$

With the entropy $S_{12} = f_s$ (steam, $H=h_{12}$, $P=P_{12}$) and the pressure P_{13} is determined using below equation 4.18, where the pressure P_{12} is known from equation (4.64).

$$P_{13} = P_{12}\ (R_{p,LPP1}) \quad (4.18)$$

Then to calculate *h*13 use isentropic efficiency of LPP1 ($\eta_{is,LPP1}$) which shown below equation (4.19). Assume $\eta_{is,LPP1}$ (isentropic efficiency for LPP1) = 0.8623 and $R_{P,LPP1}$ (constant pressure ratio for LPP1) =0.47

$$\eta_{is,LPP1} = \frac{h_{12}-h_{13}}{h_{12}-h_{13,rev}} \quad (4.19)$$

Then the temperature T_{13} and entropy s_{13} are also calculated from EES fluid property functions with the enthalpy h_{13} at the pressure p_{13} using $T_{13} = f_T$ (steam, H=h_{13}, P=p_{13}) and $S_{13} = f_s$ (steam, H=h_{13}, P=p_{13})

$$\dot{m}_{12} - \dot{m}_{13} = 0 \quad (4.20)$$

To calculate mass flow rate between LPP1 and LPP2:-

$$\dot{m}_{13} - \dot{m}_{14} - \dot{m}_{15} = 0 \quad (4.21)$$

$$\frac{\dot{m}_{14}}{\dot{m}_{15}} = R_{m,LPP1} \quad (4.22)$$

The split streams are assumed to be in the mechanical and thermodynamic equilibrim.therefore fulfil the following values: $T_{13}=T_{14}=T_{15}$, $P_{13}=P_{14}=P_{15}$, $h_{13}=h_{14}=h_{15}$ and $s_{13}=s_{14}=s_{15}$. $R_{m,LPP1}$ is constant mass flow rate for HPP1, this value changes for different days, let take for february 20,2021, $R_{m,LPP1}$= 0.02. For the case of LPP2 is the same way calculate temperature and pressure as LPP1 which shown below.

$$h_{18,rev} = f_h \text{ (steam, } S=s_{15}, P=p_{18} \text{)} \quad (4.23)$$

$$P_{18} = P_{15}\ R_{p,LPP2} \quad (4.24)$$

Then to calculate h_{18} use isentropic efficiency of LPP2 ($\eta_{is\ LPP2}$) as follow.

$$\eta_{is\ LPP2} = \frac{h_{15}-h_{18}}{h_{15}-h_{18,rev}} \quad (4.25)$$

Assume $\eta_{is\ LPP2}$ (isentropic efficiency for LPP2) = 0.8623 and $R_{p,LPP2}$(constant pressure ratio for LPP2) =0.1.

Then the temperature T_{18} and entropy s_{18} are also calculated from EES fluid property functions with the enthalpy h_{18} at the pressure p_{18} using $T_{18} = f_T$ (steam, H=h_{18}, P=p_{18}) and $S_{18} = f_s$ (steam, H=h_{18}, P=p_{18})

$$\dot{m}_{15} - \dot{m}_{18} = 0 \qquad (4.26)$$

V. Low- pressure feedwater heater (LPFH): The low-pressure feedwater heater (LPFH) is a closed type feedwater heater with a backward drain. The bled steam that comes from the pasturazation extraction between LPP1 and LPP2, is on the shell side and transfers its energy to the feedwater. Thus an energy balance between the bled steam and the feedwater is the first equation for the LPFH model.

$$\dot{m}_2 h_2 - \dot{m}_3 h_3 + \dot{m}_{17} h_{17} - \dot{m}_{21} h_{21} = 0 \qquad (4.27)$$

This equation determines the drain enthalpy h_{21} since the enthalpy h_2 is known from equation (4.2), the known from equation with equation (4.36) and the enthalpy of the bled steam, h_{17}, is known that $h_{13}=h_{14}=h_{15}$, the steam mass flow rate , $\dot{m}_{17}$, is calculated from equation (4.28). The feedwater mass flow rate, $\dot{m}_2$, is determined from the following equation 4.29 mass balance that is part of the LPFH model. Here, $h_{14} = h_{16} = h_{17}$.

$$\dot{m}_{14} - \dot{m}_{16} - \dot{m}_{17} = 0 \qquad (4.28)$$

$$\dot{m}_2 - \dot{m}_3 = 0 \qquad (4.29)$$

The mass flow rate $\dot{m}_3$ comes from equation (4.35). the drain stream leaves the LPFH with the mass flow rate $\dot{m}_{21}$ from:-

$$\dot{m}_{17} - \dot{m}_{21} = 0 \qquad (4.30)$$

Pressure drops of the feedwater heater are usually large because of the flow friction in long small diameter tubes. For the LPFH in view, the pressure P_2 is given through:-

$$P_3 = P_2 \Delta P_{LPFH} \qquad (4.31)$$

Where Assume ΔP_{LPFH} =0.5 (pressure of LPFH). The pressure P_3 is known concept of $P_3 = P_4$. the temperature T_3 and the entropy s_3 are found through EES fluid property functions as the temperature and the entropy of water with the enthalpy h_3 at the pressure P_3, using $T_3 = f_T$ (water, $H=h_3$, $P=p_3$) and $S_3 = f_s$ (water, $H=h_3$, $P=p_3$).

VI. Dearator (D) and throttle valve (TV 1): The dearetor D is direct- contact feedwater heater, Before it enters D, the extraction steam that is withdrawn between LPT 1 and LPT 2, is mixed with the drain stream of the high-pressure feedwater heater HPFH. The higher pressured drain stream passes a throttle valve to reduce its pressure to the pressure of the turbine extraction steam before the two steams merge. The pressure of the turbine extraction steem P_{16}, is calculated using this relationship: $p_{14} = p_{16} = p_{17}$ and $P_{23} = P_{16}$. Defines the outlet pressure of TV 1. No heat losses are assumed for TV 1, hence $h_{23} = h_{20}$ and the temperature is assumed to stay constant: $T_{23} = T_{20}$.

The drain enthalpy h_{20} is calculated from equation (4.38) and the drain temperature T_{20} is known using $T_{20} = f_T$ (steam, $H=h_{20}$, $P=p_{20}$). A mass balance on TV 1 yields become $\dot{m}_{20} - \dot{m}_{23} = 0$ Where the drain mass flow rate, $\dot{m}_{20}$, comes from $\dot{m}_9 - \dot{m}_{20} = 0$. The outlet entropy of TV 1, s_{23} , is calculated with EEs fluid property functions as the entropy of steam with the enthalpy h_{23} at the pressure P_{23}, using $S_{23} = f_s$ (steam, $H=h_{23}$, $P=p_{23}$).

The throttles outlet stream merges with the extraction steam of the pasteurization. Thus the fluid that enters D at the steam side has the mass flow rate $\dot{m}_{22}$ from

$$\dot{m}_{16} + \dot{m}_{23} - \dot{m}_{22} = 0 \qquad (4.32)$$

The extraction mass flow rate $\dot{m}_{14}$ is known from equations 4.22 and $T_{13}=T_{14}=T_{15}$. The enthalpy of the steam entering D, h_{22}, is determined the following energy balance

$$\dot{m}_{16}h_{16} + \dot{m}_{23}h_{23} - \dot{m}_{22}h_{22} = 0 \qquad (4.33)$$

Where the extraction steam enthalpy, h_{16}, is known from consept of $h_{13}=h_{14}=h_{15}$. the merging streams are in a mechanical equilibrium and hence $P_{22} = P_{16}$.

The steam side inlet temperature, T_{22} and entropy,S_{22} are calculated with EEs fluid property functions with enthalpy h_{22} at the pressureP_{22}: using $T_{22} = f_s$ (steam, H=h_{22}, P=p_{22}) and $S_{22} = f_s$ (steam, H=h_{22}, P=p_{22})

The deaerator is supposed to produce saturated feedwater at the extraction steam pressure.thus the enthalpy of the saturated feedwater, h_4, is calculated from EES fluid property functions as the enthalpy of saturated water at the pressure P_{22}

$$h_4 = f_h \text{ (steam, P=}p_{22}\text{, X=0)} \qquad (4.34)$$

This assumption includes that the feedwater outlet pressure of D,P_4, is the same as the steam inlet pressure p_{22}, that is $p_4 = p_{22}$. In addition, no pressure drop in the feedwater is assumed, $P_3 = P_4$. Thus the feedwater outlet temperature, T_4 and entropy, S_4 can be calculated from EES property functions with the enthalpy h_4 at the pressure P_4, using $T_4 = f_T$ (steam, H=h_4, P=p_4) and $S_4 = f_s$ (steam, H=h_4, P=p_4).

A mass balance on D has to account for the fact that the feedwater inlet stream and the steam inlet steam are mixed together and form the feedwater outlet stream. The feedwater inlet stream has the mass flow rate $\dot{m}_3$ from

$$\dot{m}_3 + \dot{m}_{22} - \dot{m}_4 = 0 \qquad (4.35)$$

Where the mass flow rate $\dot{m}_4$ is known from equation (4.9) and the steam mass flow rate $\dot{m}_{22}$ is determined from equation (4.61). The following energy balance is used to find a value for the feedwater inlet enthalpy, h_3,

$$\dot{m}_3 h_3 + \dot{m}_{22} h_{22} - \dot{m}_4 h_4 = 0 \qquad (4.36)$$

VII. High-pressure feedwater heater (HPFH): The high-pressure feedwater heater (HPFH) is like the LPFH a closed type feedwater heater with a backward drain and an energy balance is calculated using as below.

$$\dot{m}_5 h_5 - \dot{m}_6 h_6 + \dot{m}_9 h_9 - \dot{m}_{20} h_{20} = 0 \qquad (4.37)$$

Through this equation, the feedwater outlet enthalpy,h_6, is calculated since the extraction

Enthalpy, h_9, is determined from use h_8=h_9=h_{10} and the feedwater inlet enthalpy, h_5, is given through equation (4.4). The extraction mass flow rate, $\dot{m}_9$, is calculated from equations (4.16) and (4.17). The drain mass flow rate, $\dot{m}_{20}$, follows from $\dot{m}_9$ - $\dot{m}_{20}$ = 0.

The feedwater mass flow rate, $\dot{m}_5$, is determined from the following mass balance for the feedwater using $\dot{m}_5$ - $\dot{m}_6$ = 0. Where the mass flow rate $\dot{m}_6$ is an input of the power plant model.

The drain enthalpy, h_{20}, is calculated from an effectiveness equation for HPFH

$$\varepsilon_{HPFH} = \frac{h_9 - h_{20}}{h_9 - h_5} \qquad (4.38)$$

From measurement of the water inlet conditions and steam outlet conditions of the heat exchanger train, it seems that the effectiveness, ε_{HPFH}, is a function of the fraction of the two inlet mass flow rates, $\frac{\dot{m}_9}{\dot{m}_5}$, and of the feedwater mass flow rate, $\dot{m}_5$, itself. From lippke report, design values of the two mass flow rates are given. They are $\dot{m}_{50}$ = 38.969kg/s and $\dot{m}_{90}$ = 5.7319kg/s. These design values are used to define the following variable

$$B = \frac{1}{2}\left[\frac{\dot{m}_9/\dot{m}_5}{\dot{m}_{90}/\dot{m}_{50}} + \frac{\dot{m}_5}{\dot{m}_{50}}\right] \qquad (4.39)$$

That is used to estimate the effectiveness, ε_{HPFH}, from the following polynomial

$$\varepsilon_{HPFH} = 0.433509942 - 1.72903764(B) + 3.21718006(B^2) - 1.2931972(B^3) \qquad (4.40)$$

This polynomial was found through fitting measured heat exchanger train inlet water data when measured heat exchanger train outlet steam data were used as model inputs.

A constant pressure drop is considered in the feedwater and also at the steam side of the a HPFH

$$P_6 = P_5(\Delta P_{HPFH,c}) \qquad (4.41)$$

$$P_{20} = P_9(\Delta P_{HPFH,h}) \qquad (4.42)$$

Estimated from lippke report, the values for the pressure ratios are $\Delta P_{HPFH,c}$ = 0.8286 and $\Delta P_{HPFH,h}$ = 0.236. Equation (4.41) gives a value for the feedwater inlet pressureP_5, since the feedwater outlet pressure, P_6, is known from equation(4.53).

Corresponding, equation (4.42) yields a value for the drain pressureP_{20}, since the extraction pressure, P_9, is known from (P_8=P_9=P_{10}). The feedwater outlet temperature, T_6, and the feedwater outlet entropy, S_6, are calculated from fluid property functions as the temperature and entropy of water with the enthalpy h_6 at pressure P_6:using $T_6 = f_T$ (water, H=h_6, P=p_6) and $S_6 = f_s$ (water, H=h_6, P=p_6) .

Likewise, the drain temperature, T_{20}, and the drain entropy, s_{20}, are calculated from fluid property functions as the temperature and entropy of steam with the enthalpy h_{20} at the pressure P_{20}: then $T_{20} = f_T$ (steam, H=h_{20}, P=p_{20}) and $S_{20} = f_s$ (steam, H=h_{20}, P=p_{20}).

VIII. Condenser (C) and throttle valve (TV 2): the condenser C is used to condense the exhaust steam from the low pressure part of the pasteurization and thus recover the high quality feedwater for reuse in the cycle. Before the pasteurization exhaust enters the condenser, it is mixed with the drain stream of the low-pressure feed water heater (LPFH).this drain steam passes a throttle valve TV 2 before it is mixed with the exhaust stream. Since the mixing steams are in a mechanical equilibrium, the throttle valves outlet pressure, P_{24} is the same as the exhaust pressure. That is P_{24} =P_{18}. The exhaust pressure from pasturazation, P_{18} , is determined by equation (4.24). The pressure drop induced by TV 2 is given through.

$$P_{24} = P_{21}(\Delta P_{TV\,2}) \qquad (4.43)$$

Where the pressure ratio is estimated to $\Delta P_{TV\,2}$ = 0.57. This equation is used to calculate the LPFH drain pressure, P_{21}, then depend on this pressure calculate the LPFH drain temperature,(T_{21}) and the drain entropy,(S_{21}) from fluid property functions as the temperature and entropy of steam with the enthalpy (h_{21}) at the pressure (P_{21}) then T_{21} =f_T (steam, H=h_{21}, P=P_{21}) and S_{21} =f_S (steam, H=h_{21}, P=P_{21}).

The drain enthalpy, h_{21} is known from equation (4.27). The enthalpy stays constant in the adiabatic throttle valve TV 2. Therefore equation become: h_{24} =h_{21}. In addition, a constant temperature is assumed, T_{24} =T_{21}. There is no loss of mass in TV 2, hence $\dot{m}_{21}$ - $\dot{m}_{24}$ = 0. The mass flow rate $\dot{m}_{21}$ is calculated from equation (4.30). The entropy of the throttle valves

outlet stream is calculated from fluid property functions as the entropy of steam with the enthalpy h_{24} at the pressureP_{24}: then S_{24} =f (steam, H=h_{24}, P=P_{24}).

Before entering the condenser, the throttled drain stream is mixed with the low pressure pasteurization exhaust. This fact is described through the following mass balance

$$\dot{m}_{18} + \dot{m}_{24} - \dot{m}_{19} = 0 \qquad (4.44)$$

This equation is used to calculate the mass flow rate $\dot{m}_{19}$ since the exhaust mass flow rate $\dot{m}_{19}$ is known from equation 4.45. The fluid entering Condenser is in a mechanical equilibrium with the merging streams. Therefore equation become: P_{19} =P_{18}.

The enthalpy of the fluid that enters the condenser (C),h_{19}, is determined from the following energy balance.

$$\dot{m}_{18}\, h_{18} + \dot{m}_{24}\, h_{24} - \dot{m}_{19}\, h_{19} = 0 \qquad (4.45)$$

The enthalpy of the exhaust, h_{18} is known from equation 4.25. The temperature T_{19} is calculated from fluid property functions as the temperature and the entropy S_{19} of steam with the enthalpy h_{19} at the pressure. Then T_{19} =f_T (steam, H=h_{19}, P=P_{19}) and S_{19} =f_s (steam, H=h_{19}, P=P_{19}).

The mixed fluid enters the condenser and looses its energy to the circulating cooling water until it leaves the condenser as saturated liquid. Thus the enthalpy of the outlet flow, h_1, is assumed to be the enthalpy of saturated water the pressure P_{19} and is calculated from fluid property functions:-

$$h_1 = f_h \text{ (steam, P=}P_{19}\text{, X=0)} \qquad (4.46)$$

Hence the pressure is assumed to remain constant (P_1 =P_{19}) and the mass flow rate stays constant as well ($\dot{m}_{19}$ - $\dot{m}_1$=0).

The outlet temperature T_1 and the entropy s_1 are calculated from EEs fluid property functions as the tempertue and entropy of steam with the enthalpy at the pressureP_1: then T_1 =f_T (steam, H=h_1, P=P_1) and S_1 =f_s (steam, H=h_1, P=P_1).

The incoming cooling water temperature, $T_{cool\,i}$ is one of the inputs to the power plant model but does not affect the enthalpy h_1 in this implementation due to the assumption of saturated Liquid

outlet conditions in equation (4.46) of the incoming cooling water, $p_{cool\,i}$ is assumed to be the ambient pressure.

$$p_{cool\,i} = p_{atm} \quad (4.47)$$

From fluid property functions, the cooling water inlet enthalpy, $h_{cool\,i}$ is calculated as the enthalpy of water with the temperature $T_{cool\,i}$ at the pressure$p_{cool\,i}$.

$$h_{cool,i}=f\ (water,\ T=T_{cool,i},\ P=P_{cool,i}) \quad (4.48)$$

There is no pressure drop assumed in the cooling water and the cooling water outlet pressure,$p_{cool\,,o}$, is: express as $p_{cool\,o} = p_{cool\,i}$. Also the mass flow rate of the cooling water remains constant $\dot{m}_{Cooli}$ - $\dot{m}_{Coolo}$ = 0).

Where $\dot{m}_{Coolo}$ is the cooling water outlet mass flow rate and $\dot{m}_{Cooli}$ is the mass flow rate of the incoming cooling water and is estimated to be proportional to the heat exchanger train inlet mass flow rate, $\dot{m}_6$:Here, $\dot{m}_{Cooli}$ = 39.38($\dot{m}_6$).
The factor 19.38 was determined from measurement of the cooling water outer temperature to satisfy the following energy balance

$$\dot{m}_{Cooli}\ (h_{cool,o} - h_{cool,i}\ ) \ = \dot{m}_{19}\ (h_{19} - \ h_1\ ) \quad (4.49)$$

From this equation, the cooling water outlet enthalpy $h_{cool,o}$ is calculated. From this enthalpy, the temperature of the outlet cooling water, $T_{cool,o}$, is determined from fluid property functions as the temperature of water the enthalpy, $h_{cool,o}$ at the pressure $P_{cool,o}$:

$$T_{cool,o} = f_T\ (water,\ H=h_{cool,o},\ P=P_{cool,o}) \quad (4.50)$$

VIIII. Heat exchanger (HE) and reheater (RH): the heat exchanger (HE) and reheaters (RH) are very important parts of the pasteurization plant since they represent the interface between the HTF cycle and the pasteurization plant cycle. The heat transfer between the HTF and the working fluid occurs in these heat exchangers. From the HTF side, the HTF is into two streams where one stream flows into the heat exchanger and other streams flows into the reheaters.

From the pipe geometry, the amount of HTF that flows into the reheaters cannot exceed 25 percent of the entire HTF that leaves the expansion vessel. However, the splitting fraction that is not measured in the plant differs from operator.

$$\dot{m}_{HE} = F_{HE}\dot{m}_6 \quad (4.51)$$

$$\dot{m}_{RH} = F_{RH}\dot{m}_{11} \quad (4.52)$$

Where $\dot{m}_{HE}$ = the mass flow rate of the fluid is pass through heat exchanger, $\dot{m}_{RH}$ = is the mass flow rate of fluid passes through reheater, F_{HE} = feedwater fraction enter HE and F_{RH} = feedwater fraction enter RH. Those fraction determine the steam that enter heat exchanger and reheater. Based on this fraction calculate mass flow rate as above equation (4.51 and 4.52). The value of fraction varies through the day, Assume for February 20, 2021(F_{HE} =0.82 and F_{RH}=0.457) the pressures P_{HE} that develop in heat exchanger (HE) is function of the mass flow rate ($\dot{m}_{HE}$).The polynomial were found from measurement of the mass flow rate and pressure at pasturazation:-

$$P_{HE} = P_6 = 683.96 + 343.99\dot{m}_{HE} + 4.5601\dot{m}_{HE}^2 + P_{atm} \quad (4.53)$$

The temperature of feedwater into heat exchanger (T_6) and into reheater (T_{11}) are calculated using $T_{Water,HE}$ =T_6 and $T_{Water,RH}$ =T_{11} respectively. The temperature of that leaves the expansion vessel is split into heat exchanger and reheater. In other case leave heat exchanger and reheater, each with its own HTF outlet temperature and merge to form the inlet flow of the solar trough collector field. Since no HTF mass is lost on its way through heat exchanger and reheater are the inlet temperature of the solar trough collector field ($T_{HTF,inlet}$) is calculated as follow:

$$T_{HTF,inlet} = T_{HTF,HE} + T_{HTF,RH} \quad (4.54)$$

The temperature differences are become:

$$\Delta T_{HE,1} = T_{EXP} - T_{steam,HE} \quad (4.55)$$

$$\Delta T_{RH,1} = T_{EXP} - T_{steam,RH} \quad (4.56)$$

Where $T_{steam,HE}$ is the working fluid outlet temperature of Heat exchanger and $T_{steam,RH}$ is the working fluid outlet temperature of reheater. Since the overall HTF volume flow rate, $\dot{V}_{HTF}$ and

the mass flow rate $\dot{m}_6$ of the working fluid are available as measured data , the following variable is defined that is equally dependent on the HTF volume flow rate and the mass flow rate:

$$M=\frac{1}{2}\left(\frac{\dot{V}_{HTF}}{\dot{V}_{HTF,0}}+\frac{\dot{m}_6}{\dot{m}_{6,0}}\right) \quad (4.57)$$

Where, M = the different overall heat transfer coefficient area products. Here, $V_{HTF,0}$ = 0.624 m^3/s and $\dot{m}_{6,0}$ = 19.9 kg/s are the values of the HTF volume flow rate and the mass flow rate at solar noon on February 20, 2021.

The working fluid outlet enthalpies, $h_{steam,HE}$ and $h_{steam,RH}$ are calculated from fluid property functions as the enthalpies of steam at the related outlet temperatures and pressures.

$$h_{steam,HE} = f_h \text{ (steam, } T=T_{steam.HE}, P=P_{HE} \text{)} \quad (4.58)$$

$$h_{steam,RH} = f_h \text{ (steam, } T=T_{steam.RH}, P=P_{HE} \text{)} \quad (4.59)$$

Mass flow rate $\dot{m}_6$ is enter into heat exchanger and Mass flow rate $\dot{m}_7$ leave heat exchanger.

$$\dot{m}_{HE} - \dot{m}_7 = 0 \quad (4.60)$$

Where $\dot{m}_{HE} = \dot{m}_6$ (mass flow rate enter into heat exchanger).

The temperature T_7 and the enthalpy h_7 of the single stream that flows into the high pressure part of the turbine are determined from the working fluid flow fractions. Here consider $T_7 = T_{steam.HE}$ and $h_7 = h_{steam.HE}$.

The pressure T_7 is also calculated as below:-

$$P_7 = P_{HE} - \Delta P_{HE} \quad (4.61)$$

May be the pressure drop occurs in the working fluid on its way from the heat exchanger to the high pressure part of the pasturazation. This pressure drop is estimated as a function of the mass flow rate $\dot{m}_7$. The following polynomial was found from measured data:

$$\Delta P_{HE}=-9.81020 + 2.76034(\dot{m}_7) + 0.27897(\dot{m}_7^2) \quad (4.62)$$

The entropy S_7 is calculated from fluid property functions as the entropy of steam with the enthalpy h_7 at the pressure P_7 then $S_7 = f_s$ (steam,H=h_7,P=p_7). The same way for the case of reheater mass flow rate $\dot{m}_{11}$ inter reheater and mass flow rate $\dot{m}_{12}$ leave the reheater , the temperature T_{12}, the enthalpy h_{12}, the pressure p_{12} and the entropy S_{12} of the fluid that enters the low pressure part of the pasturazation (LPP): become $S_{12} = f_s$ (steam,H=h_{12},P=p_{12}). Here, consider $T_{12} = T_{\text{steam RH}}$ and $h_{12} = h_{\text{steam RH}}$.

$$\dot{m}_{RH} - \dot{m}_{12} = 0 \qquad (4.63)$$

$$P_{12} = P_{RH} - \Delta P_{RH} \qquad (4.64)$$

$$\Delta P_{RH} = -124.845 + 5.6385\dot{m}_{12} - 0.0510125\dot{m}_{12}^2 \qquad (4.65)$$

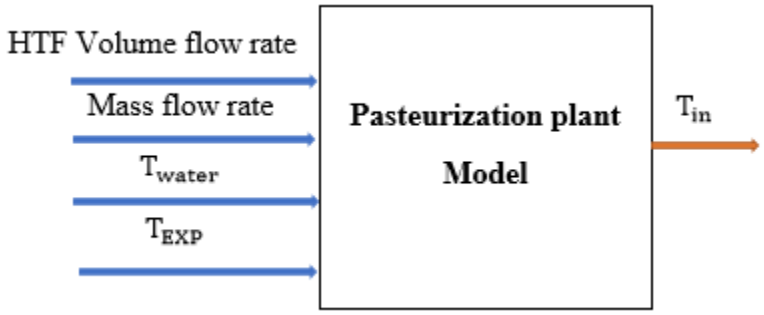

Figure 4.3: Block of pasteurization plant Model with Inputs and Outputs

4.3 Combined PTC and Pasteurization plant

Finally combine parabolic trough collector (PTC) model and pasteurization plant model to design the model predictive controller (MPC) control system. As shown in figure 4.4, the expansion vessel model is the link between parabolic trough collector and pasteurization plant model. This combined plant model take real data from specific location of the Industry, Ethiopia, Oromia Region, Bedele town. The measured input the HTF volume flow rate ($\dot{V}_{HTF}$), the steam mass flow rate ($\dot{m}(t)$), the cooling water inlet temperature (T_{water}), and environmental data (direct normal solar radiation (DIN) and ambient temperature (T_{amb})). The collector outlet temperature is the considered outputs of the plant (T_{out}), is calculated through simulation using Matlab software. The control algorithm that select for this thesis is model predictive control (MPC) controller system and its implementation performance for the plant model is described in the next chapter.

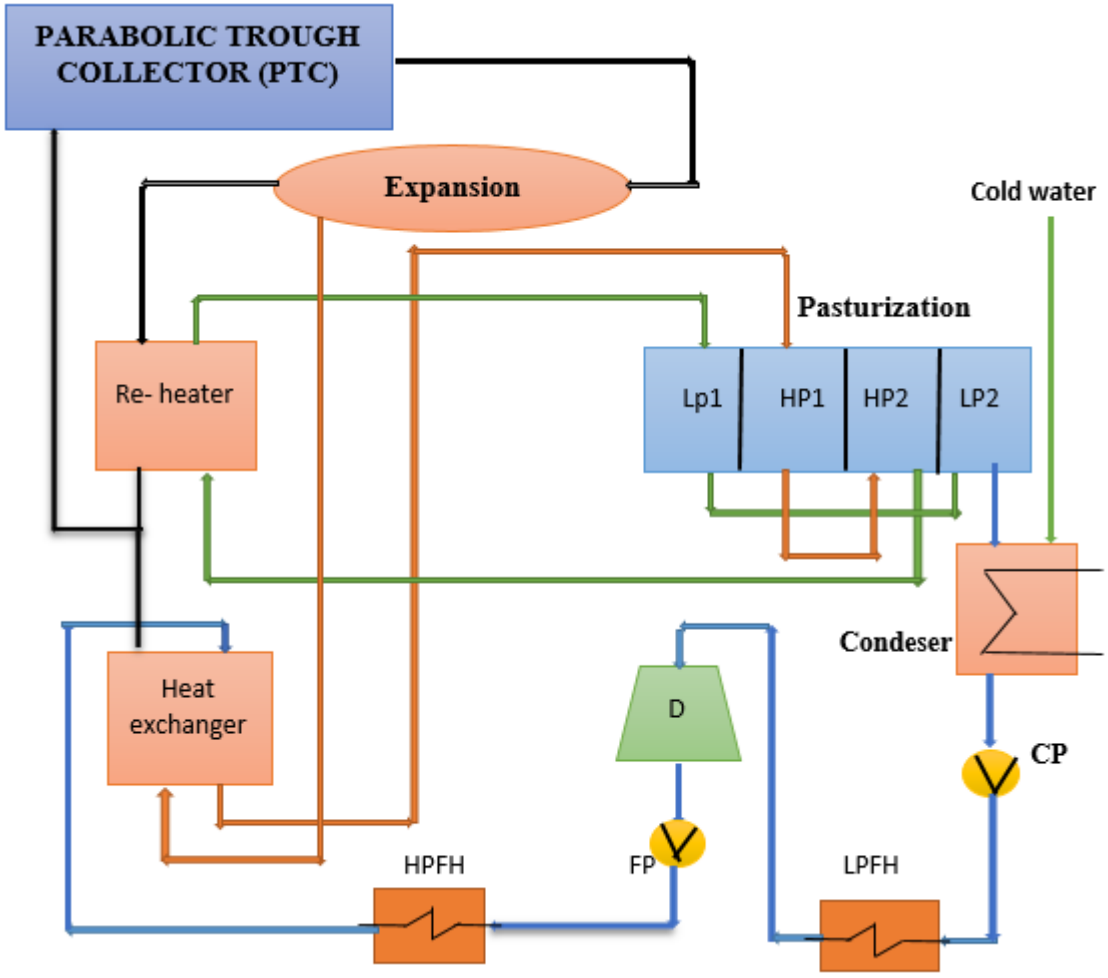

Figure 4.4: Combination of collector model and pasteurization plant model

CHAPTER 5

MODEL LINEAR MPC CONTROL

5.1 Introduction

The basic concept of model predictive control (MPC) is to use a dynamic model to forecast system behavior and optimize the forecast to produce the best decision of the control move at the current time. Because the optimal control move depends on the initial state of the dynamic system, a second basic concept in MPC is to use the past record of measurements to determine the most likely initial state of the system.

The main feature of MPC is incorporation of constraint on manipulated and controlled variables into the optimization procedure. In this work develop a linear model predictive controller steam supply for Pasteurization system using solar collector as shown in figure 5.1. To controller the steam temperature, solar radiation, ambient temperature, steam mass flow rate in the PTC plant model, heat exchanger water inlet temperature used to calculate the heat transfer fluid (HTF) and volume flow rate which drives the collectors outlet temperature into adjusting set point. Here, in this thesis design five input and one output are considered those are: Volume flow rate ($\dot{V}_{HTF}$), mass flow rate ($\dot{m}_{(t)}$), ambient temperature ($\mathrm{T_{amb}}$), heat absorbed ($\mathrm{q_{absorb}}$) and inlet temperature ($\mathrm{T_{water}}$) consider as input and Temperature steam ($\mathrm{T_{steam}}$) is consider as output of the system.

5.2 Mathematical Model of Combination Plant

For this thesis to summarize the combination plant let design as shown in figure 5.2. Let classified into four parts those are: parabolic trough collector (PTC), heat exchanger (HE), HTF pump and expansion vessel which integrate PTC with Pasteurization plant. Then calculate the differential equation for temperature in this summarize model.

- **Solar collector outlet temperature:** is one of the nonlinear equations of parabolic trough collector (PTC) outlet temperature for heat transfer fluid. An energy balance on collectors' outlet temperature leads to this differential equation which express below:

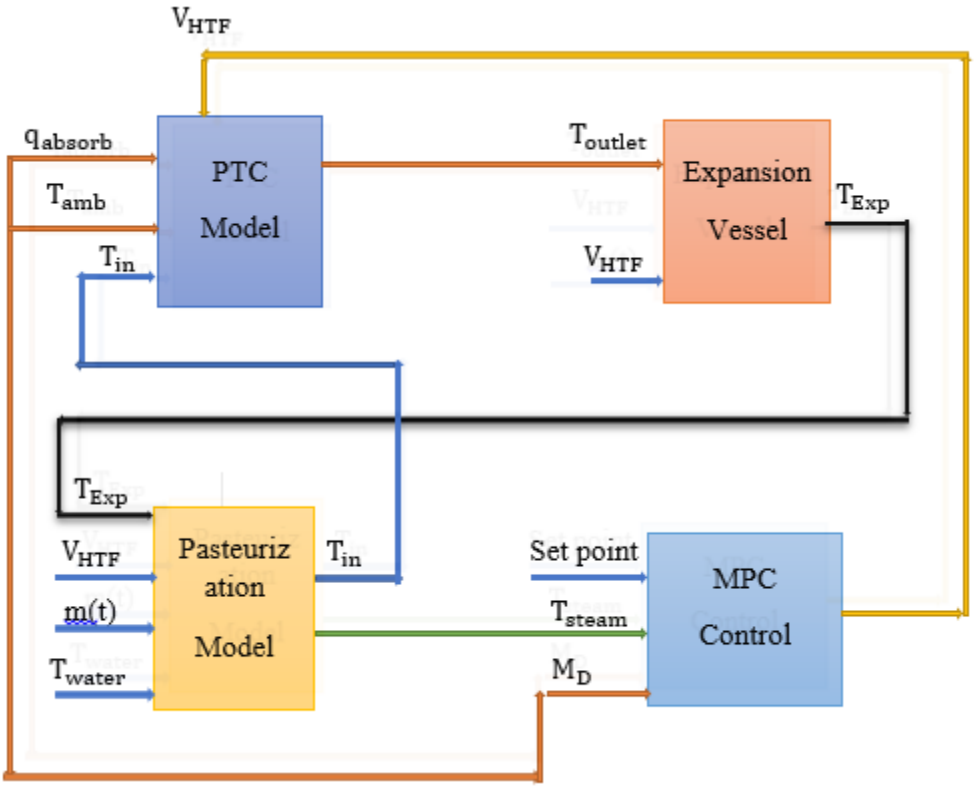

Figure 5.1: MPC controller for the plant model

$$\frac{dT_{out}(t)}{dt} = \frac{-\dot{V}_{HTF}(t)}{V_{col}} T_{out}(t) + \frac{\dot{V}_{HTF}(t)}{V_{col}} T_{in}(t) + \frac{L_{col}}{\rho_{HTF} C_{HTF} V_{col}} [\, q_{absobed}(t) - q_{ambient}(t)] \quad (5.1)$$

$$q_{ambient}(t) = h_{ambient}\, A_{ABS\,surf,i}(t)[\, T_{out}(t) - T_{amb}(t)] \quad (5.2)$$

Where, Overall volume of the solar collector calculate as $V_{col} = [(\pi/4)D_{ABS,i}^{2}](L_{col})$ and length of the solar collector become: $L_{col} = (Length)(n_{collector})$, initial condition become: $T_{out(0)} = T_{out,init}$, $h_{ambient} = 2.5 W/m^2K$ (heat transfer coefficient) and $q_{ambient}$ is heat transfer to environment.

- **Expansion Vessel Temperature:** is the second nonlinear equations used to determine the temperature of expansion vessel.

$$\frac{dT_{Exp}(t)}{dt} = -\frac{\dot{V}_{HTF}(t)}{V_{EXP}} T_{Exp}(t) + \frac{\dot{V}_{HTF}(t)}{V_{EXP}} T_{out}(t) \quad (5.3)$$

Assume, Initial condition become: $T_{Exp}(0) = T_{Exp,init}$, V_{Exp} (volume of expansion vessel) = $220 m^3$.

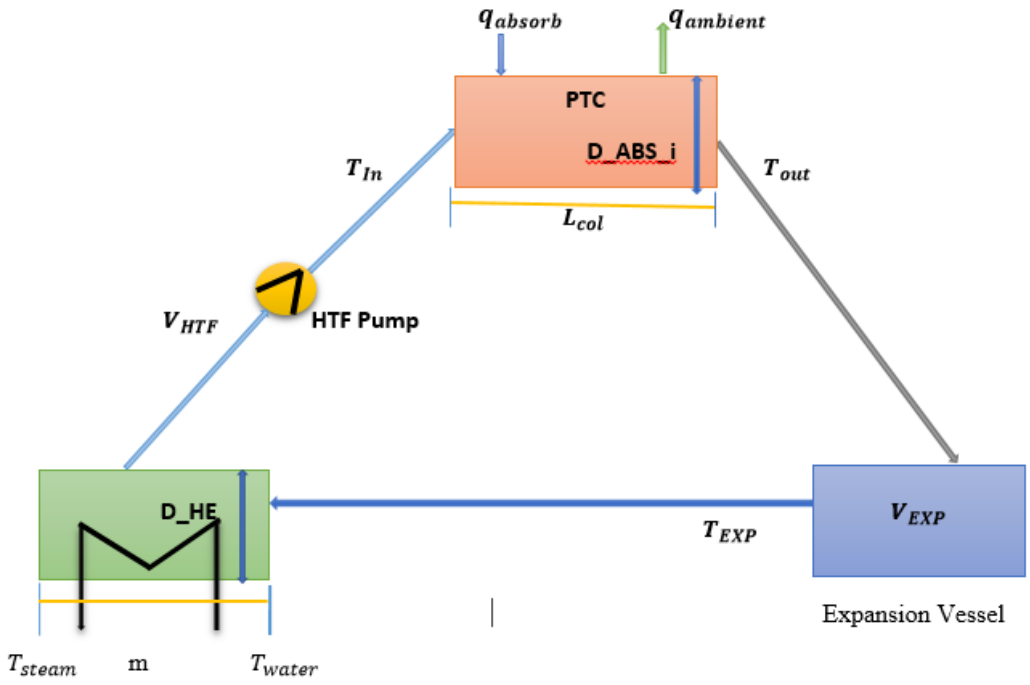

Figure 5.2: The structure of combined plant model

• **Heat exchanger temperature:** to determine input temperature through an energy balance on given heat exchanger.

$$\frac{dT_{in}(t)}{dt} = -\frac{\dot{V}_{HTF}(t)}{V_{HE}} T_{in}(t) + \frac{\dot{V}_{HTF}(t)}{V_{HE}} T_{Exp}(t) + \frac{L_{HE}}{\rho_{HTF} C_{HTF} V_{HE}} q_{transferred}(t) \quad (5.4)$$

$$q_{transferred}(t) = h_{HE}(t)\ A_{HEsurf}\ [T_h(t) - T_c(t)] \quad (5.5)$$

$$h_{HE}(t) = 120\left[\frac{\dot{V}_{HTF}(t)}{\dot{V}_{HTF,0}} + \frac{\dot{m}(t)}{\dot{m}_0}\right] \quad (5.6)$$

$$V_{HE} = \frac{\pi}{4} D_{HE}^2 L_{HE} \quad (5.7)$$

Assume $T_{in}(0) = T_{in,nit}$, m_{HE} (mass of heat exchanger) =100kg, $q_{transferred}(t)$ = the heat transfer in given heat exchanger, T_h = mean temperature of hot fluid in heat exchanger, T_c = mean temperature of cold fluid in heat exchanger, h_{HE} = heat transfer coefficient, $\dot{m}$ = mass flow rate of working fluid, $\dot{m}_0$ (Reference mass flow rate of working fluid) =19.9 kgS^{-1}, $\dot{V}_{HTF,0}$ (reference volume flow rate) = 0.624m^3S^{-1}, $A_{HE,surf}$ = surface area of heat exchanger, D_{HE} (diameter of heat exchanger)=1m, L_{HE} (length of heat exchanger) = 10m.

- **Steam temperature:** is calculate using below a heat effectiveness equation. Then convert heat effective equation into differential equation because model predictive control framework use only differential equations. Additionally, heat exchanger effectiveness is assumed to be flow rate dependent.

$$\varepsilon_{HE}(t) = \frac{T_{steam}(t) - T_{Water}(t)}{T_{Exp}(t) - T_{water}(t)} \quad (5.8)$$

$$\frac{dT_{steam}(t)}{dt} = 0.01[-T_{steam}(t)\,\varepsilon_{HE}(t)\,[T_{Exp}(t) - T_{water}(t)] + T_{water}(t)] \quad (5.9)$$

$$\varepsilon_{HE}(t) = (-0.1)\left(\frac{\dot{V}_{HTF}(t)}{\dot{V}_{HTF,0}} + \frac{\dot{m}(t)}{\dot{m}_0}\right) + 0.36 \quad (5.10)$$

Here, Initial condition become: $T_{steam}(0) = T_{stream,nit}$. Factor 0.01 s^{-1} was introduced to adjust the time constant of this differential to the time constant range of the entire system in order to avoid a stiff differential equation system.

5.3 Model for Linear MPC

The models in linear MPC are discrete-time linear models in state space form. Therefore, Above non linear system convert into this model. First, the linear model in state-spaced form is explained, later explain the time discretization of this thesis model.

- **State-space form :** the general expression form of state space is as shown below eqaution.

$$\dot{x}(t) = A(t)x(t) + B(t)u(t) \quad (5.11)$$

$$y(t) = C(t)x(t) + D(t)u(t) \quad (5.12)$$

Where, $x(0) = x_{init}$ is initial condition for equation (5.11). For this thesis use time- invariant state space form, where the matrices A, B, C and D are constant as shown in equation (5.13) and (5.14).

$$\dot{x}(t) = Ax(t) + Bu(t) \quad (5.13)$$

$$y(t) = Cx(t) + Du(t) \quad (5.14)$$

Since above nonlinear equation (5.1), (5.3), (5.4) and (5.9) are not express in state space model convert it using the time constant $1/t_{col}(t) = \dot{V}_{HTF}(t)/V_{col}$. Where, A_{col} = cross-sectional area of

the collector and overall heat transfer coefficient area product calculate as $UA_{col} = h_{ambient} A_{ABS,surf,i}$. With these definitions, the differential equation for the collector outlet temperature (5.1) written as:

$$\frac{dT_{out}(t)}{dt} = \frac{1}{t_{col,}(t)}\left(T_{in}(t) - T_{out}(t)\right) + \frac{q_{absorbed}(t) - UA_{col}\left(T_{out}(t) - T_{amb}(t)\right)}{A_{col}\rho_{HTF}(T_{out}(t))C_{HTF}(T_{out}(t))} \quad (5.15)$$

There is a time constant for expansion vessel is: $1/t_{Exp}(t) = \dot{V}_{HTF}(t)/ V_{Exp}$. Thus the differential equation for the expansion vessel temperature (5.6) becomes:

$$\frac{dT_{Exp}(t)}{dt} = \frac{1}{t_{Exp}(t)}[T_{out}(t) - T_{Exp}(t)] \quad (5.16)$$

The heat exchanger time constant is calculated as: $1/t_{HE}(t) = \dot{V}_{HTF}(t)/ V_{HE}$.

Where, Overall heat transfer coefficient area product calculate as: $UA_{HE}(t) = h_{HE}(t)A_{HEsurf}$ and A_{HE} is cross sectional area of the heat exchanger. With these definitions, the differential equation for the collector inlet temperature in equation (5.4) result in:

$$\frac{dT_{in}(t)}{dt} = \frac{1}{t_{HE}(t)}[T_{Exp}(t) - T_{in}(t)] - \frac{UA_{HE}(t)(T_{Exp}(t) - T_{in}(t) - T_{steam}(t) - T_{water}(t)}{2 * A_{HE}\rho_{HTF}(T_{in}(t))C_{HTF}(T_{in}(t))} \quad (5.17)$$

The differential equation for steam outlet temperature of the heat exchanger in equation (5.9) is:

$$\frac{dT_{steam}(t)}{dt} = 0.01\left[(-T_{steam}(t) - \varepsilon_{HE}(t)\left(T_{Exp}(t) - T_{water}(t)\right) + T_{water}(t)\right] \quad (5.18)$$

According to state space model from above equation (5.15),(5.16),(5.17) and (5.18) introduced four state vector and five input vector respectively as follow:

$$x(t) = \begin{bmatrix} T_{out}(t) \\ T_{Exp}(t) \\ T_{in}(t) \\ T_{steam}(t) \end{bmatrix} \tag{5.19}$$

$$u(t) = \begin{bmatrix} q_{absorbed}(t) \\ T_{ambient}(t) \\ V_{HTF}(t) \\ m(t) \\ T_{water}(t) \end{bmatrix} \tag{5.20}$$

And the initial condition is given through:

$$x(0) = \begin{bmatrix} T_{out,init} \\ T_{Exp,init} \\ T_{in,init} \\ T_{steam,init} \end{bmatrix} \tag{5.21}$$

The model defined by the four differential (5.15), (5.16), (5.17) and (5.18) is not of the linear state-space form as defined above. Considering again the vector definitions made in (5.19), (5.20) and (5.21), the simplified model is of the very general form:

$$\dot{x}(t) = f\,[x(t), u(t), t] \tag{5.22}$$

Equation (5.22) stands for:

$$\begin{bmatrix} \frac{dT_{out}(t)}{dt} \\ \frac{dT_{Exp}(t)}{dt} \\ \frac{dT_{in}(t)}{dt} \\ \frac{dT_{steam}(t)}{dt} \end{bmatrix} =$$

$$\begin{bmatrix} \frac{1}{\tau_{col}(t)}\left(T_{in}(t) - T_{out}(t)\right) + \frac{q_{absorbed}(t) - UA_{col}\left(T_{out}(t) - T_{amb}(t)\right)}{A_{col}\rho_{HTF}\left(T_{out}(t)\right)C_{HTF}\left(T_{out}(t)\right)} \\ \frac{1}{\tau_{Exp}(t)}\left(T_{out}(t) - T_{Exp}(t)\right) \\ \frac{1}{\tau_{HE}(t)}\left(T_{Exp}(t) - T_{in}(t)\right) - \frac{UA_{HE}(t)(T_{Exp}(t) - T_{in}(t) - T_{steam}(t) - T_{water}(t)}{2\,A_{HE}\rho_{HTF}\left(T_{in}(t)\right)C_{HTF}\left(T_{in}(t)\right)} \\ 0.01\,[(-T_{steam}(t) - \varepsilon_{HE}(t)\left(T_{Exp}(t) - T_{water}(t)\right) + T_{water}(t)] \end{bmatrix} \tag{5.23}$$

Here, this equation is not required form for linear MPC control algorithm, let approximate it and convert to state space form.

5.3.1 Model linearization

The linearization procedure, taken from [24], is first presented theoretically by starting with the general form of the system (5.22). Suppose that $u_{nom(t)}$ is a given input to system and $x_{nom(t)}$ is a known solution of the state differential equation. Then $x_{nom(t)}$ satisfies. The target is to find approximation to neighboring solutions for small deviation for both nominal input and nominal state. Here, use forward difference approximation method of linearization is use.

$$\dot{x}_{nom}(t) = f[x_{nom(t)},\ u_{nom(t)}, t] \quad (5.24)$$

$$u(t) = u_{nom(t)} + \tilde{u}(t) \quad (5.25)$$

$$x(t) = x_{nom(t)} + \tilde{x}(t) \quad (5.26)$$

Where, time is $0 \leq t \leq t_{end}$, u_{nom} is nominal input, x_{nom} is nominal trajectory, $\tilde{u}(t)$ is small perturbations input and $\tilde{x}(t)$ is small perturbations state and initial conditions for equation (5.26) become: $x(0) = x_{nom}(0) + \tilde{x}(0)$.

Substituting equation (5.25) and (5.26) into the state differential equation (5.22), then Taylor expansion is made as follow:

$$\dot{x}_{nom}(t) + \dot{\tilde{x}}(t) = f[x_{nom(t)},\ u_{nom(t)}, t] + J_x[x_{nom(t)},\ u_{nom(t)}, t]\,\tilde{x}(t) + J_u[x_{nom(t)},\ u_{nom(t)}, t]\,\tilde{u}(t) + hot \quad (5.27)$$

Here J_x and J_u are the Jacobian matrices of f with respect to x and u. That is, J_x become: $(J_x)_{i,j} = \partial f_i / \partial \varepsilon_j$ matrix the (i, j)-the element. Where, $0 \leq t \leq t_{end}$, J_x= Jacobian matrices of f with respect to x, J_u= Jacobian matrices of f with respect to u, Here, J_x is a matrix the (i,j)-th element, f_i = the i-th component of f and ε_j = the j-th component. For the case of J_u also the same case. Higher order hot is neglect it since it is small respect to $\tilde{x}$ and $\tilde{u}$. Then simplify above equation as follow:

$$\dot{\tilde{x}}(t) = J_x[x_{nom(t)},\ u_{nom(t)}, t]\,\tilde{x}(t) + J_u[x_{nom(t)},\ u_{nom(t)}, t]\,\tilde{u}(t) \quad (5.28)$$

Where A(t)= $J_x[x_{nom(t)}, u_{nom(t)}, t]$ and B(t)= $J_u[x_{nom(t)}, u_{nom(t)}, t]$.

Here, approximately satisfy a linear equations (5.11) and the above equations (5.28) called linearized state differential equation. Therefore using this method linearize equation (5.23):

$$\begin{bmatrix} f_1[x(t),u(t),t] \\ f_2[x(t),u(t),t] \\ f_3[x(t),u(t),t] \\ f_4[x(t),u(t),t] \end{bmatrix} =$$

$$\begin{bmatrix} \frac{1}{t_{col}(t)}\left(T_{in}(t) - T_{out}(t)\right) + \frac{q_{absorbed}(t) - UA_{col}\left(T_{out}(t) - T_{amb}(t)\right)}{A_{col}\rho_{HTF}(T_{out}(t))C_{HTF}(T_{out}(t))} \\ \frac{1}{t_{Exp}(t)}\left(T_{out}(t) - T_{Exp}(t)\right) \\ \frac{1}{t_{HE}(t)}\left(T_{Exp}(t) - T_{in}(t)\right) - \frac{UA_{HE}(t)(T_{Exp}(t) - T_{in}(t) - T_{steam}(t) - T_{water}(t)}{2 * A_{HE}\rho_{HTF}(T_{in}(t))C_{HTF}(T_{in}(t))} \\ 0.01 * ((-T_{steam}(t) - \varepsilon_{HE}(t)(T_{Exp}(t) - T_{water}(t)) + T_{water}(t)) \end{bmatrix} \quad (5.29)$$

Here, it needed to determine both J_x and J_u matrix for this system. From definition of jacobian matrix equation (5.28) calculate J_x as follow:

$$J_x[X(t), U(t), t] = \begin{bmatrix} \frac{\partial f_1}{\partial T_{out}} & \frac{\partial f_1}{\partial T_{Exp}} & \frac{\partial f_1}{\partial T_{in}} & \frac{\partial f_1}{\partial T_{steam}} \\ \frac{\partial f_2}{\partial T_{out}} & \frac{\partial f_2}{\partial T_{Exp}} & \frac{\partial f_2}{\partial T_{in}} & \frac{\partial f_2}{\partial T_{steam}} \\ \frac{\partial f_3}{\partial T_{out}} & \frac{\partial f_3}{\partial T_{Exp}} & \frac{\partial f_3}{\partial T_{in}} & \frac{\partial f_3}{\partial T_{steam}} \\ \frac{\partial f_4}{\partial T_{out}} & \frac{\partial f_4}{\partial T_{Exp}} & \frac{\partial f_4}{\partial T_{in}} & \frac{\partial f_4}{\partial T_{steam}} \end{bmatrix} \quad (5.30)$$

According to equation (5.30) derivate each equation respect each four state vector, then J_x matrix calculate below:

$$J_x[X(t), U(t), t] = \begin{bmatrix} r_1 & 0 & \frac{1}{\tau_{col}(t)} & 0 \\ \frac{1}{\tau_{Exp}(t)} & \frac{-1}{\tau_{Exp}(t)} & 0 & 0 \\ 0 & r_3 & r_4 & r_2 \\ 0 & 0.01\varepsilon_{HE}(t) & 0 & -0.01 \end{bmatrix} \quad (5.31)$$

Where, $r_1 = -\frac{1}{\tau_{col,1}(t)} - \frac{1}{\tau_{col,2}(t)} - \frac{UA_{col}}{A_{col}\rho_{HTF}(T_{out}(t))C_{HTF}(T_{out}(t))} - n(t)$,

$$r_2 = \frac{UA_{HE}(t)}{2*A_{HE}\,\rho_{HTF}(T_{in}(t))C_{HTF}(T_{in}(t))}$$

$$r_3 = \frac{1}{\tau_{HE,1}(t)} + \frac{1}{\tau_{HE,2}(t)} - r_2$$

$$r_4 = -\frac{1}{\tau_{HE,1}(t)} - \frac{1}{\tau_{HE,2}(t)} - r_2 + n_{HE}(t),$$

$$n(t) = \frac{\left(\frac{\partial\rho_{HTF}}{\partial T_{out}}C_{HTF} + \rho_{HTF}\frac{\partial C_{HTF}}{\partial T_{out}}\right)}{A_{col}(\rho_{HTF}(T_{out}(t))C_{HTF}(T_{out}(t)))^2}\left[q_{absorbed}(t) - UA_{col}(T_{out}(t) - T_{amb}(t))\right]$$

$$n_{HE}(t) = \frac{UA_{HE}(t)\left[\frac{\partial\rho_{HTF}}{\partial T_{in}}C_{HTF} + \rho_{HTF}\frac{\partial C_{HTF}}{\partial T_{in}}\right]}{2*A_{HE}\,(\rho_{HTF}(T_{in}(t))C_{HTF}(T_{in}(t)))^2}\left(T_{in}(t) + T_{Exp}(t) - T_{steam}(t) - T_{water}(t)\right)$$

For the case J_u matrix the same way according to equation(5.30) derivate each equation respect to five input vector and finally calculate the matrix J_u.

$$J_u[X(t), U(t), t] = \begin{bmatrix} \frac{\partial f_1}{\partial q_{absorbed}} & \frac{\partial f_1}{\partial T_{amb}} & \frac{\partial f_1}{\partial \dot{V}_{HTF}} & \frac{\partial f_1}{\partial \dot{m}(t)} & \frac{\partial f_1}{\partial T_{water}} \\ \frac{\partial f_2}{\partial q_{absorbed}} & \frac{\partial f_2}{\partial T_{amb}} & \frac{\partial f_2}{\partial \dot{V}_{HTF}} & \frac{\partial f_2}{\partial \dot{m}(t))} & \frac{\partial f_2}{\partial T_{water}} \\ \frac{\partial f_3}{\partial q_{absorbed}} & \frac{\partial f_3}{\partial T_{amb}} & \frac{\partial f_3}{\partial \dot{V}_{HTF}} & \frac{\partial f_3}{\partial \dot{m}(t)} & \frac{\partial f_3}{\partial T_{water}} \\ \frac{\partial f_4}{\partial q_{absorbed}} & \frac{\partial f_4}{\partial T_{amb}} & \frac{\partial f_4}{\partial \dot{V}_{HTF}} & \frac{\partial f_4}{\partial \dot{m}(t)} & \frac{\partial f_4}{\partial T_{water}} \end{bmatrix} \qquad (5.32)$$

According to equation (5.32) derivate each equation respect each four state vector, then J_u matrix calculate below:

$J_u[X(t), U(t), t] =$

$$\begin{bmatrix} r_5 & r_6 & \frac{(T_{in(t)} - T_{out(t)})}{V_{col}} & 0 & 0 \\ 0 & 0 & \frac{(T_{out(t)} - T_{exp(t)})}{V_{exp}} & 0 & 0 \\ 0 & 0 & r_7 - \frac{K(t)}{2\,A_{HE}\rho_{HTF}(T_{in}(t))C_{HTF}(T_{in}(t)\dot{m}_0} & \frac{UA_{HE(t)}}{2\,A_{HE}\rho_{HTF}(T_{in}(t))C_{HTF}(T_{in}(t))} & \\ 0 & 0 & \frac{-0.0005(T_{exp(t)} - T_{water(t)})}{\dot{V}_{HTF,0}} & \frac{-0.0005(T_{exp(t)} - T_{water(t)})}{\dot{m}_0} & 0.01(1 - \varepsilon_{HE(t)}) \end{bmatrix}$$

(5.33)

Where, $r_5 = \frac{1}{A_{col}\rho_{HTF}(T_{out}(t))C_{HTF}(T_{out}(t))}$

$$r_6 = \frac{UA_{col}}{A_{col}\rho_{HTF}(T_{out}(t))C_{HTF}(T_{out}(t))}$$

$$r_7 = \frac{a\,(T_{exp(t)} - T_{in(t)})}{V_{HE}} - \frac{k(t)}{2\,A_{HE}\rho_{HTF}(T_{in}(t))C_{HTF}(T_{in}(t)\dot{V}_{HTF,0}}$$

$$K(t) = 36000A_{surfHE}(T_{Exp}(t) + T_{in}(t) - T_{steam}(t) - T_{water}(t))$$

To obtain a time-invariant linearized state differential equation from (5.28), a steady-state situation as nominal solution is considered, where all quantities are constant. A constant input to the system means that absorbed solar energy, ambient temperature, HTF volume flow rate, mass flow rate and water temperature are held constant. For such a constant input, temperatures will evolve throughout the plant that stay constant with ongoing time if no further change in the input variables occurs. The constant input together with the constant temperatures is called a steady-state situation. If the constant input is taken as nominal input, (u_{nom})) and the evolved constant temperatures as nominal trajectory, (x_{nom}) then the Jacobian matrices (J_X) and (J_u) have constant elements if evaluated for this nominal solution.

In this case, the linearized state differential equation (5.28) is time-invariant and a model of the form (5.13) is found that can be applied to the MPC algorithm.

5.3.2 Discrete time models

Since MPC work with discrete time system, convert linear time-invariant continuous time system to equivalent discrete system as follow.

$$\tilde{x}_{k+1} = A_d\,\tilde{x}_k + B_{m,d}\tilde{U}_{m,k} + B_{d,d}\,\tilde{U}_{d,k} \qquad (5.34)$$

$$\tilde{y}_k = C_d\,\tilde{x}_k \qquad (5.35)$$

Where, $\tilde{x}_k$ = the state and $\tilde{U}_{m,k}$, $\tilde{U}_{d,k}$ the inputs at time instants t_k ,k=0, 1,2..,the initial condition is $\tilde{x}_0$. The sampling period, Δ, is the constant difference between two time instants:

$$\Delta = t_{i+1} - t_i \qquad (5.36)$$

A derivation of the following transformation for the discrete-time system can be found in [24] and yields are: ($A_d = e^{A\Delta}$) ,($B_{m,d} = A^{-1} (A_d - I) B_m$),($B_{d,d} = A^{-1} (A_d - I) B_d$),($C_d = C$):

Through these equations, the discrete-time equations that represent the continous-time system are obtained. In the following only the discrete-time system is considered and the d-index at the matrices is omitted,bearing in mind that the system matrices are the matrices of discrete time system. Before the linear discrete-time model is used in the MPC algorithms, equation (5.37) is augmented by the input step disturbance d_k. This results in:

$$\tilde{x}_{k+1} = A\tilde{x}_k + B_m(\tilde{u}_{mk} + d_k) + B_d\, \tilde{u}_{d\,k} \qquad (5.37)$$

Where, d_k is serves the purpose of adding integral control.

Constraints are at output side the steam temperature and at input side volume flow rate of HTF is considered.

$$\tilde{T}_{steam\ min} \leq \tilde{T}_{steam\ k} \leq \tilde{T}_{steam\ max} \qquad (5.38)$$

$$\dot{\tilde{V}}_{HTF,min} \leq \dot{\tilde{V}}_{HTF,k} \leq \dot{\tilde{V}}_{HTF,max} \qquad (5.39)$$

For other case also possible to express as:

$$\tilde{y}_{min} \leq \tilde{y}_k \leq \tilde{y}_{max} \qquad (5.40)$$

$$\tilde{u}_{m,min} \leq \tilde{u}_{m,k} \leq \tilde{u}_{m,max} \qquad (5.41)$$

The time-invariant linear discrete time model given through (5.37) and (5.35) together with the constraints (5.40) and (5.41) is now ready for use in the MPC framework which explain below.

5.4 The Model predictive control framework

Cost function is to be minimized for optimal control must increase with an increasing difference between the forecasted steam temperature and the set point temperature. Additionally, it must increase with an increasing rate of change in the HTF volume flow rate and mass flow rate.

$$\emptyset_k = \frac{1}{2} \sum_{j=0}^{\infty} [Q(\tilde{T}_{out,k+j} - \tilde{T}_{outset})^2 + S(\Delta\dot{\tilde{V}}_{HTF,k+j}^2 + \Delta\dot{m}(k+j))] \qquad (5.42)$$

Where, Q is a penalty parameter on the difference between the steam temperature and the set point temperature with Q > 0. The parameter S with S > 0 is a penalty parameter on the addition rate of the HTF volume flow rate as input.

CHAPTER 6

RESULT AND DISCUSSION

6.1 Sun Tracking Result

Maximum Power Point Tracking (MPPT) is a technique that to collect solar radiation intensity get the maximum possible power from one or more PTC or photovoltaic devices. The output power of a PTC system can be maximized by continuously tracking the maximum power point of a system and the maximum power point is dependent on the solar temperature, solar irradiation and on the load connected. Thus maximum power point can be tracked continuously by using LDR sensor.

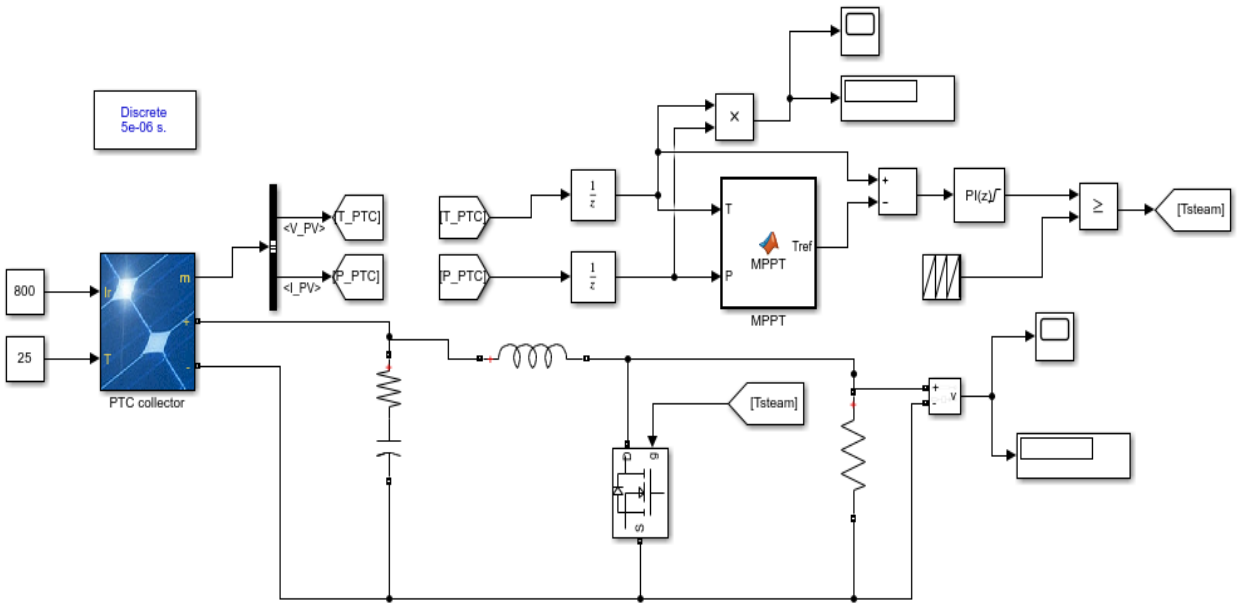

Figure 6.1: Solar Tracking Simulink Model

In this thesis before regulate the output steam temperature first model and Simulink the sun tracking system weather collect the necessary level of solar radiation intensity exist or not. Therefore, I model and Simulink the sun tracking system as shown below for both clear day and partial cloud day.

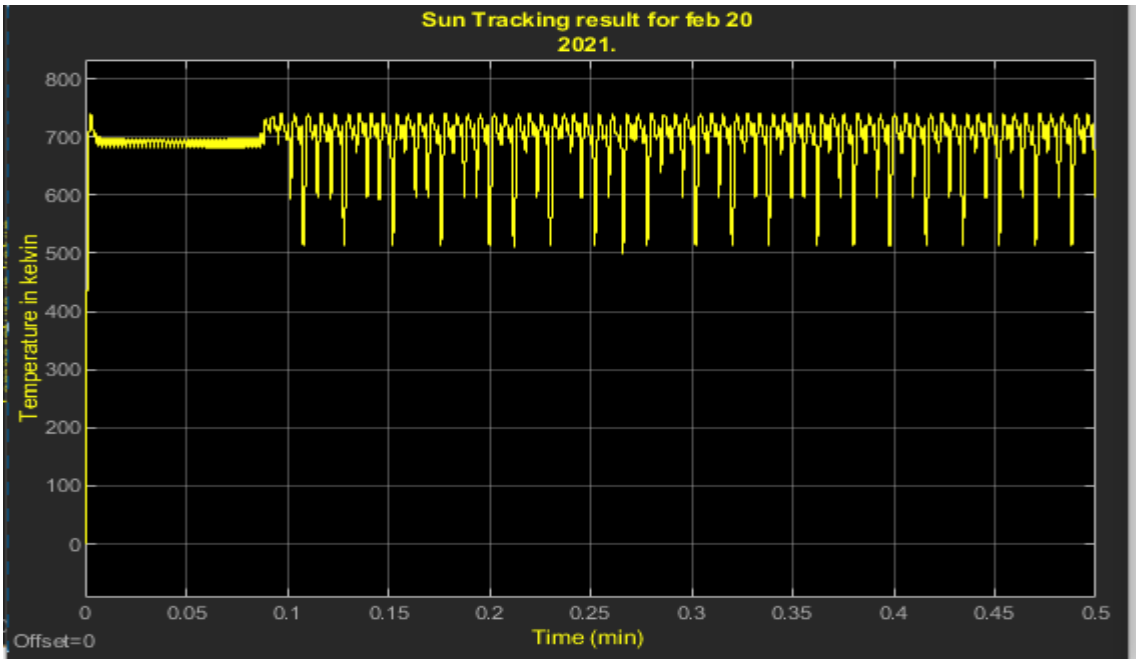

Figure 6.2: Sun tracking result for February 20, 2021

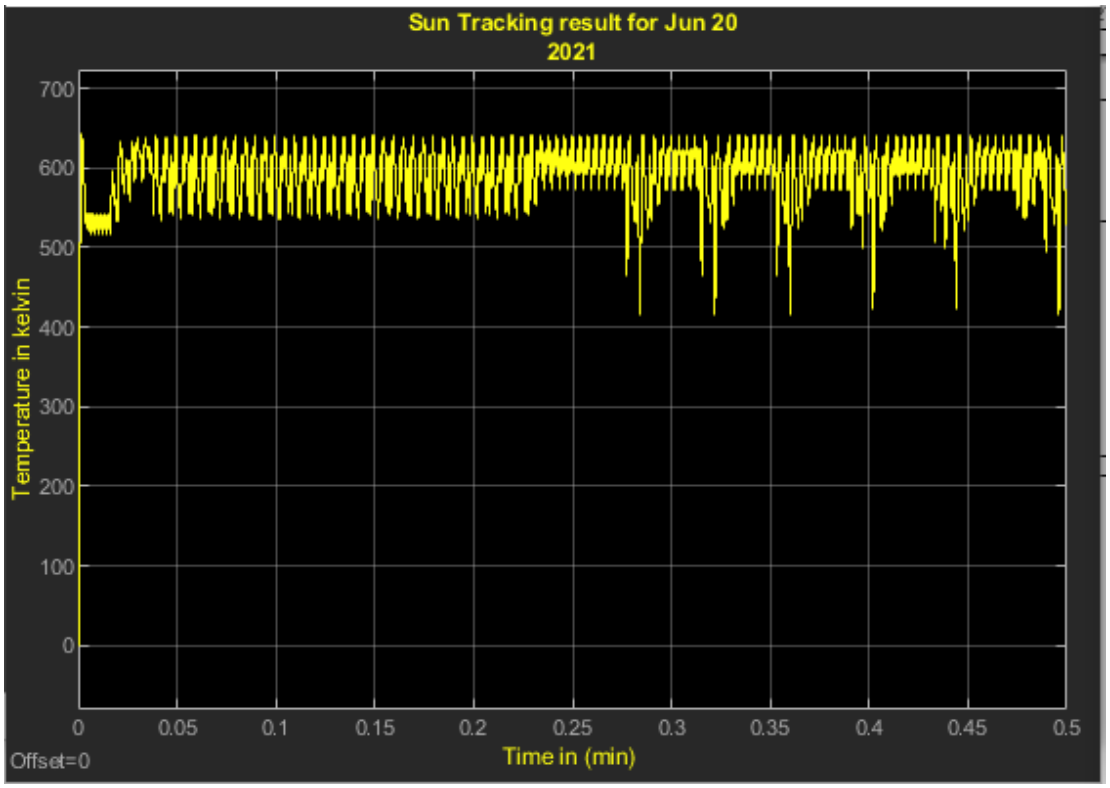

Figure 6.3: Sun tracking result for June 20, 2021

6.2 Steam Temperature Control Result

Controllers are a tool for regulating the dynamical systems so that desirable behavior is obtained. The goal is to control temperature of steam which supply to pasteurization plant. There are several controllers that can be used for controlling steam temperature. Among this controlling system for this thesis used PID and MPC controller to control collector output temperature. First discuss proportional integral derivative controller result and second discuss Model predictive controller result. Finally compare both type of controller result.

6.2.1 Proportional-Integral-Derivative control result

Proportional-Integral-Derivative controllers are one of the most commonly used types of controllers both in academic and industry. It's widely used because of its good performance. The performance of this controller evaluated based on transient response and steady state response result. Here, in this thesis the result of the controller is evaluated for two different days in 2021. As shows in figure 6.4 (a) and (b) the steam temperature and Inlet temperature of the system for February 20, 2021 using PID controller respectively.

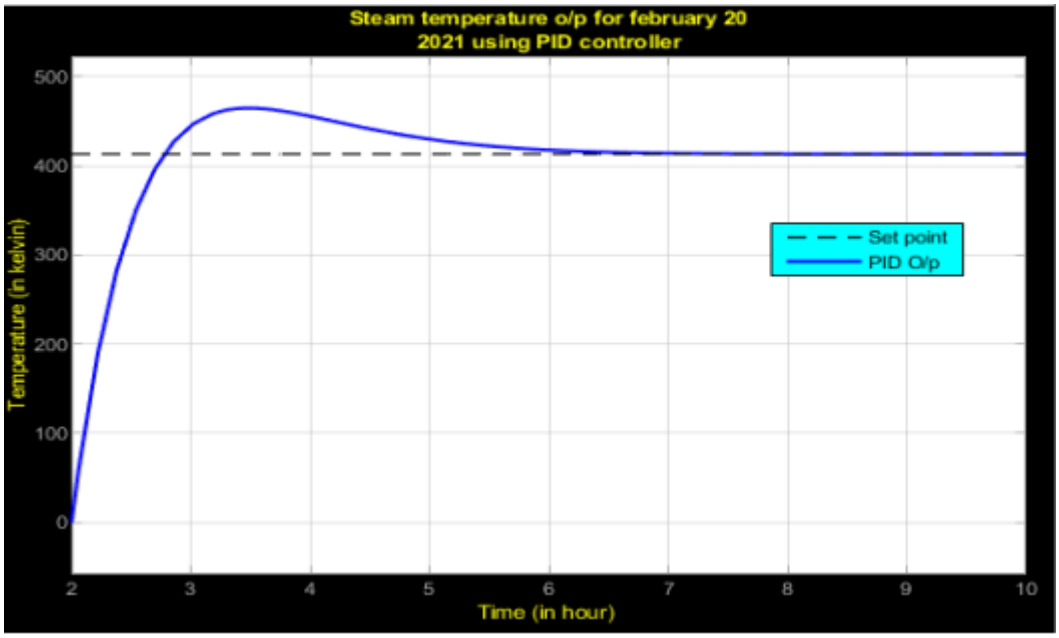

(a)

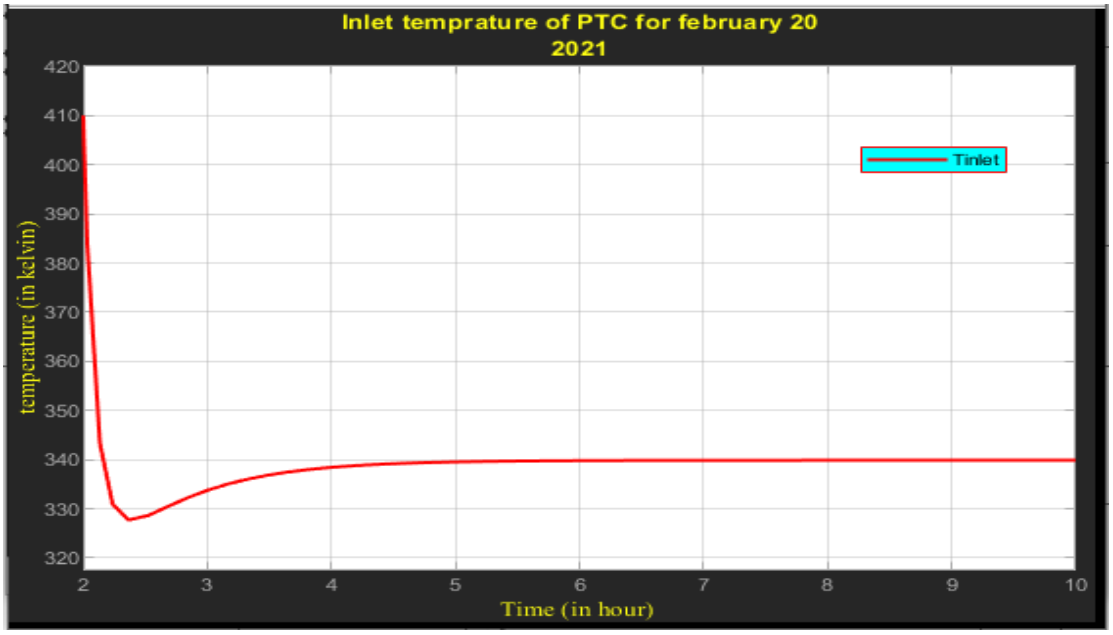

(b)

Figure 6.4: (a) Steam temperature and (b) Inlet temperature for Feb 20, 2021 Using PID.

Here, the PID controller obtains the Ability to hold the steam temperature more approximate to set point (413k) for a long time throughout the day. According to this MATLAB simulation results revealed the PID controller was less capability to providing fast settling time and its have maximum overshoot.

For other case, as shows in figure 6.5 (a) and (b) the steam outlet temperature and Inlet temperature using PID controller for June 20, 2021, for partially cloudy day is considered respectively. Here, the occurring drop in the collector outlet temperature through the adjustment of the HTF volume flow rate. Here, the PID controller obtains the ability to hold the steam temperature more approximate to set point (413k) for a long time throughout the day. But, According to this MATLAB simulation results the PID controller was less capability to providing good settling time and minimum overshoot. While reaching its lower bound. The MPC controller obtains the ability to hold the steam temperature at a constant set point (413k) for a long time throughout the day. The MPC controller is constraint in its control action; it can hold the collector outlet temperature more approximate to its set point. According to this PID control result there is some overshoot values and delay settling time. The variation of set point is because of solar radiation intensity variation.

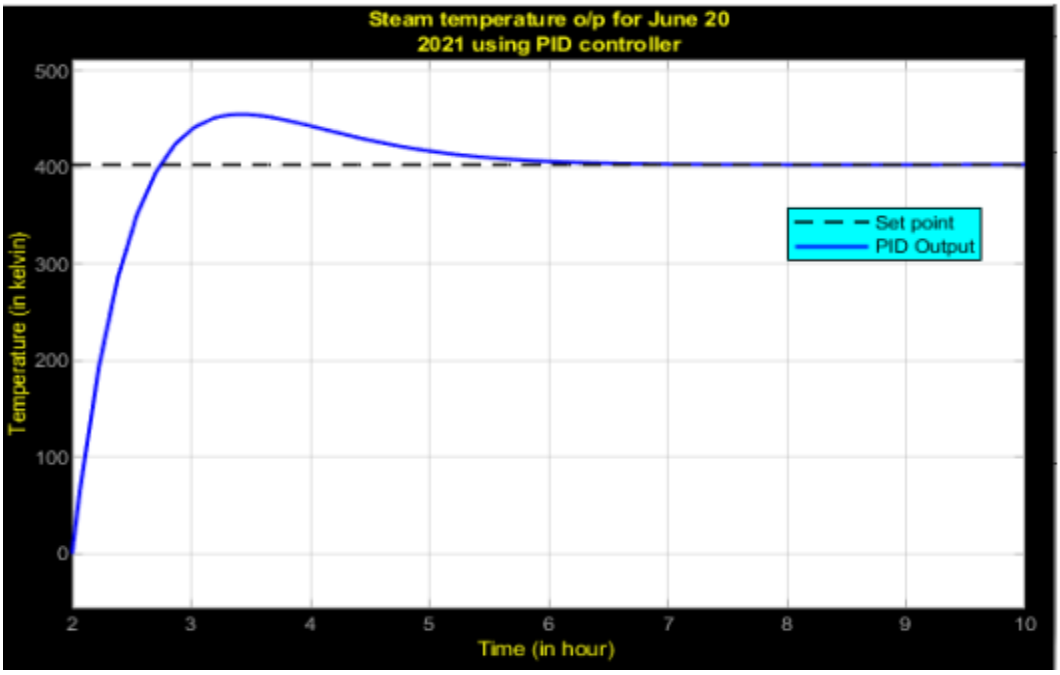

(a)

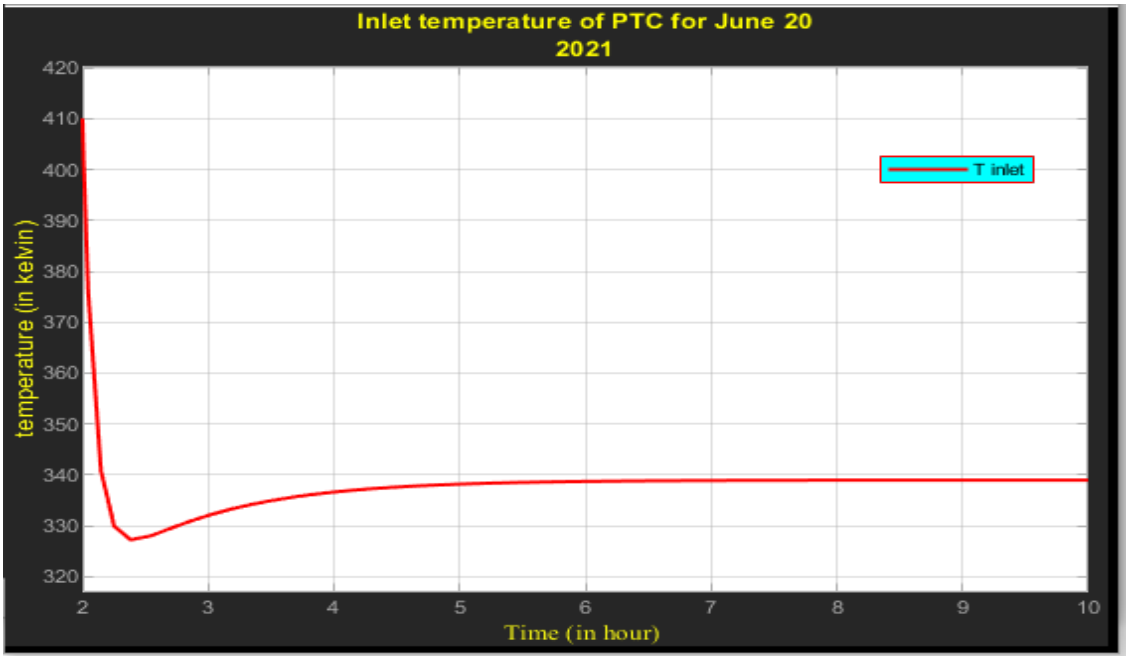

(b)

Figure 6.5: (a) Steam temperature and (b) Inlet temperature for June 20, 2021 Using PID.

6.2.2 MPC control output

As it is shown in figure 6.6 the block diagram of overall model of MATLAB Simulink show that Model Predictive controller control the steam temperature output from the combined plant model. Here, constraints are at output side the collector outlet temperature and at input side volume flow rate of HTF is considered. The MPC is the advanced prediction based controlling method. The result indicate that the plant model described in this thesis is very useful to predict the collector outlet temperature. For this model, a control algorithm has to be found that obtains the ability to hold the collector outlet temperature at a constant set point through the adjustment of the HTF volume flow rate. The controlling algorithm that was chosen for this thesis is model predictive control.

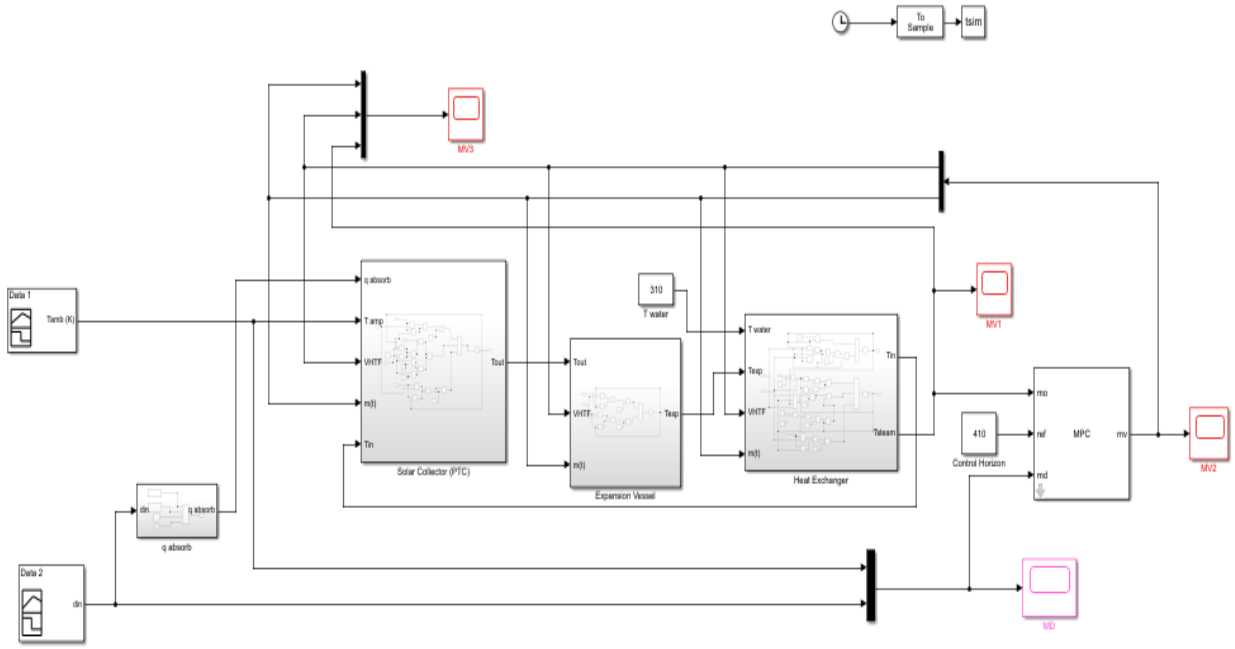

Figure 6.6: Over all Model Matlab Simulink

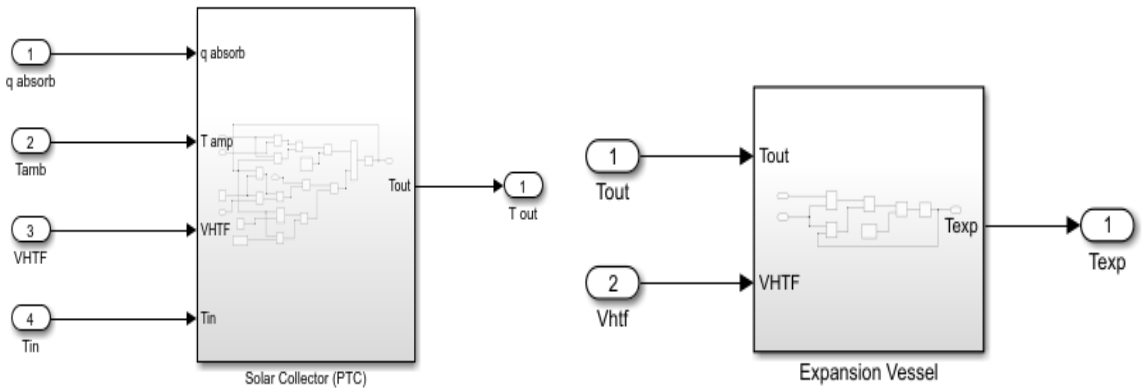

(a) (b)

Figure 6.7: (a) Matlab output of PTC, (b) Matlab output of expansion vessel

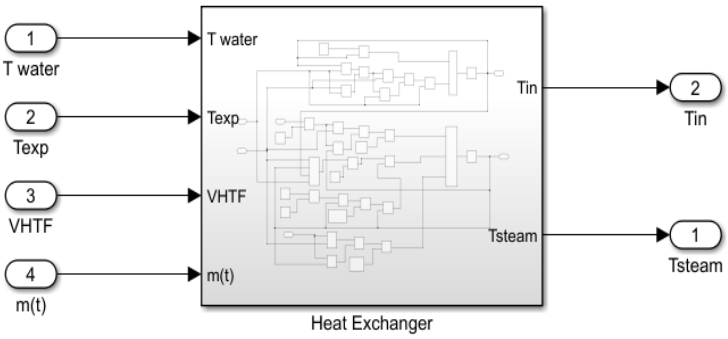

(a)

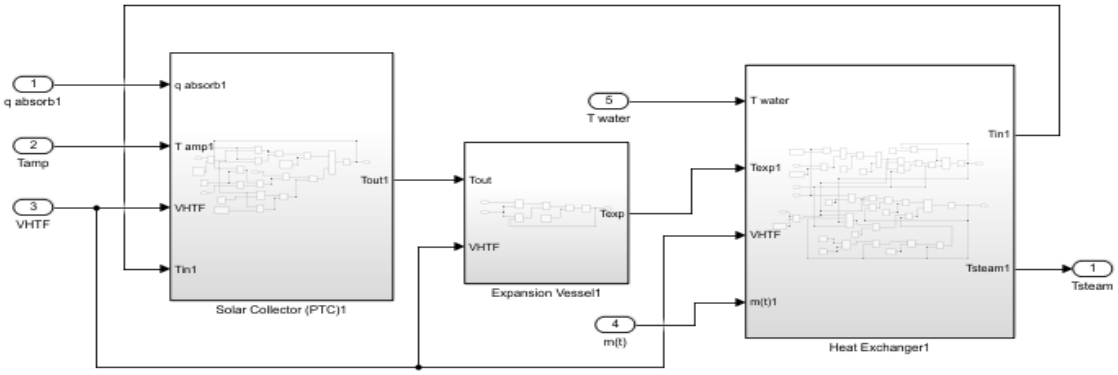

(b)

Figure 6.8: (a) Matlab output of Heat Exchanger (T_HE) and (b) MPC-Lab-1 Simulink

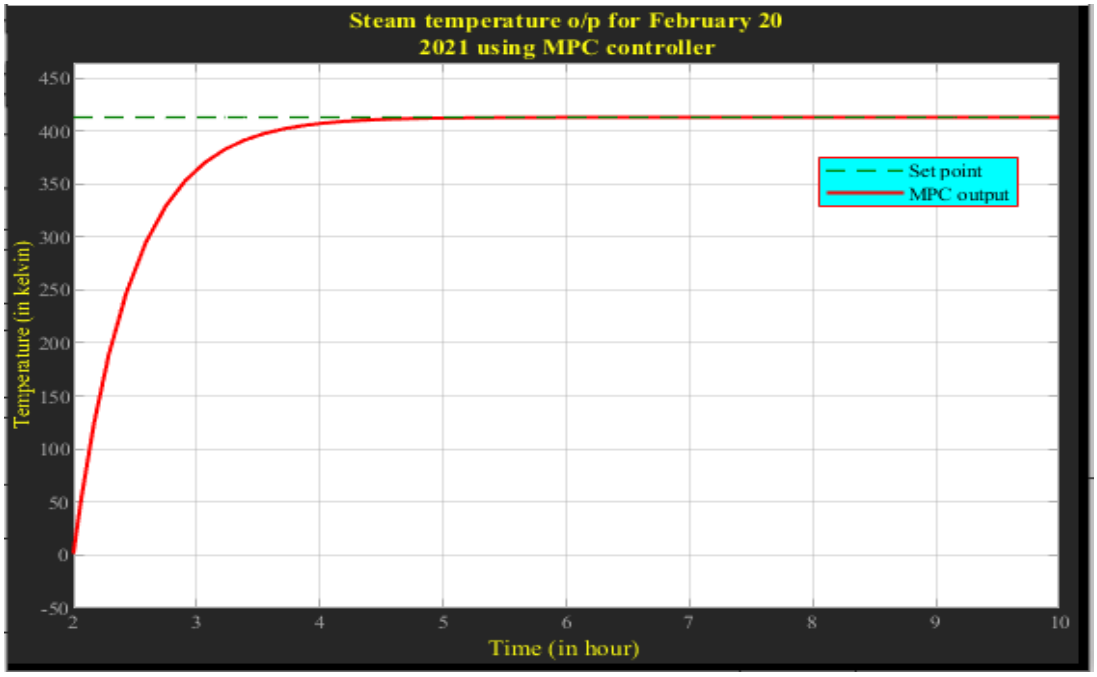

(a)

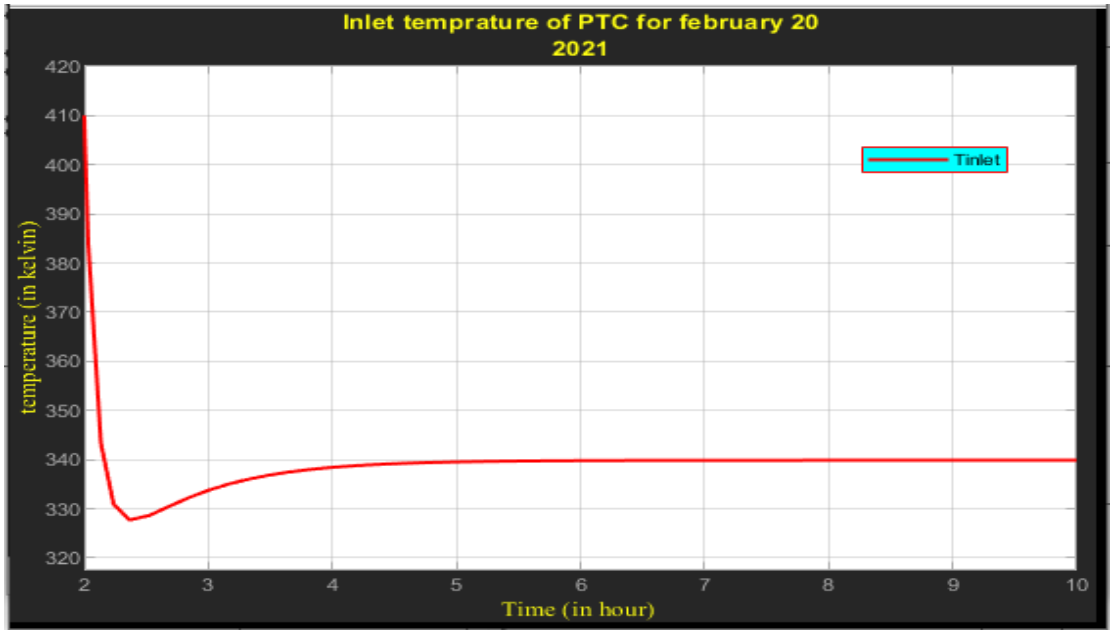

(b)

Figure 6.9: (a) Steam temperature and (b) Inlet temperature For Feb. 20, 2021 Using MPC.

As shows in figure 6.9 (a) and (b) steam temperature and Inlet temperature for February 20, 2021 using MPC controller present respectively. Here, MPC controller obtains the ability to hold the steam temperature more approximate to set point (413k) for a long time throughout the day. The MPC control action results in steam temperature that is held constantly in the set point. But, slight oscillations occur. Therefore, T_{steam} represent a steam outlet temperature when using HTF volume flow rate consider as manipulated variable for model predictive controller (MPC).

For other case, as shows in figure 6.10 (a) and (b) indicate the steam temperature and Inlet temperature using MPC controller for June 20, 2021, a partially cloudy day is considered respectively. Here, the occurring drop in the steam temperature through the adjustment of the HTF volume flow rate. While reaching its lower bound. Here, MPC controller obtains the ability to hold the collector outlet temperature at a constant set point (413k) for a long time throughout the day. The MPC controller is constraint in its control action and it can hold the collector outlet temperature.

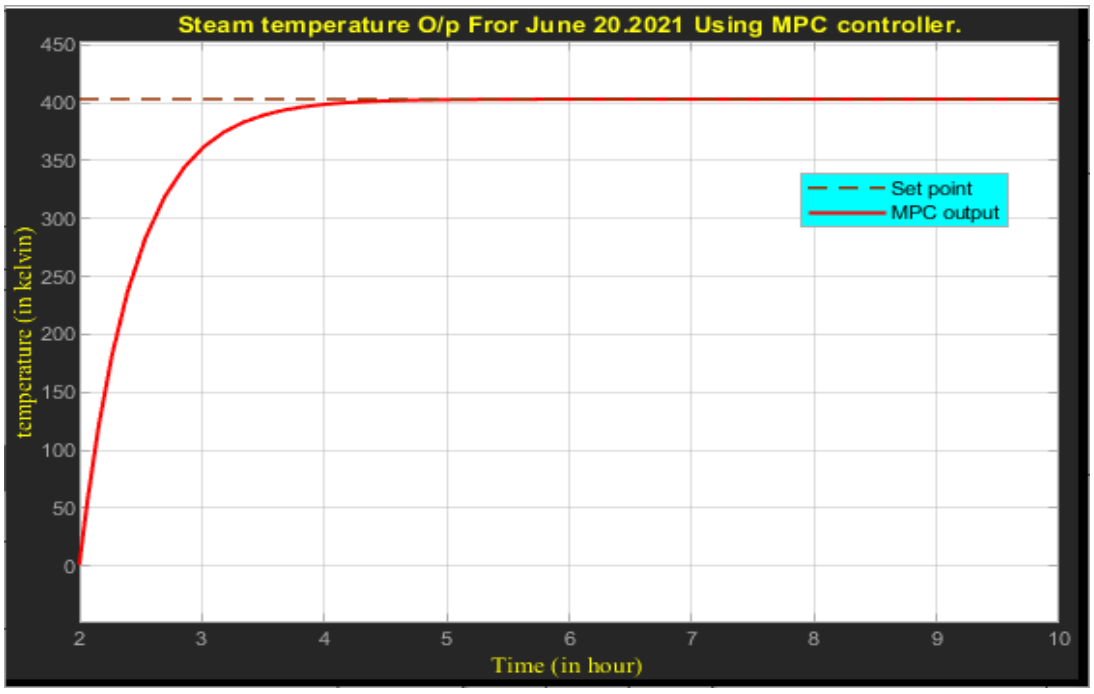

(a)

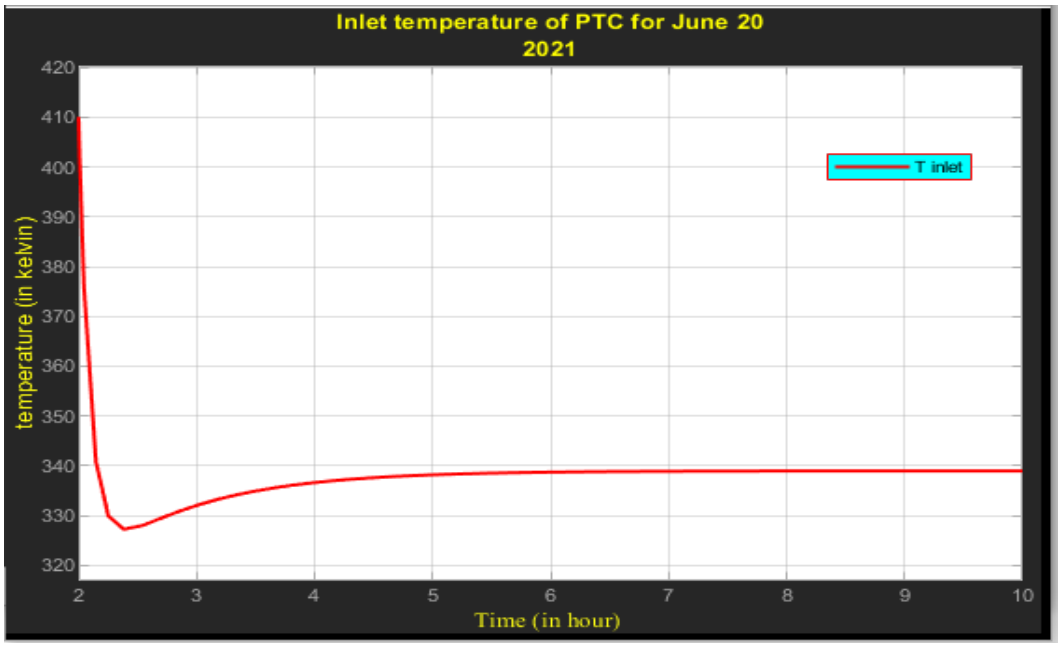

(b)

Figure 6.10: (a) Steam temperature and (b) Inlet temperature for June 20, 2021 Using MPC

6.3 Performance comparison of PID and MPC controller

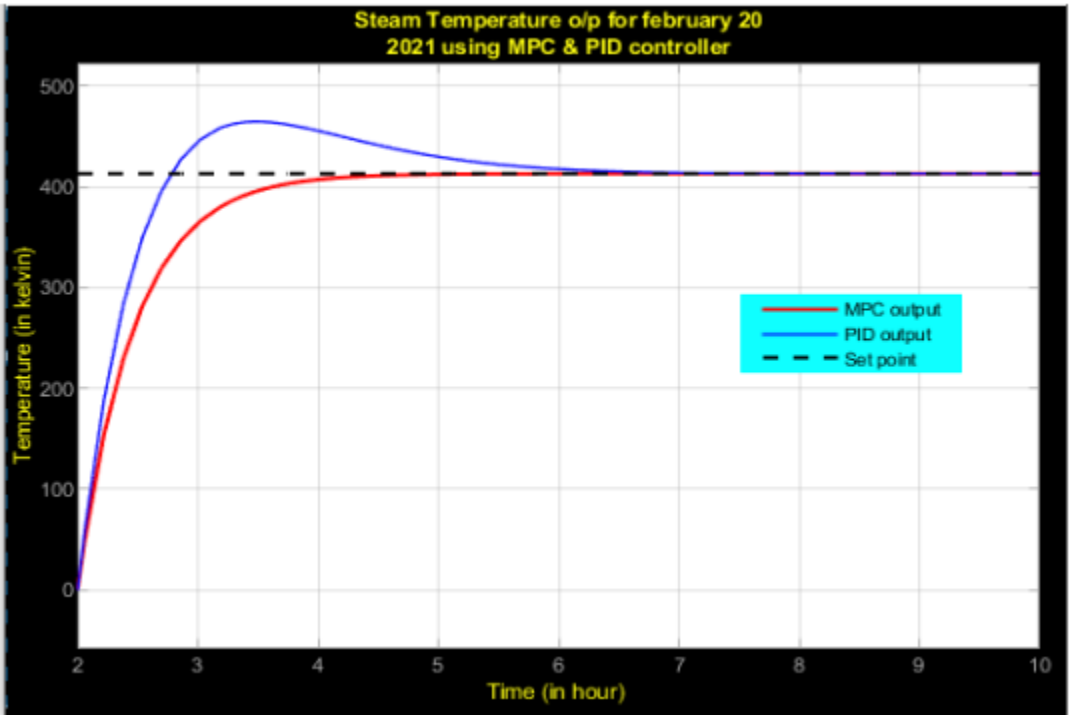

Figure 6.11: Steam temperature for February 20, 2021 Using PID and MPC controller.

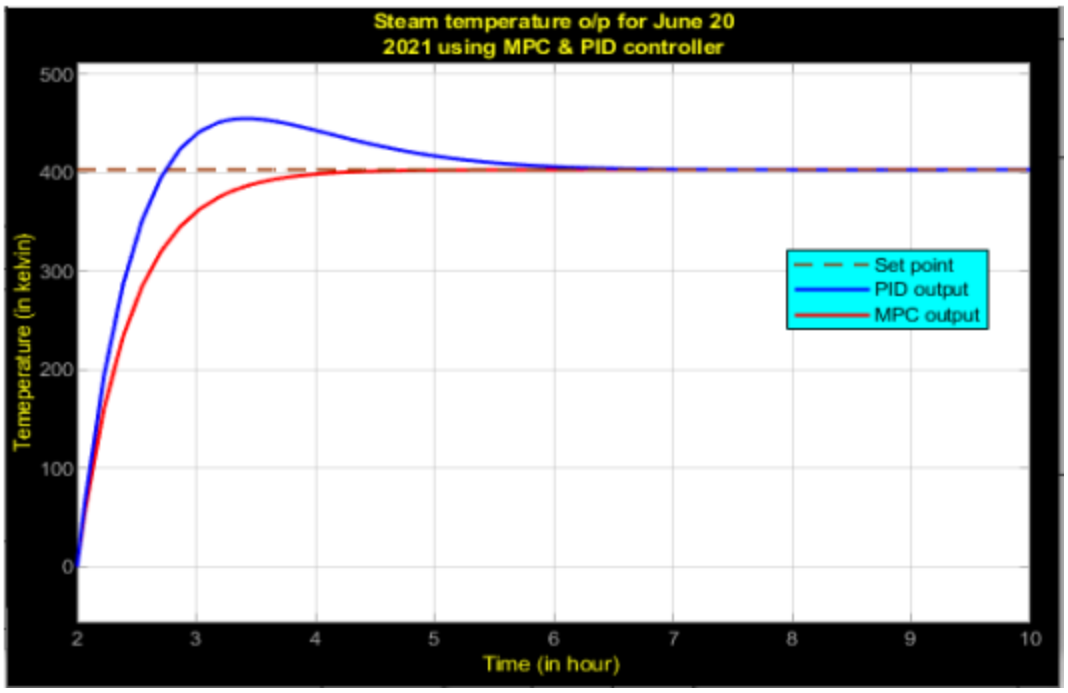

Figure 6.12: Steam temperature for June 20, 2021 Using PID and MPC controller.

Generally, the performance of this controller evaluated based on transient response and steady state response. According to above MATLAB simulation result revealed that the MPC controller reduce steady state error almost to zero and explain transient response parameter such as settling time, rise time and percentage of overshoot in below table 1. Finally conclude that MPC controller result is more preferable than PID controller for this plant. On the other hand, a drawback is that the controller can be quite complex to derive compared to a PID controller.

Table 1: Performance analysis parameter

Controller	Rise time (min)	Setting time (min)	Percentage overshoot (%)
PID	28	155	0.0278
MPC	51	83	0.0012

CHAPTER 7

CONCLUSION AND RECOMMENDATION

7.1 Conclusion

The goal of this thesis is to control the collector outlet temperature which supply to pasteurization plant utilizing a parabolic through collector (PTC). A nonlinear pasteurization plant model using a parabolic trough plant has been developed. First, the collector field model was presented by partial differential equations. Then, the calculation of the absorbed solar energy from the direct normal solar radiation was explain with necessary mathematical equation. Here, the environmental data collect from specification area of the factory. The performance of this model was evaluated through Matlab software.

Secondly, model pasteurization plant using energy balance concept, then collector field model and the pasteurization plant model were combined to an entire plant model that was implemented in EES. A model predictive controller was developed for combined plant model. Its task is to maintain a constant outlet temperature throughout the days by adjusting the heat transfer fluid volume flow rate while solar radiation changes. It was implemented in MATLAB. The control performance was evaluated through simulation for two different days in 2021 and compare output result from prospective of PID controller result. Here, the MPC controller result better than PID controller Interim's of transient response and steady state response.

7.2 Recommendation

Parabolic trough collector design in this thesis has been applied to produce steam and control this steam temperature using model predictive control by adjusting the volume flow rate of heat transfer fluid. In this thesis such control approach has also used for increasing the stability of the plant output and for prediction. The main future works to this thesis are:

- In this thesis work only use solar energy for steam production and supply to pasteurization plant. To have stable steam output it is recommended that use other additional heat source to avoid the reduction of collect heat.
- Analyzing the effect by controlling both the HTF volume flow rate and the steam mass flow rate in the system plant.
- In this thesis work MPC control only temperature of steam which supply at the center of pasteurization plant. It is recommended to design model predictive control strategy for each section of the pasteurization plant with different temperature set point.

Reference

[1]. K. Hennecke, T. Hirsch, D. Krger, A. Lokurlu and M. Walder, Pilot Plant for Solar Process Steam Supply, 2014.

[2]. Paul Verrax. Model Predictive Control Applied to Ground Source Heat Pumps, 2018.

[3]. Hafed Efheij,Abdulgani Albagul,Nabela Ammar Albraiki, Comparison of Model Predictive Control and PID Controller in Real Time Process Control System, 2019.

[4]. Massimo Fiorentini, Hybrid model predictive control of residential heating, ventilation and air conditioning systems with on-sit e energy generation and storage, 2016.

[5]. Sanan T.mohammad and Hussain H.AL-kayiem, an integrated program of a standalone parabolic trough solar thermal power plant, 2018.

[6]. Stefano Poppi, Nelson Sommerfeldt, Chris Bales, Hatef Madani, Per Lundqvist Techno-economic review of solar heat pump systems for residential heating applications, 2018.

[7]. Massimo Fiorentinia, Paul Cooper, Zhenun Maaand Duane A. Robinson Hybrid model predictive control of a residential HVAC system with PVT energy generation and PCM thermal storage, 2015.

[8]. Zhenun Maaand, Simulation of Parabolic Trough Concentrating Solar Power Generation System, 2017.

[9]. Md Adulselam, Automatic control of the 30 MWe SEGS VI parabolic trough plant, 2016.

[10]. Md Mafizul Islam,Md Abdul Salam, Modelling and Control System design to control Water temperature in Heat Pump, 2013.

[11]. Singh, R.; Ierapetritou, M.; Ramachandran, R.Modellig,transient simulation and paameric studies of parabolic trough collector with thermal energy storage, 2017.

[12]. Xiaolei Li and Ershu Xu, Modeling and dynamic simulation of a steam generation system for a parabolic trough solar power plant, 2018.

[13]. Alexander Arnitz, Model based predictive control of a heat pump system, 2017.

[14]. Song, C.; Wu, B.; Li, P, A hybrid model-based optimal control method for nonlinear systems using simultaneous dynamic optimization strategies, 2012.

[15]. Mohanad Abdulazeez Abdulraheem Alfellag, Modelling and Experimental Investigation of Parabolic trough solar collector, 2014.

[16]. T. G. Ling, M. F. Rahmat, A. R. Husain, R. Ghazali, System Identifi- cation of Electro Hydraulic Actuator Servo System, Faculty of Electrical Engineering, Universiti Teknologi Malaysia,81310 Skudai, Malaysia, IEEE, 2011.

[17]. John H, Lienherd,A Heat transfer textbook, Third edition, 31 Jan, 2008.

[18]. Giampaolo Torrisi, Sergio Grammatico, Andrea Cortinovis,Mehmet Mercangz, Manfred Morari, Model Predictive Approaches for Active Surge Control in Centrifugal Compressors,2017.

[19]. Techn. Ren Rieberer. Model based predictive control of a heat p ump system, 2014.

[20]. Honggui Han, Member, IEEE, and Junfei Qiao,Member, IEEE Nonlinear ModelPredictive Control for Industrial Processes: An Application to Wastewater Treatment Process,2014.

[21]. Mohammad B. Shadmand, Robert S. Balog,Haitham Abu-Rub, Senior Member,IEEE Model Predictive Control of PV Sources in a Smart DC Distribution System: Maximum Power Point Tracking and Droop Control, 2014.

[22]. H.J.Palanth,S.Lacy, J.B.Hoagg an D.S.Bernstein, Subspacebased Identification for Linear and Nonlinear Systems,American Control Conference, pp.2320-2334,2005.

[23]. Clara VERHELST,Model Predictive Control of Ground Coupled Heat Pump Systems for Office Building, 2012.

[24]. Kwakernaak, H. and Sivan, R. (1972) Linear Optimal Control Systems. 1st Edition, Wiley-Interscience, Hoboken, 1972.

[25]. Klein, S.A. (2001), EES Engineering Equation Solver, F-Chart Software, USA.

[26]. Karche A. S, Wagh M. M, Kulkarni V.V. Review on Performance Evaluation of Parabolic Trough Collector. 2018.

[27]. Niclas BJorsell, Control strategies for heating systems, University Collage of Gavle-Sandviken, 801 76 Gavle, Sweden.2010.

[28]. Duffie, Jouh A. and William A. Beckman, Solar engineering of thermal processes 3rd. New Jersey,John Wiley and Sons, 2006.

[29]. Tiwari, G. N, Solar energy fundamentals design, modelling and applications, New Delhi, Alpha science international. 2006.

[30]. Foster, Robert, Majed Ghassemi and Alma Cota. Solar energy: renewable energy and the environment. Boca Raton: CRC press, 2010.

[31]. Goswami, D. Yogi, Frank Kreith and Jan F. Kreider. Principles of solar engineering.2nd. Philadelphia: Taylor and Francis, 1999.

[32]. Kalogirou, Soteris A. Solar energy engineering: Processes and Systems. 1st. USA: Elsevier, 2009.

[33]. Dubey, Swapnil and G.N. Tiwari. Fundamentals of photovoltaic modules and their Applications. Cambridge: The royal society of chemistry, 2010.

[34]. Eduardo F.Camacho and Antenia J.Gallego: Model predictive control in solar trough plant, 2017.

[35]. Ministry of Water and Energy, April 15-04-2011, Ethiopian Energy Potential and Five Year Energy Sector GTP.

[36]. https://en.wikipedia.org/wiki/Bedele.

Appendix 1

PTC design

I. PTC Dimensions

No.	Parameter	Values
1	Technology	Parabolic trough
2	Location	Bedele, Ethiopia
3	$n_{collector}$	60
4	Length	10m
5	$D_{Abs,i}$	0.058m
6	$D_{Abs,o}$	0.078m
7	$D_{Env,i}$	0.088m
8	D_{Env}	0.094m
9	A_{Env}	0.00053
10	$A_{Abs,i}$	0.0003421
11	A_{Abs}	0.0004273
12	V_{Exp}	220
13	W	8m
14	D_{HE}	2m
15	C_{HTF}	100
16	L_{HE}	3.2m

II. Environmental Data of Bedele on February 20, 2021

Time(hr)	Ambient Temperature (℃)	Wind speed (m/s)	Solar radiation
2	294.	2.2	320
2:30	294.3	2.2	350
3	294.8	2.3	410
3:30	295.1	2.5	422
4	295.7	2.5	483
4:30	296.0	2.55	520
5	296.4	2.71	590
5:30	296.8	2.72	630
6	297.1	2.72	720
6:30	297.3	2.75	748
7	297.7	2.76	772
7:30	298	2.76	790
8	298.2	2.91	805
8:30	298.34	3.01	812
9	298.4	3.2	801
9:30	298.65	3.34	796
10	297.8	3.42	742
10:30	297.5	3.53	680
11	297.3	3.61	638
11:30	297.1	3.7	610

III. Environmental Data of Bedele on June 20, 2021

Time(hr)	Ambient Temperature (℃)	Wind speed (m/s)	Solar radiation
2	291.14	1.96	311
2:30	291.32	1.97	324
3	292.81	2.01	372
3:30	292.14	2.02	378
4	292.20	2.14	410
4:30	292.01	2.21	439
5	292.15	2.28	473
5:30	293.8	2.32	522
6	294.1	2.33	610
6:30	294.3	2.36	676
7	294.7	2.39	710
7:30	295	2.39	712
8	295.2	2.41	769
8:30	295.18	2.53	781
9	295.14	2.56	780
9:30	295.02	2.61	774
10	294.48	2.67	713
10:30	294.35	2.66	632
11	294.3	2.66	546
11:30	293.9	2.69	521

Appendix 2

Matlab Simulink

I. Parabolic collector Matlab Simulink

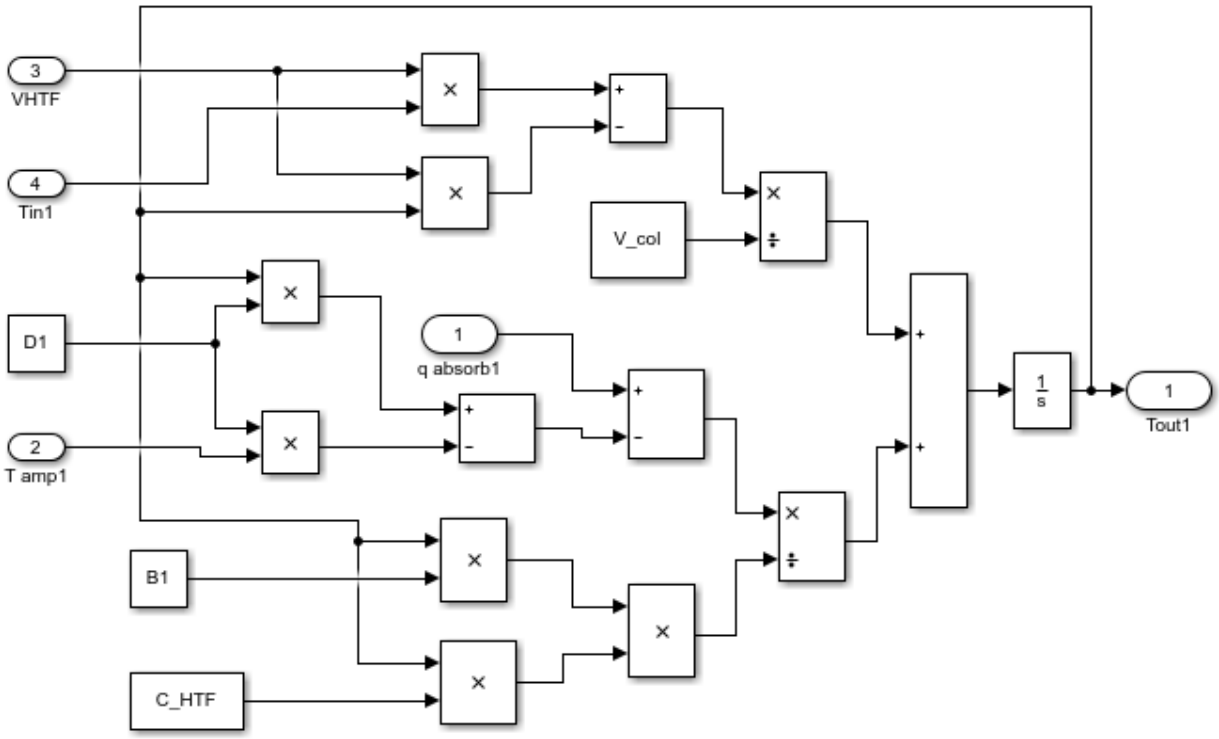

II. Expansion vessel matlab simulik

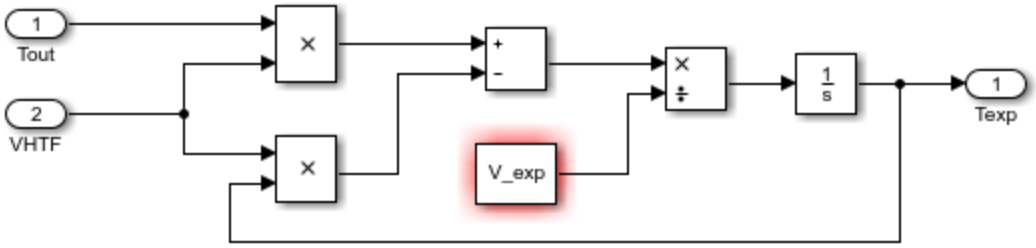

III. Heat exchanger matlab simulik

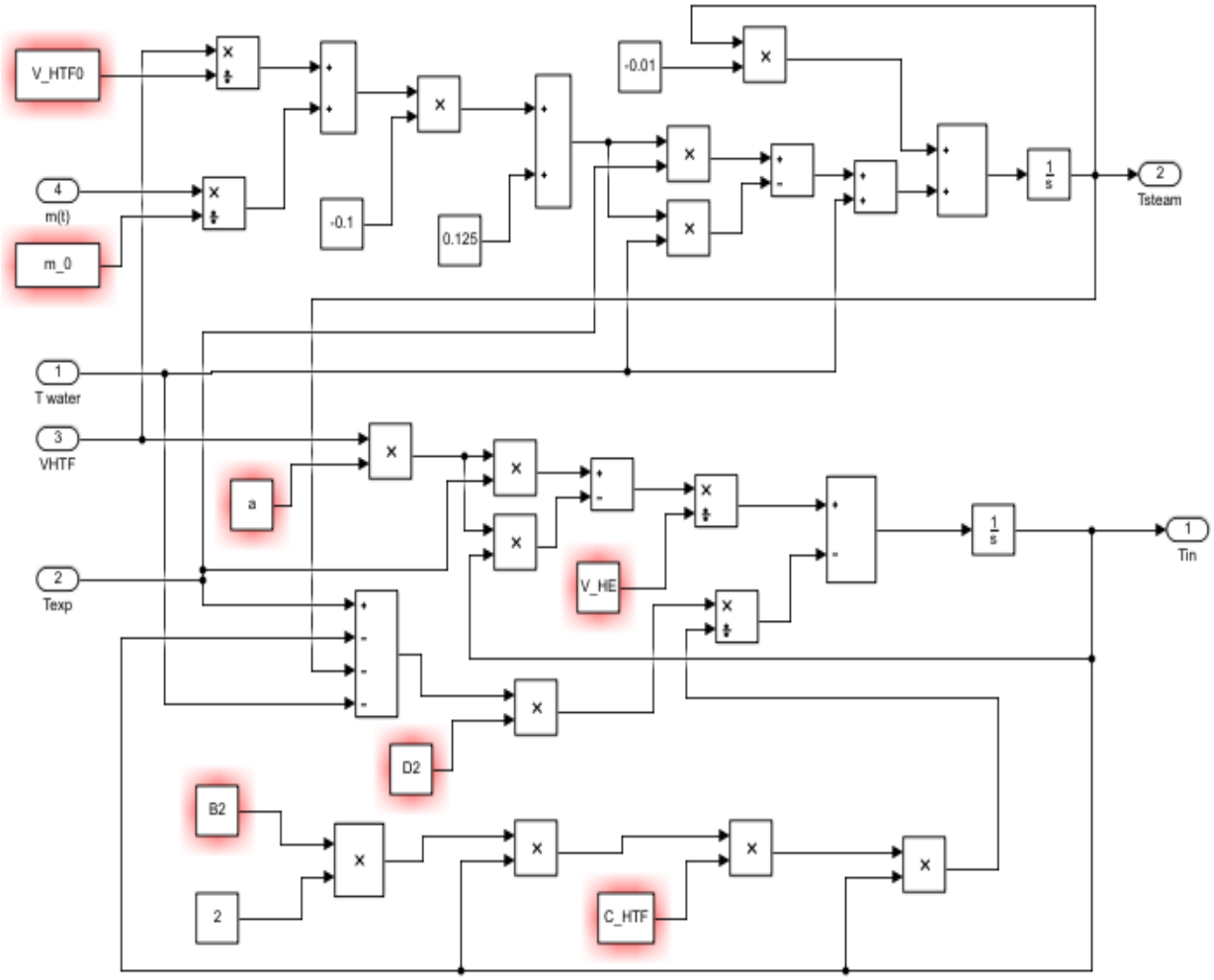

Appendix 3

Matlab code

I. Parabolic trough collector (PTC)

data = xlsread("Desktop:ptc:bedeledataa")

T s = 1

samples = length(data(:, 1)

t = -T s

load(0steadestate:mat0;0 ss0)

x0 = ss

T_{emp} = x0

n = size(x0;,1)

InT = 298

T_{amp} = data(:, 2)

DNI = data(:, 3)

$n_{collector}$ = 60

V_{HTF}= 0.7225

dx = 10

W = 8

A_{ABS} = 0.0004273

$A_{ABS,i}$ = 0.003421

A_{Env} = 0.0005349

$D_{ABS,i}$ = 0.058

$D_{ABS,o}$ = 0.07

$D_{Env,o}$ = 0.115

$D_{Env,i}$ = 0.112

V_{wind} = data(:, 1)

theta = 11.4136

C_{Env} = 840

C_{ABS} = 460

ρ_{ABS} = 7850

ρ_{ENV} = 2400

Cp- a = 1498

Cp- b = 2.414

Cp- c = $5.9591 * 10^{-3}$

Cp- d = $2.9879 * 10^{-5}$

Cp- e = $4.4172 * 10^{-8}$

rho1 - a = 1083.25

rho1 - b = 0.90797

rho1 - c = 0.00078116

rho1 - d = $2.367 * 10^{-6}$

v_a= 544.149

v_b= = 11443

v_c= = 2.59578

kfa = 0:137743

kfb = $8:19477 * 10^{-5}$

kfc = $1:92257 * 10^{-7}$

kfd = $2:5034 * 10^{-11}$

kfe = $7:2974 * 10^{-15}$

$A_{ABS,surf\,o} = \pi * D_{ABS,o}$

mirrorRefreflectance = 0.94

transmittance = 0.93

absorptance = 0.94

interceptfactor = 0.92

IAM = $1 - 0.00384 * \theta - 0.000143 * \Theta^2$

eta - peak = mirrorRefreflectance $*$ transmittance $*$ absorptance $*$ interceptfactor $*$ IAM

II. Sun Tracking

```
Function Tref = MPPT(T,P)
Trefmax = 450;
Trefmin = 0;
Trefinit = 375;
deltaVref = 1;
persistent Told Pold Trefold;
dataType = 'double';
if isempty (Told)
   Told = 0;
   Pold = 0;
   Trefold = Trefinit;
end
   dT = T- Told;
   dP = P- Pold;
   if dP ~= 0
      if dP<0
         if dT<0
         Tref=Trefold+ deltaTref;
      else
         Tref=Trefold - deltaTref;
      end
   else
      if dT<0
         Tref=Trefold - deltaTref;
      else
         Tref=Trefold + deltaTref;
      end
   end
 else
      Tref = Trefold;
   end
if Tref>=Trefmax | Tref<=Trefmin
   Tref=Trefold;
end
Trefold=Tref;
Told = T;
Pold = P;
```

III. Model predictive control

$D_{ABS,i}$ = 0.058

eta-peak = 3.98

TrackingError = 0.92

W = 8

a = 1

U = 9.6525

Length = 10

$n_{collector}$ = 60

A_{col} = 21

A_{HE} = 1418

p_{HTF}= 100

D_{HE}= 2

L_{HE} = 3.2

L_{col} = Length ∗ ncollector

V_{col} = L_{col} ∗ pi=4 ∗ DABSi2

V_{HE} = L_{HE} ∗ pi=4 ∗ DHE2

V_{Exp} = 220

R_{HTF} = 800

B1 = A_{col} ∗ p_{HTF}

B2 = A_{HE} ∗ p_{HTF}

C_{HTF} = 120

D1 = U ∗ A_{col}

D2 = U ∗ A_{HE}

p1 = tf(1; 1; 1; 1; 1; [4:51]; [31]; [7:51]; [14]; [:512])

plant = ss(p1,' min')

[A; B; C; D] = ssdata(plant)

x0 = [0; 0; 0; 0;]

T s = 0.5

p = 5

m = 2

if mpccheckboxinstalled('simulink')

return end.

I. Specify signals

plantDSS = c2d (plant; T s)

plantDSS.InputGroup.MeasuredDisturbances = [1 2]

plantDSS.InputGroup.ManipulatedV ariables = [3]

plantDSS.InputGroup.nunMeasuredDisturbances = [4 5]

plantDSS:OutputGroup:Measured = 1

plantDSS:InputName = $'q'_{absorb,}$ $'T'_{amb,}$ $'V'_{HTF}$,'m(t)', $'T'_{water}$

plantDSS:OutputName = $'T'_{out}$

T stop = 1

ref:time = 0 : T s : (T stop + p ∗ T s)

ref.signals.values = double(ref.time > 10)

md.time = ref.time

md.signals.values = double(md.time > 30)

if mpccheckboxinstalled('slcontrol')

return end

II. Create operating point specification.

plant - mdl =' MPC - Lab – 1'

op = operspec(plantmdl)

op:Inputs(1).u = 710

op:Inputs(1).Known = true

op:Inputs(2).u = 298

op:Inputs(2).Known = true

op:Inputs(3).u = 0.722

op:Inputs(3).Known = true

op:Inputs(4).u = 19.82

op:Inputs(4).Known = true

op:Inputs(5).u = 313

op:Inputs(5).Known = true

```
[op – point, op - report] = findop(plant – mdl. op)
x0 = op – report.States(1).x
y0 = op – report.Outputs(1).y
u_o = [op - report:Inputs(1):u; op - report:Inputs(2):u; op - report:Inputs(3):u; op -
report.Inputs(4).u; op - report:Inputs(5).u]
sys = linearize(plant – mdl, op - point)
plant = c2d(sys, T s)
mpcobj = mpc(plantDSS, T s, 5, 2)
mpcobj:MV (1).Min = 0
mpcobj:MV (1).Max = 2:776
mpcobj:MV (1).RateMin = 0
mpcobj:MV (1).RateMax = 2
mpcobj
if mpcchecktoolboxinstalled('ident')
return end
mdl =' mpc – optimalcost'

open - system(mdl)
sim(mdl)
```